Eugene S.Struminsky M.Eng. July 1971

Civil Engineering & Applied Mechanics

LOW-CYCLE FATIGUE STUDY OF FIBERGLASS-REINFORCED PLASTIC LAMINATES

Abstract

This experimental investigation into the low-cycle fatigue response of fiberglass-reinforced polyester laminates considered the effects of varying test mode (tension/flexure),fiberglass/resin ratio,and minimum stress level,in an aqueous environment at ambient temperatures.Quasi-static strength tests,on which a formal factorial analysis of variance was performed,served as reference data.It was established that the energy input during cyclic testing is more significant than the material properties,and that longer fatigue lives and less strength degradation are generally apparent in the flexural stressing mode,the higher fiberglass/resin ratio and the non-zero (20% of ultimate) minimum stress level.

STRUMINSKY E.S. LOW-CYCLE FATIGUE STUDY OF FRP LAMINATES M.ENG. COPY I

Low-Cycle Fatigue Study

of

Fiberglass-Reinforced Plastic Laminates

Eugene S. Struminsky

A Thesis submitted to the

Faculty of Graduate Studies and Research

in partial fulfilment of the

requirements for the degree of

Master of Engineering

in

Civil Engineering

Department of Civil Engineering and Applied Mechanics

McGill University

July, 1971

Abstract

This experimental investigation into the low-cycle fatigue response of fiberglass-reinforced polyester laminates considered the effects of varying test mode (tension/flexure), fiberglass/resin ratio, and minimum stress level, in an aqueous environment at ambient temperatures. Quasi-static strength tests, on which a formal factorial analysis of variance was performed, served as reference data. It was established that the energy input during cyclic testing is more significant than the material properties, and that longer fatigue lives and less strength degradation are generally apparent in the flexural stressing mode, the higher fiberglass/resin ratio and the non-zero (20% of ultimate) minimum stress level.

Acknowledgement

It is with pleasure that the author thanks his research director, Dr. Joseph Nemec, Jr., for his many helpful suggestions and guidance throughout this project.

Acknowledgement is also due to Mr. Axel Mothes, of the School of Architecture, for manufacturing most of the specimens, and to Mr. Torquel Bowen for making the electrical circuits.

Financial support for this project was provided by the Defence Research Board of Canada under grant No. 7555-09. This support is gratefully acknowledged.

Table of Contents

List of Figures

(Appendix A)

List of Tables

Low-Cycle Fatigue Study of Fiberglass-Reinforced Plastic Laminates

1. Introduction

1.1 General

Current uses of composite materials include various military and similar structures such as those in aerospace and deep-submergence structures (1), transportation vehicle components (2), sub-terranean structures (3) and buildings (4), (5). The decisive criteria motivating the increased utilization of composites are their high strength/weight ratios and good corrosive properties. Furthermore, it is often possible to take advantage of the variety of matrix and reinforcing materials and the fabrication processes to achieve a directionally reinforced and particularly shaped composite component to specifically suit the designer's needs. Against the attractive properties of composites, one must consider their relative high cost and sensitivity of mechanical properties to long-term stress and higher temperature exposures. Fiberglass-reinforced resins are used most in structural applications and increased use is being made of higher strength composites using boron and carbon fibers (6),(7).

The requirements for design vary with the particular application. In all cases data is required as to the stiffness of the material, stiffness variation with orientation of reinforcement, and the behavior of the material subjected to fatigue, which can be defined generally as a progressive weakening of a test piece or component with increasing time under load, such that loads supported satisfactorily at short times produce failure at long times. The term fatigue can then be qualified by subdivision into two main classes - static and dynamic, in order to differentiate between the behavior of plastics subjected to continuous and to cyclic loading. This project examines the behavior of a fiberglass-polyester laminate under low-frequency cyclic loads in a controlled environment (see sec. 1.3).

1.2 Review of Research on Fatigue of FRP's

The following is a brief outline of research carried out on the mechanical fatigue properties of plastics reinforced with cloth, filament and mat fiberglass. Reference to the conclusions drawn from this body of work which are particularly relevant to this project shall be made in sec. 4 and sec. 5. Research which has been primarily concerned with relating mechanical to micro-material behavior of FRP's shall be discussed in sec. 2. It may be noted that almost all results are empirical, qualitative and specialized, but can serve to illustrate the approaches to and presentations of fatigue experimentation.

The first extensive investigations of FRP fatigue were conducted by Boller and his associates Kimball, Stevens, Werren et al (8), (9) at the Forest Products Laboratory, Wisconsin, between 1952 and 1961. Various resins and reinforcements, as well as effects of moisture absorption, temperature, notching of specimens (stress concentrations) and loading variables were studied. Tests were run on standard axial tension specimens cut from laminate sheets, at a frequency of 900 rpm, reference temperature and humidity generally being 73^{o}F and 50%. In all, 53 stress-fatigue life (SN) curves were developed in the 10^{3}-10^{7} cycle range, and several master diagrams showing the relationship between mean stress and stress amplitude at different lifetimes were derived from these. However, Boller himself stated in (8), that "... No theories are intentionally advocated ... the data themselves point to the fatigue characteristics".

In 1951 Lazar (11) presented an accelerated method for predicting the fatigue limit of plastics using the Prot Progressive Loading technique. Time savings of about 90% over conventional methods were obtained. Tests were carried out in reversed axial (tensile - 0 - compressive) stressing on gear nylon and two types of glass-cloth-reinforced plastics under different tensile mean stresses, at a frequency of 1900 rpm on a modified rotator. In all cases the Prot extrapolated endurance limits agreed very well with the standard Wohler check tests.

A study of dynamic and static fatigue was carried out by Thompson (10) in 1962. Seventy resin formulations were considered and an epoxy reinforced with glass fabric was chosen for the aircraft application required. The program covered three test conditions (unnotched, dry; unnotched, in water bath; notched, in water bath) and four types of loading (0 - tension, 0 - compression; tension - 0 - compression; between two levels of tensile load). All tests were at 0^{o} to warp, at a frequency of about 100 cpm, with a maximum 1000 cpm for the lowest load tests. SN curves and master diagrams were developed and quantitative conclusions drawn.

Carswell and Borwick (12, 1965) conducted creep rupture, tensile and repeated loading tests on chopped-mat-polyester sheet specimens at three strain rates (0.002, 0.05, 2.0 ipm tension; 0.3, 10, 60 cpm cyclic) to assess the sensitivity of the material to frequency of cyclic loading. An Instron machine was used. A microscopic examination was made to reveal similarities of failure between the static and dynamic tests, and the relation to the creep rupture failures.

Low-cycle flexural fatigue tests on a thin (3-ply) epoxy laminate were carried out by James, Appl and Bert (13). Strain (rather than stress) vs. cycles-to-failure data were obtained for speeds of 25, 150, 425 cpm.

The British team of Owen, Smith and Dukes conducted fatigue experiments on chopped-strand-mat polyester laminates (14, 15, 1968-9) using a specially designed pulsator. Glass contents varied between 29-36% by weight for the two resins used. Test frequency was generally 74 cpm. Stress rupture tests were used in conjunction with SN diagrams to develop master Goodman curves. Throughout the program extensive statistical control tests were undertaken to determine effects of specimen batches and different loading frames. It was suggested that failure be defined as the onset of cracking or debonding in specimens and that SN curves be correlated to strain at debonding, not only stress (load) at failure.

Dally and Carillo (16, 1969) conducted fluctuating tension fatigue tests, using a stress ratio of 0.05 and frequency of 600 cpm, on glass-fiber reinforced thermoplastics to determine the effects of length of discontinuous fibers and strength elongation characteristics of different matrix materials. Glass content was 40% by weight in all cases. The classical SN curves were generated and residual strength vs. cycles endured was also evaluated. Failure mechanisms were studied by a comprehensive microscopic examination of fatigued specimens.

Cessna, Levens and Thomson (17, 1969) investigated flexural fatigue of thermoplastics as a function of cyclic stress level, frequency, viscoelastic polymer parameters, and matrix-to-fiber stress transfer capacity. The effects of dissipative heating of a "working" specimen and efficient stress transfer mechanisms were emphasized. Test frequencies varied from 100 - 2200 cpm.

Dally and Broutman (18, 1967) carried out a program to determine the effects of cyclic frequency, in a range of 1-40 cps, on tensile fatigue characteristics of non-woven glass-fiber-reinforced plastics, using many fiber orientations. Equations were developed to predict temperature distributions due to hysterisis heating, (using 1 cycle closed-loop tests), the time to achieve steady state at intermediate points, and steady state surface temperatures. The effect of frequency on fatigue life was also observed. For a crossply laminate and $(\sigma_{max}/\sigma_{ult}) = 0.46$, the difference was about 1500 cycles (4000 to 5500) over the range 1 - 40 cps.

Boller (19, 1965) investigated the effect of pre-cyclic stresses on the tensile fatigue life of epoxy-glass laminates by measuring fatigue life at two stress levels after damage had been programmed at either higher or lower stress levels for 1, 3, or several hundred cycles. The three levels were 80%, 60% and 40% of ultimate strength. Twenty-five groups of specimens, with different reinforcement orientations and resin formulations, were tested in all, at 73^{o}F, 50% RH, 900 cpm for continuous and 6 cpm for precyclic stressing. A statistical analysis led Boller to conclude that GRPs do not obey the usual damage laws and precycling may even improve life of a laminate if the number of precycles is smaller compared to life fatigue.

Fatigue characteristics of glass-filament-reinforced plastics were investigated by Freund and Silvergleit (20, 1966), using unaxial and biaxial compression and interlaminar shear on short bars and Naval Ordinance Laboratory (NOL) rings, and biaxial compression at 20,000 psi on thick-walled cylinders. The lower limit SN curves developed represented data collected between 1962-65. Very large scatter was observed and no attempt was made to define variables such as resin content, specimen size and moisture conditions.

An analytical analysis of the effect of combining roving glass cloth with mat in polyester laminates was made by Fujii and Mizukawa (21, 1969). Using both pulsating tension and cantilever bending tests to support the theory, they concluded that fatigue strength under tensile load is a function of the layers' relative proportions and glass content, whereas in bending, fatigue strength varies primarily according to the ordering of the layers.

McAbee and Chmura (22, 1961) investigated the effect of loading rates on tensile properties of polyesters reinforced with mat, woven roving and cloth glass fibers. The standard ASTM rate of 0.05"/min. of crosshead separation, producing failure in about two minutes, was compared to a high rate on special testing equipment, producing failure in 7 - 10 milliseconds. The stress-strain curves produced showed that high-rate tests exhibit two distinct linear portions separated by a "knee" and greater strengths, whereas low rate tests exhibit a linear then non-linear curve. Interlaminar shear values were also observed to increase with loading rate. It was also noted that slow rates produced a series of individual minor failures prior to final rupture. This was not seen in the high rate tests where the stress-strain curves were smooth rather than "stepped".

Analytical and empirical correlations between matrix properties and torsional fatigue life of uni-directional fiber-reinforced polyester and epoxies at different temperatures (R.T., 76°C - 196°C) were developed by Lavengood and Anderson (23, 1969), using NOL ring tests and a frequency of 150 cpm. Matrix properties were determined by flexural tests on unreinforced rods.

Hagerup (24, 1962) used a modified version of the Prot test and a Sonntag rotator to evaluate flexural fatigue properties of unsaturated polyesters at resonant frequencies. Glass reinforcement was incorporated as two layers of fabric corresponding to the outermost plies in a laminate. Plastic, brittle, and tough resins were characterized depending on their capacity to dissipate local stress concentrations. The effect of a glass/resin interface as stress raiser was investigated.

Opp, Skinner and Wiktorek (23, 1969) of IBM Systems Development Division developed an analytical model for predicting the fatigue life of polymers from their stress-strain curves and physical constants. The model is based on a total hysterisis energy concept, taking into account both mechanical and thermal energy, which is taken as being constant per cycle. Tests on six polymers, including glass-reinforced nylon, generally support the theory and show its promise under further development and refinement. The theory at present accounts for effects of frequency of loading, thickness of material, ambient temperature, stress concentrations, rest periods and type of loading waveform.

Scop and Argon (26, 1967) presented a statistical approach to the theory of strength of laminated composites. Unaxial tension tests on a glass-ribbon composite were used to support the theory, and extensions were made to include the biaxial tension case also. Laminate strength was completely specified in terms of distribution of flaw strengths, i.e. number of flaws per unit area which produce failure at some stress σ , the number of sheets, dimensions of each sheet and glue shear strength.

Gotham (27, 1969) presented a unified approach to the problem of static and dynamic fatigue of thermoplastics by relating static (creep) fatigue and dynamic (cyclic) fatigue (in the unaxial tension mode) to a common stress-strain-time-temperature frame of reference. Use of a square waveform in cyclic loading permitted easy conversion to "total time elapsed at maximum stress" for any test. A comprehensive discussion of failure criteria was given. Effects of temperature and environmental stress cracking were also evaluated.

For additional references on FRP fatigue and mechanical properties in general, (4), (6), (7) may be consulted.

1.3 Project Objectives

The purpose of this experimental project is to establish correlation between the tensile and flexural modes of fatigue behavior of a common FRP laminate under a limited range of material and loading variables, while controlling the environmental variables of temperature and wetness exposure. Properties established from quasi-static strength tests in tension and flexure serve as reference data. Most of the fatigue tests for FRP laminates reported in the literature are in tension, whereas relatively little data is available on the flexural fatigue response. Since bending action is predominant in many structural shapes, such correlation is considered valuable in design. With these objectives in mind, the testing program was organized as a factorial design (see sec. 3.1 and sec. 3.4) and correlations are established by a statistical analysis of variance, as well as by more general interpretations of strength retention characteristics.

2. Fatigue Behavior of Fiber-Reinforced Plastics

2.1 Influencing Factors

The factors which influence the fatigue behavior of FRPs may be categorized into three classes: material properties, environmental variables, and stress variables. Let us consider them in turn.

2.1a Material Properties

Type of matrix material, i.e. resin, greatly affects fatigue endurance (8), (9). For example, epoxies are stronger but more brittle than polyesters, while with a given type the more brittle formulations cause premature failures (24). Sensitivity of the resin to hysterisis heating at high frequencies will also shorten fatigue life (25). In some cases, elastomeric fillers are added as dispersions to the matrix material, where they act as crack arresters (40), (41). Low reactivity resins were observed to be slightly superior to high reactivity resins under various conditions of mean and alternating stress (45). The differences are more apparent at high stresses (short fatigue lives) than at low stresses (long lives).

Type of glass reinforcement also greatly affects fatigue life (8), (9), (16), (21). Highest strengths are shown by uni-directional filament or fiber-reinforced laminates where loading is applied parallel to reinforcement. Fabric and cross-ply laminates exhibit orthotropic properties, while lowest strengths are shown by mat or chopped-strand laminates which may be considered isotropic.

Changing glass content has a considerable effect on the ultimate strength of FRPs. At short lives, the fatigue strength reflects the difference in UTS, but at long lives the differences tend to disappear (45). Because of substantial damage to the resin matrix early in a fatigue test, the rate of stress transfer to the glass reinforcement is high at the start, and becomes almost insignificant after a large number of cycles. Thus the glass/resin ratio is important initially but plays little role in a much fatigued specimen.

The orientation of reinforcement greatly alters fatigue strength, depending also on the orientation of loading. Fabric-reinforced materials, for example, show high strengths at 0^{o} and 90^{o} to warp but significantly lower strengths at 45^{o}. Filament-wound reinforcements are highly directional and advantage is taken of this in such applications as pressure vessels and rocket casings. In low-strength molded applications, however, the isotropy of mat or chopped filament reinforcement is more desirable.

The bonding agent used between glass/resin layers, curing temperature and curing time, as well as laminating pressure, contribute to provide an effective G/R interface, i.e. effective stress transfer from resin to glass. The quality of this bond affects endurance under repeated loads inasmuch as it determines progressive damage at any point. It should be noted that the G/R interface is a region of high stress concentration since the curing, laminating and bonding process in fact producestensile forces on the reinforcement (42). The G/R interface will be discussed further in sec. 2.2.

The effect of surface conditions, whether natural imperfections such as scratches, or artificial such as notches or holes, is to uniformly lower fatigue strength (8), (9), (10), (34). Such regions of stress concentration act as nuclei for the failure mechanisms discussed in sec. 2.2. The shape of specimens is specified such that fillets reduce stress concentrations at gripping points, and span/depth ratios for flexural tests are chosen so as to minimize effect of interlaminar shear on properties measured, i.e. elastic moduli. The thickness of laminates also affects their strength properties.

Youngs (33) found that maximum strength in tension, compression and flexure appears to be greatest for thicknesses of 1/16 to 1/8 inch, with an abrupt decrease below and gradual decrease above these levels. Modulus of elasticity was found to be virtually non-sensitive to laminate thickness (32), (33), but to increase slightly with an increase in space/depth ratio in bending tests, probably due to decreasing effects of shear (32). Density of cracking was observed to decrease with increasing specimen cross sections by (12). An approach to laminate strength based on statistical flaw distributions and number of plies has been developed in (26).

2.1b Environmental Variables

The exposure of laminates to moisture or wetness has been shown to have a deleterious effect on strength in reported immersion and boiling tests (8), (9), (10), (28), (30), (31) for stressed and unstressed conditions, the effect diminishing with number of cycles sustained. Resin content appears to have much less effect after long exposures, than in the short-term tests (31). Modulus of rupture, yield stress, and fiber stress at the proportional limit have been degraded by as much as 30%, but modulus of elasticity was observed to decrease only very slightly (28). A comprehensive analysis of the mechanisms of water attack on the glass-resin bond is given in (30). Hydrolysis of the glass and its protection by the coupling agent, resin swelling and degradation, and composite bond life in boiling water are discussed. Response of the resin to water depends on its diffusivity, and the swelling may be large enough to exceed the original thermal shrinkage occurring after cure. The G/R interface is then subjected to a radial stress which tends to cause debonding and to accelerate hydrolysis. The resin is also stressed by swelling and may develop cohesive cracks. Water absorbed between polar groups of polymer chains tends to plasticize the resin, and it will also hydrolyze the ester links in polyesters leading to serious reductions in cross-link density. Furthermore, the acidic degradation products of resins have a catalytic effect on hydrolysis of other components. The glass surface may be directly hydrolyzed, implying destruction (at least locally) of the G/R bond. This hydrolysis releases small amounts of Na^+ and K^+ in E-type glass, which raises the pH at the interface and further catalyzes hydrolysis of all components. Effects of hydrolysis on the coupling agent seem to be linked more to conditions of its application and curing process than to type, although a carbon chain network joined to glass by Si-C bonds appears to show greater promise than siloxane networks. It is proposed in (30) that G/R debonding in a hot and wet environment consists of two overlapping stages. First there is swelling of resin due to absorption, developing a radial stress at the interface. A slower hydrolytic degradation then follows in the whole composite until localized cleavage occurs. Gross physical separations at interfaces do not occur until the radial compression due to thermal shrinkage has been approximately cancelled by the absorptive swelling. Thus bond life of the composite consists of the time for swelling to counterbalance shrinkage plus the time for hydrolysis to reduce cross-link density to the point where the interface cannot sustain the combined effects of swelling and any applied external pressures.

Corrosive non-aqueous liquids or gases may degrade one or more phases of an FRP composite, depending on the components' chemical resistance and surface finish of the laminate. Effects vary in type (e.g. blistering, scaling, corrosion) and severity. Some useful typical data is presented in (31), and detailed information is usually available from the manufacturer. The strength degradation of polyester-fiberglass laminates in an underground environment is discussed in (3).

The incidence of ultraviolet light, whose main source is the sun, on unprotected plastics is known to have degrading effects (29) in the range of 300 - 400 nano-meters wavelength. The potential energy of UV radiation is very high compared to that of visible and infrared wavelengths and is sufficient to split organic molecules. Complete inhibition of this effect is not possible, but a proper choice of processing stabilizer, pigmentation and light stabilizer will enhance the life of a plastic laminate. Generally, UV absorption will produce similar effects to those of thermal oxidative degradation, leading to discoloration, embrittlement and a general reduction in desirable physical properties (29). The UV impingement process of degradation is believed to promote the initiation of free-radical degradation processes in polymers. The propagation reactions are believed to involve the reaction of free radicals with oxygen, peroxide formation, and breakdown into more radicals,coupled with hydrogen extraction from the polymer (29). The process initiates at the surface and progressively attacks underlying layers.

Since the polymeric resins used in FRP laminates are viscoelastic materials, they are temperature sensitive. Elevated temperatures during testing tend to relieve original shrinkage stresses and hasten debonding, but may also serve to relieve regions of stress concentration. If the heat-distortion temperature is exceeded, flow of resin may occur at highly stressed points. High temperatures may also relieve water-swelling pressures in an aqueous medium (30). The hysteresis heating of a specimen undergoing cyclic fatigue has been investigated in (18), where surface temperatures as high as 265°F have been measured. Elevated temperatures also magnify creep and relaxation phenomena in FRPs (35).

2.1c Stress Variables

In a specimen subjected to cyclic fatigue, two parameters are required to describe its state of stress completely. With the aid of Figure 1 and the accompanying equations, this can readily be seen. For this project maximum and minimum stresses were used. The most usual representation of the effect of stress variables on fatigue life is the Goodman diagram, or a modified version thereof, in which stress amplitude (or stress range = 2 x stress amplitude) is plotted against mean stress for several given fatigue lives expressed in numbers of cycles to failure. A typical Goodman diagram is shown in Figure 2 (8). Other examples may be found in (9), (10), (14), (15). It is apparent that at least 4 or 5 combinations of stress variables must be used to develop sufficient data (SN curves) from which to draw such a master diagram. When the alternating stress amplitude is zero, the abcissa intercepts are equal to the steady stress (obtained from stress-rupture tests) which can be sustained for a period corresponding to the number of cycles for a particular curve. It should be noted that for the test conditions shown,(unnotched, heat-resistant polyester resin /181 glass fabric, Volan A finish, 500^{o}F), the compressive strength is considerably less than the tensile strength and somewhat higher stress amplitudes can be sustained at low mean stress levels than at zero mean stress. However, the tensile and compressive strengths are generally similar and it can be seen that the effect of lowering stress amplitude (for given mean stress) or lowering mean stress (for a given amplitude) will increase fatigue life.

The effects of frequency of cyclic tests, or rate of straining, have been examined in (12), (13), (18), (22). In general, significant differences in mechanical properties or fatigue life for laminated FRPs are observed only at differences of several orders of magnitude in frequency or rate of strain, (see sec. 1.2).

The influence of a precyclic stress history on fatigue life has been studied (19), but results did not permit a general rule to be deduced. Both improvements and losses of endurance were noted, depending on the test conditions and materials, (see sec. 1.2).

The stress distribution over specimen cross-section will also affect fatigue performance. The most obvious manifestations of this occur when stress raisers such as artificial defects are introduced to achieve localized concentrations of stress which are much higher than the maximum stresses due to the external loading applied, as shown in Figure 3a. Significantly lower fatigue strengths result (8), (9), (10), (34). The stress distribution can also be altered, however, by altering the mode of testing. For example, uniaxial tensile and simple flexural modes constitute two different stress distributions over a laminate cross-section of thickness t (see Figures 3b, c). As will be seen in sec. 2.2, moreover, the stress distribution in flexure changes with time, i.e. the neutral axis shifts, since progressive damage in the specimen occurs. If σ_{max} (flexure) equals σ_{max} (tension), greater fatigue endurances should be apparent in bending tests. The influence of stress distribution may also be noted from the work of Thompson (10) who concluded, on the basis of testing with four different stress patterns, that the energy input into the specimen, rather than the maximum stress reached, is the governing factor in fatigue life achieved. The energy concept, of course, is the most successful basis for theoretical models of fatigue behavior (29). Finally, it may be possible to evaluate creep and relaxation effects in dynamic fatigue tests by using appropriate waveforms (e.g. square wave, as in (27)), or by programming the sequence of cycling. As has been pointed out in (27), correlation between static and dynamic forms of fatigue is desirable.

2.2 Progressive Damage and Failure Mechanisms

In contrast to metals and alloys, glass-reinforced plastics develop extensive cracking very early in their fatigue lives, even at low stress levels, and show marked decreases in strength and stiffness progressively. While this degradation usually does not impair the structural integrity of an FRP laminate critically, it may affect serviceability by causing excessive deflections or by permitting ingress of water or some other fluid (see sec. 2.1). Thus the nature, initiation and progression of internal damage are important to structural designers using FRPs, and constitute the subject of this section.

Internal microcracks in the resin matrix cause the degradation of FRPs under load. Minute cohesive failures at localized high stress concentrations multiply and grow in size, ultimately resulting in gross discontinuities which impair the combined action of the composite (40). Desai and McGarry (38) proposed a mechanism for the initiation of such cohesive microcracks in cloth-reinforced FRPs in 1959. In a woven fabric, the glass yarns are bent as they pass over and under each other, rendering the fabric much less stiff than filamentary glass. Under tension straightening of the yarns occurs, imposing high tensile and shear strains on the attached matrix. The high local displacements, combined with contraction of the resin due to the Poisson effect, cause brittle resin to fracture at relatively low stresses. In compressive loading the resin effectively supports the yarns against local buckling and also expands against them because of the Poisson action. While 20 - 30% of ultimate may produce significant damage in tension, Broutman (44) reported that as much as 80% of ultimate may be required to initiate microcracking in compression of filament-reinforced specimens. Figure 4 (38) schematically illustrates the mechanisms involved.

The formation of microcracks is almost invariably initiated at the glass-resin interface or in the adhesive zone between the two (42), (43), (44), (46). In a photoelastic study of resin "tricornes" enclosed by a "container" of glass filaments, West and Outwater (42) have shown that the glass surface is under severe tension, in the order of several thousands psi, resulting from thermal shrinkage of the resin surrounded by unyielding glass. In the case of cloth lay-up FRPs, the resin is believed to be "contained" at the cross-overs of strands, where the curing pressure would tend to squeeze fiber plies together around resin interstices. The tension is due to the adhesive bond between resin and glass, and may be increased disadvantageously by post-cure. The effects of sizing (a cohesive binder to impart glass-strand integrity in order to improve handling properties of reinforcements) and coupling agents on the G/R bond was investigated by Throckmorton et al (43) using NOL rings and a constant deflection fatigue test method. Microphotographs showed G/R bond separations at about 0.2 micron from the glass surface, i.e. in the adhesive zone. No cracks were reported originating in bulk-phase resin nor through fracture of glass filaments. Loss of adhesion between bulk-resin and the filament surface was cited as the originator of stress failure, independent of fault zones caused by resin-lean areas (caused by glass "sized" in absence of vinyl silane coupling agents). Higher moduli and rigidity under cycling were observed for coupled filaments, but damage still initiated from the interfacial region. Broutman (44) reached similar conclusions based on compressive, compressive creep and compressive fatigue tests of filament FRP and tensile fatigue tests of crossply laminates (46).

Microcracking in stressed FRPs is primarily dependent on stress concentrations in the matrix between adjacent fibers and on resin brittleness. Kies (47) has shown on simplified composite models that the local strain amplification between fibers is directly proportional to the modulus ratio of fiber to matrix and inversely proportional to fiber separation. Cracks are also most often formed parallel to fibers which are perpendicular to the tensile load direction. Crack planes parallel to the applied force were rarely observed (40). Owen, Dukes, and Smith (45) have defined internal damage in FRPs as occurring in two stages. The first stage consists of separations of G/R bonds within fiber strands perpendicular to the load. This effect is intensified by the repetition or increase of the load. In mat or fabric laminates with relatively high resin contents, the next distinct stage is resin cracking, accompanied by debonding of fibers parallel to the load. In nonwoven glass laminates having relatively high resin contents, the second stage is delamination at ply interfaces. It may be noted that a numerical analysis of a square array of fibers in a brittle matrix reported in (45) supports the conclusions of (43) (47) and (42) in establishing importance of interfacial stresses and strain-and-stress concentration factors between fibers, as a function of fiber arrangement and density. The progression of cracking as determined by the direction of reinforcement has also been studied by Broutman and Sahu (46), using cross-ply epoxy laminates. They observed considerable cracking forming very early in sections which exposed the ends of fibers perpendicular to the load. The crack density increased rapidly, then reached a saturation value after a few hundred cycles. In sections where fibers parallel to the load were exposed for microscopic examination, cracks did not appear after one cycle and only traces of cracking were visible after a thousand cycles. After that a continual increase occurred until fatigue life was reached. At higher stress levels, cracks in this direction formed earlier. Thus cracking perpendicular to the applied stress gave little idea about progressive damage during fatigue, whereas cracking parallel to the applied stress could be used as a quantitative indicator of damage. On the basis of EM studies at 25,000 X, the crack propagation was characterized. Cracks first form in plies with fibers perpendicular to load, originating at the G/R interface in regions of high fiber density. The rate of formation and numbers depend on the stress level. Once formed these cracks tend to propogate throughout the width of the ply, extending to adjacent ply interfaces. Then propagation can continue along the interfaces or into the plies with fibers parallel to the load. Most of the delamination is observed to occur at a later stage. It is caused by large shear stresses at crack tips or tensile stress concentrations parallel to crack tips, where the cracks from transverse plies have their "leading edges" at the interface of adjacent longitudinal plies. The delamination itself, of course, can also initiate cracking (44), (46) due to transverse stresses caused in the matrix by load parallel to fibers. The magnification of such stresses is a function of the difference in Poisson's ratios of fiber and matrix (46). Fibers and ply interfaces were also observed to act as crack arresters or deflectors causing bunching of cracks (44). Visually, crack development may be noticeable in changes in colour of a stressed specimen. The specimen may become opaque or whitish even at the first application of load and this opacity may initially disappear during no-load or compressive parts of the loading cycle, but it gradually becomes permanent and intensifies until rupture.

Several techniques may be suggested to reduce or inhibit the formation of microcracking in FRPs (exclusive of using better coupling G/R agents or large design safety factors). Resin formulations giving more flexible matrices are a possibility, but the resulting loss of stiffness and very low moduli usually negate the advantages of using these FRPs. Another feasible though not often practical method would be to exercise strict control on filament or fiber ply spacing to minimize regions of high stress concentration. The most promising technique consists of toughening the resin matrix by a dispersed inclusion of elastomeric particles (40). This method is based on fracture phenomena in glassy polymers, where it has been observed that cold drawing and molecular orientation accompany the passage of cracks in layers several Angstroms thick on both fracture surfaces. The energy absorbed by these mechanisms is of order 100 X greater than that derived from simple covalent bond cleavage in the polymers. If fracture surface work (44) is defined as the amount of work required to create a new surface by the passage of a crack, it is apparent that for highly crosslinked epoxies and polyesters fracture surface work is decreased due to reduced mobility of their polymeric chains. High cross-link density will result in greater temperature resistance and produce higher moduli, but incurrs the penalty of increased susceptibility to crack propagation. The inhibiting influence on crack propagation of elastomeric particles in a resin matrix is due, therefore, to crazing, cold drawing and orientation in the adjacent resin phase prior to fracture. This absorbs considerable mechanical energy and impedes the progress of cracks (44). Triaxial stress fields set up in this way in the matrix induce crazing throughout a significant portion of the matrix volume, instead of confining it to thin layers on the fractured surfaces. This virtually eliminates the differential water absorption observed with crack propagation and has been observed to reduce modulus degradation by as much as an order of magnitude (41).

Let us now turn from the micro-mechanical to a macro-mechanical consideration of progressive damage in FRP laminates. McGarry and Willner (40) reported that if the fracture area in a stressed specimen becomes of the order 0.1% or more of the interface area, macroscopic effects can be observed as the material is mechanically deteriorating. Quantitative measurements of internal damage, which would also indicate the structural consequences, include weight gain immersion tests, monitoring of stiffness properties (modulus, Poisson's ratio) throughout a test, evaluation of mechanical hysterisis and various acoustical, ultrasonic (48) and X-ray techniques presently under development.

The early work of Chambers, McGarry and Desai (39), (36), (38) was based on simple absorption tests and interply strain measurements using bonded electric foil gages. One-cycle load-unload tests revealed that the tensile stress-strain curve can be approximated by two straight lines, intersecting at a point called the "knee", leading to a definition of primary and secondary moduli for the material. Similar characteristics were obtained by Broutman (46) for cross-ply laminates and Owen et al (45) for chopped-strand-mat composites. For cloth-reinforced FRPs Chambers (36) found that in the first tensile unloading, the modulus was less than the initial but greater than the secondary. No changes in compressive modulus occurred throughout the entire loading cycle. Hysterisis decreased or disappeared upon subsequent loadings, however, and both moduli continued to decrease and approach the compressive modulus in value. One-cycle bending tests showed a strain distribution that was approximately linear until the outer 2/6 of beam thickness, where strains became slightly magnified. It was postulated that partial tensile failure controls flexural behavior, because as the stiffness of the tensile portion of the beam was being reduced by increasing or repeating loads, the neutral axis was observed to shift towards the compressive face, and exposed an ever-greater volume of the beam to tensile strains and stresses. The volume of material at a particular stress was also cited by Broutman (44) as an important factor in compressive strength evaluation. The internal damage appeared to be irreversible and hysterisis measurements indicated that most, though not all, of the mechanical degradation is accomplished during the first cycle. From water absorption tests, it became clear that specimens stressed in tension past the "knee" absorb more water, leading to the conclusion that the internal degradation consists of fine fractures in the resin or at the G/R interface. This was, of course, later elaborated on in more detailed studies (40), (41), (44), (45), (46), and may be summarized as follows (46). The primary modulus (measured at the origin of σ-ε curve) decreases continuously until the end of fatigue life. Cracks develop during the first cycle if there are fibers oriented at 90^{o} to the tensile load axis and if the stress is greater than at the knee of the stress-strain curve. Cracks along fibers parallel to the stress direction will form if the stress is much higher, e.g. 75% of ultimate. These increase very rapidly with the number of cycles, then the rate becomes constant until the last stage of rapid increase. Crack density in plies at 90^{o} to the stress direction reaches a maximum value approximately during the first 1% of fatigue life. The residual strength of the FRP under fluctuating tension decreases with number of cycles until it equals the cyclic fatigue stress at which time failure occurs. This is shown schematically in Figure 5 (46). The rate of decrease depends on the stress range during the cycle. When the cyclic stress imposed on an FRP is near or below the knee, then after any number of cycles, the knee will reappear in a σ-ε curve, i.e. when the material is loaded in tension to failure. If a higher stress level is used, the knee will not appear even after a small number of cycles. Broutman (46) also measured a slight increase in the secondary modulus during the initial part of fatigue life, and a similar increase in the primary modulus after a sharp initial decrease. Both moduli were then observed to decrease slowly until failure. This occurred in cases where the knee disappeared from the original σ-ε curve after one cycle so that the secondary modulus after the first cycle was actually measured (by interrupting the fatigue test) at the origin of a σ-ε curve. Broutman offers as a partial explanation for this phenomenon the saturation with cracks in the direction perpendicular to the load, if the applied stress is greater than that at the knee, with some recovery occurring at the first unloading. Owen et al (45), however, reported steady degradation of modulus of mat FRPs with repeated loadings, and related the damage to the loss in modulus quantitatively. Debonding at the G/R interfaces was observed to correspond to about 2.5% loss as measured in simple tensile tests, and onset of resin cracking (in the bulk phase) to about 8 - 10% loss. These criteria were used to define failure in fatigue tests, and consequently banded SN diagrams were produced, as shown schematically in Figure 6 (45). Debonding and cracking regions appear to merge. At the onset of resin cracking in fatigue, the residual strength is only slightly lower than the original ultimate tensile strength. Another interesting relationship showing strength retained as a function of original properties and fatigue life was proposed by Broutman (46). Plotting ($\sigma_{max}/\sigma_{UTS}$) vs. the remaining static strength after cycling, i.e. $\sigma^*_{UTS}/\sigma_{UTS}$, on a percentage scale, it was found that for various numbers of cycles, expressed as percentages of fatigue life, the relationships were linear and converged at 100%, as shown in Figure 7 (46). The implication is that one could predict the static strength after a given % of fatigue life (at all stress levels) by testing simply one specimen for ultimate tensile strength after cycling it for the given % of life at one stress level.

In rigorous analysis, both shear and normal stresses contribute to total deflection of flexural members. Having discussed the micro and macro behavior of FRP laminates primarily under uniaxial tensile and compressive loadings, and having postulated that partial tensile failure controls flexural behavior, it is appropriate to consider the effects of shear on flexural properties also. In an early exploratory paper, Chambers (39) remarked that if severe shear stresses were imposed on the resin phase of a typical laminate (by appropriate orientation of load with respect to the arrangement of reinforcement) the resin may not be relied upon to fully transfer distortions and therefore stresses from a given ply to adjacent plies, leading to relative ply displacements and marked deviation from ideal laminate theory. Under less contrived conditions and with orthotropic cloth reinforcement in tensile tests, this effect did not appear to be significant because a relatively large percentage of the reinforcement was parallel to the load direction, but a definite influence of shear on flexural modulus was consistently observed in later investigations (37). Pure bending was applied to the central portion of laminate beams by quarter-point loading, producing no shear between the points of load application. This was compared to simple midspan-point loading of similar beams. The influence of shear on flexural modulus was shown by loss of beam stiffness as span-depth ratio was decreased, or conversely, as span/depth ratio was increased, the apparent (simple bending) modulus E_{BA} asymptotically approached true (pure bending - no shear) modulus E_{BT}, which was independent of the span depth ratio. Values of E_{BT} corresponded to the averages of the tensile and compressive moduli of the material, provided these were not greatly different. Shear in simple bending (as per ASTM span/depth specifications) was observed to reduce the flexural modulus measured, the magnitude being dependent on laminate characteristics. For the centrally loaded beams, failures usually occurred by buckling delamination of compressive fibers near the loading roller. For quarter-point loaded beams (no shear in the central portion) failures consisted of compressive delaminations of the specimens throughout the central half-span. The interlaminar shear modulus was observed to be essentially that of the resin, leading to the postulate that the stiffness of the laminate perpendicular to the thickness depends on stiffness of the resin component as a first approximation, with fabric/resin interaction having an effect as yet undetermined. Uniaxial compressive strengths were similar to flexural strengths in pure bending. Thus the simple calculation of flexural stresses at failure is open to question on two counts - shift of the neutral axis due to progressive reduction of the tensile modulus with repeated or increased stresses, and the pronounced effect of the low shear modulus of resins on E_{BA}. Shear may also contribute to the apparently lower moduli observed in tension, as compared to flexure (39). Tractive forces applied to a tensile specimen through grip friction may also cause significantly higher strains in the outermost fibers.

3. Experimental Program

3.1 Design of the Experiment

Structural fatigue tests are usually expensive and time-consuming and, in general, relatively few specimens are tested. It is, therefore, necessary to design the fatigue testing program using standardized specimens in the most efficient manner to permit extraction of a maximum in meaningful data with statistically defined confidence. We have already seen the complexity and multitude of factors affecting the fatigue performance of FRP laminates, and therefore make a selection of variables consistent with the aims set forth in sec. 1.3. This project studies the effects of the following on fatigue performance of the FRP laminate chosen for study (see also sec. 3.2):

1. Loading mode:
   - (a) Unaxial Tension
   - (b) Simple Flexure (midpoint loading)
2. Percent of fiber reinforcement, by weight:
   - (a) 56% (nominally 60%)
   - (b) 42% (nominally 40%)
3. Stress pattern in cyclic loading to 80%, 60% and 40% of ultimate:
   - (a) Minimum stress = 0
   - (b) Minimum stress = 20% of ultimate

Considering the three mentioned variables each at two "levels", the project may be regarded most efficiently as a 2^3 factorial experiment (49), wherein the effects of the factors are investigated simultaneously. The compact factorial approach is particularly advantageous to this subject because the effects of the factors are not independent of each other. In order to conduct an experiment on a single factor, e.g. A, some decision must be made about the levels of other factors B, C, D, etc. that are to be used in the experiment. Such a "single-factor" experiment reveals the effects of A on the desired property, e.g. fatigue life, for this particular combination of B, C, D, etc., but no information is provided for predicting the effects of A with any other combination. With a factorial approach, on the other hand, the effects of any variable, e.g. A, are examined for every combination of B, C, D, etc. that is included in the experiment. Thus much information is accumulated both about the effects of the factors and their interrelationships or interactions, by making use of a formal statistical analysis of variance on quantitative characterizations of performance taken from experimental data. This systemized method for the factorial design used is considered in greater detail in sec. 4. In this section the physical scope of the project is delineated.

The 2^3 factorial design described above consists of eight fatigue test series or treatments. Let the integer 1 denote the "lower" (a) level of all parameters and lower case letters t, f, and s the "higher" (b) levels of mode, reinforcement and minimum stress respectively. Now if we let products of 1's and letters represent combinations of test parameters, the eight series may be conveniently abbreviated as:

Series	Loading Mode	% fiberglass, by wt.	Minimum stress, % ult.
1	Tension	42	0
t	Flexure	42	0
s	Tension	42	20
ts	Flexure	42	20
f	Tension	56	0
tf	Flexure	56	0

Series	Loading Mode	% fiberglass, by wt.	Minimum stress, % ult.
fs	Tension	56	20
tfs	Flexure	56	20

For each series, several specimens were tested quasi-statically to determine elastic moduli, Poisson's ratios, and ultimate strengths. These are, of course, the 100% of ultimate tests that yielded the stress-strain and lateral vs. longitudinal strain curves presented in sec. 3.4. They are analyzed in sec. 4 as a 2^2 factorial experiment with a replication factor of two, since the "minimum stress" variable quite naturally has no meaning in this case. Each one of the eight fatigue series consisted of running about five specimens at each of 80% and 60%, and generally one at 40% (due to prohibitively long test times) of the ultimate strengths to produce the conventional stress vs. $\log^N$(cycles-to-failure) curves or so-called SN diagrams. Straight lines were fitted to the data using a one-degree polynomial regression program (see sec. 4.2). Monitoring the transverse and longitudinal strains (see sec. 3.3) for the fatigue tests also enabled moduli and Poisson's ratios to be plotted against log N to yield information on progressive loss of strength and stiffness (see sec. 4).

All tests were conducted at room temperature ($73^oF \pm 5^oF$) in an air-conditioned laboratory. To simulate a possibly critical environment, all fatigue tests were run with the specimens submerged in tap water at the ambient temperature. Effects of moisture absorption have been discussed in sec. 2.1b. The water bath can be supposed to have one beneficial effect, however, in acting as a dissipating medium for the hysterisis heat generated in cycling. The effects of the test variables (strain rate, frequency) are discussed in sec. 3.3.

3.2 Specimen Manufacture and Preparation

The laminate chosen for the investigation was manufactured by Panomer Ltd. of Montreal. It consists of 16 plies of commercial F-80 polyester resin and 181-weave fiberglass cloth, prepared as a 3' x 3' sheet by the hand lay-up process. The required glass/resin ratio was achieved by spreading weighed quantities of resin between plies of fabric. Sheets thicknesses were about 0.20 to 0.25 depending on the composition. The exact compositions of the two types of laminates ordered were determined in accordance with A.S.T.M. specification D2584-D68, "Standard Method of Test for Ignition Loss of Cured Reinforced Resins". Values of 42% and 56% fiberglass by weight were recorded for nominal %'s of 40% and 60% respectively.

Tensile specimens with warp direction along the major axis were formed by a Tensil-Kut (Reg. T.M., USA) machine from strips 3/4" wide cut from the sheets using a high-speed band saw. The dimensions are in accordance with A.S.T.M. specification D638-68, "Standard Method of Test for Tensile Properties of Plastics", producing a central portion 0.50" wide (Type I). The grip sections were made slightly longer to ensure a good fit into the Instron. Tensil-Kut is a high speed contour milling machine and achieves machining by a series of light cuts with a carbide tool rotating at 20,000 RPM. The individual depths of cut are adjustable from 0.0005" to 0.250" by a precision micrometer screw and combined with the high RPM achieve a very low chip load and reduce cutting pressures to a minimum, producing machined edges, within configuration tolerances of ±0.0005", free of distorsion or heat deformation. Heavier cuts were used for roughing the specimen while light cuts were used for finishing. The laminate strip was clamped in the master template for ASTM Tensile Specimen Type I and manually moved across the Tensil-Kut table for the milling process. The Tensil-Kut machine and templates are shown in

Figure 8 and the tensile specimen in Figure 9.

Flexural specimens were laminate strips or beams 3/4" wide x 5" long, for testing flatwise on a 4" span, in the simply-supported, single mid-span-point-load mode. Roller supports and a rounded loading nose were used. The dimensions of specimens, rollers and nose conform to ASTM specification D790-66, "Standard Method of Test for Flexural Properties of Plastics". The strips were cut on a bandsaw and finished on the Tensil-Kut using precision-machined spacing blocks and bars. The spacers and bars are shown in Figure 8 (bottom) and the flexural test specimen in Figure 9.

Dimensional quality control checks were made on all specimen batches, based on a $\pm 3\%$ deviation from the mean cross-sectional area. This lead to the rejection of several specimens per batch, the thickness producing the major variation. Quality checks using densities, void contents or ignition loss measurements were not made on a large scale because material properties were observed to be quite consistent in the limited number of such tests that were performed to determine the compositions.

All specimens were conditioned prior to testing in accordance with ASTM specification D618, Procedure D. This consisted of soaking the specimens in distilled water for the 24 hours immediately preceding the test, at a temperature of $23^{\circ}C$ (i.e. room temperature). Specimens intended for ultimate strength determinations were lightly wiped of excess moisture and tested in air.

3.3 Testing Equipment and Procedures

The hydraulic-drive testing machine used for both static and dynamic tests was the Instron Model TK-50, shown in Figure 10. It has a maximum load capability of 50 kips in tension, cross-head speeds ranging from 0.0005 to 10.0 inches/min., chart speeds from 1.0 to 50.0 inches/min., a two pen (load and strain) recorder of maximum sensitivity 100 lbs. full-scale deflection, or 10 lbs./inch. The recorder can also be used as an X-Y plotter. The Instron has cycling controls and counter, and mechanical limit switches for motion of the crosshead. Cross-head displacement (with respect to a chosen and preset gage length), specimen strain (measured by a clip-on extensometer connected to one recorder pen), and applied load (tensile or compressive) can all be cycled between preset limits either manually or automatically using cams and electric switches in the load-cell activated pen circuit. Of course not all parameters can be controlled concurrently. Fatigue testing for this project made use of the load-monitoring facility, i.e. cycling between constant loads of 0 (or 20%) to 40%, 60%, or 80%s of ultimate. Good accuracy (about ±2% of nominal load) was obtained throughout. For any particular set of tests, the limits of cycling were calibrated using a dummy specimen to achieve the required accuracy. The tensile and flexural apparati used for testing under water are shown in Figures 11 and 12 respectively.

Longitudinal and lateral strains were measured using the Sanborn 320 and Hewlett-Packard 7100B two-channel strip-chart recorders. The latter is a particularly sensitive instrument, capable of a 5mV full scale deflection, or 0.5 mV/inch sensitivity, to 100V full scale, or 10V/inch. The 7100B has chart speeds ranging from 1 inch/hr. to 2 inches/sec. The maximum sensitivity of the 320 is 0.5mV/mm, and it has a top chart speed of 1mm/sec. Both were judged accurate and sensitive enough for the measurements required and only availability dictated use of one or the other. The strain-sensing devices were polyester-backed electrical-resistance bonded strain gages, manufactured by Tokyo Sokki Kenkyujo Co. Ltd., TML types PL-5 and PS-5, connected to the bridge circuit, regulated DC power supply and recorder as shown in Figure 13. Eastman 9-10 was the bonding agent used. The gages were effective up to about 10,000 cycles maximum at low stress levels. Water proofing the gages and lead wires with beeswax proved to be an economic and very satisfactory technique, since not only protection but the ductility required for cyclic loadings was achieved. The two gages (one longitudinal, one transverse to the axis of major stress) on the flexural specimen were mounted on the tension face at the quarter-spans (i.e. one inch on either side of center), rather than close together at midlength as on the tensile specimens. This was done because it was found that a small offset resulted in the necessity to apply large (and uncertain) correction factors due to the relatively small span length. Furthermore, check tests run on five specimens revealed that quarter-span strain measurements were indeed 0.50 of those at midspan up to about 45% of ultimate, and fell only to about 0.46 near the ultimate strength. Strains and load were monitored continuously for about 1000 cycles and periodically thereafter for the 60% and 40% tests and continuously for the short 80% cyclic tests. Moduli and Poisson's ratios were calculated directly from the cyclic load and strain records, rather than from static tests on specimens taken from interrupted fatigue tests, and hence may be termed "dynamic". From these data modulus and Poisson's ratio vs. log N plots were generated.

The fixed and limited range of crosshead speeds available produced certain differences in strain rates for the tensile and flexural tests. The rates have been calculated for the speeds used from the strain-time recordings and typical values are as follows:

		Crosshead Speed	Strain Rate
Static tests:	Tension	0.2 ipm	0.015 in/in/min.
	Flexure	0.2 ipm	0.012 in/in/min.
Dynamic tests:	Tension	5.0 ipm	0.265 in/in/min.
	Flexure	10.0 ipm	0.505 in/in/min.

The 10 ipm was chosen for flexural fatigue tests because it enables low-stress level tests to be performed in a reasonably short time at a frequency comparable to that in tensile tests at 5.0 ipm. Since the deflection at midspan required to produce a small strain is relatively large compared to the direct relationship of extension and strain in tensile tests, the same crosshead speed for both would have resulted in inordinately long testing times in flexure. However, the differences were judged to be insignificant, because the values were of the same order of magnitude (see sec. 2.1c).

The frequencies in all series were predetermined by both crosshead speed and the desired amplitude of load. The typical ranges presented below are quite low compared to early US practice (1800, 900 cpm) and common British values (30 - 724 cpm) but are realistic in terms of structural applications of loads.

	Frequencies, cpm	
Stress Range, %'s ult.	Tension	Flexure
0 - 80	20 - 25	15 - 25
20 - 80	33 - 35	30
0 - 60	30 - 34	20 - 30
20 - 60	55 - 60	47 - 65
0 - 40	47 - 50	37 - 45
20 - 40*	54 - 70	54 - 75

*Crosshead speed was reduced to 2.0 ipm in Tension, 5.0 ipm in flex.

The differences were considered insignificant for reasons similar to those cited in the discussion of strain rates (see sec. 2.1c).

3.4 Results

In summary, five curves represent the "untreated" output of each of the eight series, which include the 2^3 factorial design of fatigue tests and the 2^2 factorial design (with replication 2) of the quasi-static tests. These relationships are given symbolically as:

1. $\sigma_{1max}/\sigma_{1ultimate}$ vs. log N (SN curves)*
2. σ_1 vs. ε_1 (stress-strain curves)
3. ε_2 vs. ε_1 (Poissons ratio curves)
4. E/E_0 vs. log N (Modulus retention)
5. μ/μ_0 vs. log N (Poisson's ratio retention)

The graphs showing these relationships for the series are appended as Figures 14 - 53. In some cases not all experimental points are actually plotted to avoid congestion and improve clarity. Characteristics for the analysis of variance that follows are taken from relations 2 and 3. Progressive damage and residual strength are discussed qualitatively in terms of 1, 4 and 5. The investigation is termed low-cycle because low-frequencies have been used for the fatigue tests and attention is concentrated on the fatigue life range up to 100,000 cycles only.

*Subscript 1 denotes principal stress or strain
Subscript 2 denotes transverse stress or strain
Subscript o denotes original value

4. Analysis of Experimental Data

4.1 Quasi-static Tests

The stress-strain curves for the eight test series are shown in Figures 15, 20, 25, 30, 35, 40, 45, 50, and the strain relationships determining Poisson's ratios, derived from the same quasi-static tests, are shown in Figures 16, 21, 26, 31, 36, 41, 46, 51. Data for the four series in which a minimum stress of 20% of ultimate was imposed during the cyclic tests form an experimental replicate of the values obtained in the other four series. The results of the quasi-static tests are conveniently summarized in the Table below.

Table 1 Quasi-static Test Data

	56% fiberglass		42% fiberglass		
	Tension	Flexure	Tension	Flexure	
Primary modulus, psi x 10^6	2.50 2.50	3.10 2.90	2.00 2.00	2.10 2.10	replicate 1 replicate 2
Secondary modulus, psi x 10^6	2.04 1.96	2.45 2.40	1.20 1.20	1.80 1.70	r 1 r 2
Stress at the "knee", % of ult.	39.0 28.0	21.0 24.0	40.0 37.0	22.0 22.0	r 1 r 2
Ultimate strength, ksi	38.0 36.0	51.6 48.0	26.7 26.7	41.0 41.0	r 1 r 2
Primary Poisson's ratio	0.150 0.140	0.133 0.131	0.150 0.150	0.150 0.150	r 1 r 2
Secondary Poisson's ratio	0.087 0.084	0.100 0.097	0.086 0.095	0.110 0.120	r 1 r 2

It may be observed from the graphs that the two laminates tested (56 and 42% fiberglass) exhibit the characteristic dual moduli, which are also reflected in the graphs showing longitudinal vs. lateral strains. The first linear portion of a typical stress-strain curve represents polyester matrix and fiberglass reinforcement acting as a cohesive unit; the "knee" represents the onset of significant resin cracking; the final linear portion represents a lower modulus due to the loss of internal structural integrity of the composite (i.e. loss of binding action by the resin). In this region the glass fibers may be assumed to carry most of the load and hence determine the material's response. From Table 1, it is apparent that in the flexural mode both primary and secondary moduli and ultimate strength are considerably higher, whereas no definite pattern is discernible for Poisson's ratios.

To define the effects of testing mode and percent reinforcement in a statistical manner, the data in Table 1 were regarded as a randomized complete block factorial experiment (2 factors at 2 levels each, the entire experiment being replicated twice and the order of treatment or factor combination being randomly chosen (51)). The analysis of variance was performed using the McGill University Computer Center's Scientific Subroutine Package (SSP) program ANOVA, with only slight format modifications (see Appendix B). The printed output of the program for each problem (i.e. primary modulus, secondary modulus, etc ...) included the numbers of levels of each factor (supplied in input data), the mean of all data in the set, a list of sources of variation (main effects and interactions), and the corresponding sums of squares, degrees of freedom and mean squares. The outputs are summarized in Table 2. For a detailed account of the theory underlying ANOVA, reference should be made to (50), (51). To complete the analysis of variance from these standard tables, it was necessary to pool certain elements (sources of variation) into an error variance term. In a randomized complete block, it is assumed that there is no interaction between replicates and treatments, and that any such interactions are in fact confounded in the error term (51). Thus if the factors are designated as T (test mode), F (percent fiberglass), S (minimum stress level) and R (replication), the mean squares from the ANOVA table which are combined to produce the error variance are T x R, F x R and T x F x R. The degrees of freedom for these interactions must also be added to give the degrees of freedom of the error term. The mean squares for the other factors and interactions are then divided by the error term to yield the F values commonly used in testing statistical significance at given confidence limits. In this case the reference F values were (50):

$$F_{5\%,1,3} = 10.1 \qquad F_{1\%,1,3} = 34.1$$

Comparing the F values calculated in Table 2 with the ones above, the effects of the factors T, F and R may be analyzed.

For the primary modulus, only the effect of fiberglass content was significant at the 1% level, but both fiberglass content and test mode became significant at the 5% level. For the secondary modulus T and F were significant at both 1% and 5%, but F much more so. Thus the F factor had a highly significant effect on the static moduli, a decrease in fiberglass content of 14% leading to an average decrease in moduli of about 30%. The flexural mode of test (T factor) produced an average increase of 23% in moduli.

No factors were found significant for the stress at the knee, expressed as a % of the ultimate stress, for the chosen confidence limits, but based on the calculated F values, test mode had by far the most pronounced effect at F = 6.95, the tensile tests producing the knee at higher %'s of ultimate.

Table 2 ANOVA for Quasi-static Tests

Levels of Factors

T	2
F	2
R	2

	Source of Variation	Degrees of Freedom	Mean Squares	F Values
Primary Modulus	T	1	0.180	12.00
	F	1	0.980	65.33
	TF	1	0.080	5.33
	R	1	0.005	0.33
	TR + FR + TFR	3	0.015	-
Secondary Modulus	T	1	0.475	158.33
	F	1	1.088	362.67
	TF	1	0.008	2.76
	R	1	0.007	2.33
	TR + FR + TFR	3	0.003	-
Stress at "Knee"	T	1	378.13	6.95
	F	1	10.13	0.19
	TF	1	15.13	0.29
	R	1	15.13	0.29
	TR + FR + TFR	3	54.38	-
Ultimate Strength	T	1	367.20	80.53
	F	1	182.40	40.00
	TF	1	1.13	0.25
	R	1	3.92	0.86
	TR + FR + TFR	3	4.56	-
Primary Poisson's Ratio	T	1	0.00008	2.00
	F	1	0.00026	6.50
	TF	1	0.0008	2.00
	R	1	0.0002	0.50
	TR + FR + TFR	3	0.0004	-
Secondary Poisson's Ratio	T	1	0.00070	8.75
	F	1	0.00023	2.88
	TF	1	0.00007	0.88
	R	1	0.00002	0.25
	TR + FR + TFR	3	0.00008	-

Ultimate strength was found to be significantly affected by both T and F factors at 1% and 5%, test mode being about twice as significant as fiberglass content. Flexure tests yielded values about 44% higher on average.

Values of Poisson's ratios showed no definite dependence on any of the factors or interactions at both confidence limits.

4.2 Fatigue Tests

The fatigue life or SN curves were developed as described in sec. 3.1. To fit curves to the eight sets of data points values of ($\sigma_{max}/\sigma_{ult}$) expressed as a percentage were used as Y and log N as X in a SSP library program called POLRG (Polynomial Regression) (see Appendix B). This routine generates powers of an independent variable to calculate polynomials of successively increasing degrees. If there is no reduction in the residual sum of squares between two successive degrees of polynomials the problem is terminated before completing the analysis for the highest degree polynomial specified (up to 10th degree). Following the usual practice of representing SN data by straight lines on a semi-logarithmic plot, only the first degree polynomial fit was made. Regression coefficients in such a case are of course the Y intercept and slope. The eight SN diagrams are shown in Figures 14, 19, 24, 29, 34, 39, 44 and 49. The ratio ($\sigma_{max}/\sigma_{ult}$) was now taken as the allowable stress, % of ultimate, for a life of N cycles. Based on the generated lines, values were calculated for 10, 10^2, 10^3, 10^4 and 10^5 cycles and the results are shown in Table 3.

Since the fatigue life data (2^3 factorial experiment as described in sec. 3.1) has a replication factor of only 1, it was not possible to use ANOVA as was done previously. In a factorial analysis of variance for single replication all interactions are confounded with the error term (51).

Table 3 Fatigue Life Data

		56% fiberglass		42% fiberglass	
		Tension	Flexure	Tension	Flexure
% reduction per decade of N (slope of SN)	0% min. stress	13.27	12.50	12.98	10.60
	20% " "	12.85	10.40	12.82	12.52
	Allowable stresses, %'s of ultimate, for lives of N				
Number of Cycles 10	0% min. stress	92.88	94.10	91.71	85.02
	20% " "	94.86	94.72	94.79	97.72
10^2	0% " "	79.61	81.59	78.73	74.42
	20% " "	82.01	84.32	81.97	85.20
10^3	0% " "	66.34	69.08	65.75	63.82
	20% " "	69.16	73.92	69.15	72.68
10^4	0% " "	53.07	56.57	52.77	53.22
	20% " "	56.31	63.52	56.33	60.16
10^5	0% " "	39.80	44.06	39.79	42.62
	20% " "	43.46	53.12	43.51	47.64

In order to obtain an estimate of the error, some independent information may be used, or higher order interactions must be pooled into the experimental error variance. For the 2^3 design used this would require the unfounded assumption (in the absence of substantiating external data) that no second order interactions exist (51) since the only interactions available are TF, TS, FS and TFS. This method is thus only appropriate for larger numbers of factors (say 2^4 or 2^5) where the presence of higher order interactions is much more unlikely, so that it is fairly conservative to assume no four-way, five-way, etc. interactions. Even if these were present, they would be difficult to explain in practical terms. For these reasons the data of Table 3 were analyzed in a quantitative graphical manner as outlined below.

To observe the effect of each of the main factors T, F and S on the values of Table 3, four data sets from the eight available series may be compared for any given factor. For example the test mode difference can be studied using four Flexure/Tension pairings, i.e. for F = 56, S = 20; F = 56, S = 0; F = 42, S = 20; and F = 42, S = 0. The comparisons were made by taking ratios of the tabulated values for the two levels of the main factors. In the test mode example, since flexural values were predominantly greater than tensile values, the ratio was (% allowable stress in flexure/% allowable stress in tension) for a given N, with the other factors F and S being consecutively those for the four combinations given above. The ratios were then plotted vs. N to indicate trends in the factor effects. The results of these analyses are presented in Figures 54, 55 and 56. From the diagrams several general relationships may be deduced:

(1) The ratio of allowable stress in flexure to allowable stress in tension was generally $>$ 1.0 (the exception being the F = 42, S = 0 combination up to 5000 cycles) for a given N. The trend was consistently more pronounced with increasing N, and the ratio reached a maximum of about 1.22 at 10^5 cycles. A significant T x S interaction is indicated since the combinations with 20% of ultimate minimum stress levels yielded higher ratios than those with the 0% level.

(2) The ratio of allowable stress for the 20% of ultimate minimum level to that for the 0% minimum level was $>$ 1.0 in all cases. On the average this S effect was greater than the T effect discussed in (1), especially in the medium range of N. Here a likely T x S interaction was again indicated as the S effect was considerably greater for combinations with the flexural mode.

(3) The fiberglass (F) effect was less pronounced than either the T or S effect, the maximum ratios reaching about 1.10. In general, the higher fiberglass content produced greater allowable stresses; the differences tended to be more significant at low values of N, and also greater for the flexural mode, pointing to the presence of the T x F interaction.

To conclude this section it must be noted that the SN curves showed the scatter that is to be expected in fatigue testing of brittle materials such as FRPs, but the differences noted between curves in absolute values were not very great (i.e. max. ratio $\sim$ 1.20). Hence the trends of the major T, S and F effects must be regarded in light of the scatter and marginal overlap of data points. Furthermore the actual 14% difference in fiberglass contents, compared to the 20% based on 40% and 60% contents nominally supplied by the manufacturer, may not have been sufficiently large to produce effects comparable to those of test mode (i.e. stress distribution) and minimum stress level. Finally, the converging trend of most of the positive ratio curves at large N values suggests that the interactions present are more effective early in the fatigue life rather than at later stages. This may be due to the decreased importance of the F factor, hence also the TF and FS interactions, with increasing N.

4.3 Changes in Mechanical Properties with Time

The strength retention characteristics of the FRPs tested were derived from monitored stresses and strains as described in sec. 3.3 and sec. 3.4. The normalized ratios E/E_0 (Modulus at N/Initial Modulus) and μ/μ_0 (Poisson's ratio at N/Initial Poisson's ratio) plotted against N are given in Figures 17, 22, 27, 32, 37, 42, 47, 52 and Figures 18, 23, 28, 33, 38, 43, 48, 53 respectively. All experimental points are not shown in order to improve clarity of the graphs. The average initial values (for N = 1) are presented in Table 4 below. Ranges rather than averages are reported for Poisson's ratios due to the scatter and overlap observed for this parameter. The approach seems justified in the light of the significance tests in sec. 4.1.

Table 4 Initial Values of Fatigue Test Moduli and Poisson's Ratios

Moduli, psi x 10^6					
Max. Stress (% ultimate)	Min. Stress (% ultimate)	56% fiberglass		42% fiberglass	
		Tension	Flexure	Tension	Flexure
40	0	2.86	2.70	2.10	2.09
	20	2.85	2.95	2.00	2.02
60	0	2.70	2.70	1.65	2.00
	20	2.60	2.95	1.62	1.85
80	0	2.65	2.70	1.45	1.95
	20	2.45	2.85	1.45	1.85
Poisson's Ratios					
Max. Value	0	0.160	0.166	0.155	0.185
	20	0.174	0.183	0.159	0.166
Min. Value	0	0.115	0.125	0.088	0.130
	20	0.112	0.125	0.087	0.134

With increasing maximum stress, moduli values were perceptably lower in tension, but little difference was observed in flexure. For 56% fiberglass content, most values fell well within 10% of the quasi-static moduli values and for the 42% fiberglass content the correspondence was much closer. No value of fatigue test modulus fell below the corresponding value of the secondary quasi-static modulus.

The ratio E/E_0 may be regarded as the % strength remaining for any particular N. Based on the experimental curves, the values for 10, 50, 100, 500, 1000, 5000 and 10,000 cycles (higher N only at lower maximum stresses of course) are shown in Table 5 below. Table 6 presents percentages of Poisson's Ratio retained for various numbers of cycles. In a few cases extrapolation was considered reasonable and such values are shown in brackets. Even though 3 to 6 stress-strain recordings, i.e. tests, were run for a given curve, they were regarded as essential to define with confidence that one curve and cannot be regarded as true replicates, i.e. repetitions of the entire experiment. Thus an analysis similar to the one for SN data (see sec. 4.2) was performed on the data of Tables 5 and 6. The graphical results for modulus ratios are presented in Figures 57, 59, 61 for the 40% maximum stress level and in Figures 58, 60, 62 for the 60% level. Figures 63, 65, 67 and 64, 66, 68 show the Poisson's ratio graphical analysis for the 40% and 60% levels respectively. Due to the short lives obtained at the 80% level, ratios for this level were not plotted vs. N. However, it can be seen from the limited data that trends are similar to those observed at lower levels.

Two general observations may be made regarding the E/E_o and μ/μ_o data. In almost all cases, there is a marked difference between the curves at 40 and 60% of ultimate maximum stress levels and between the 60 and 80% levels, the degradation (or negative slope) of the curves being progressively accentuated by increasing values of maximum stress. There is some evidence from the 40% plots, however, that after a large number of cycles the rate of degradation diminishes considerably and that the E/E_o and μ/μ_o ratios may in fact approach nearly constant values. Secondly, it is obvious from Tables 5 and 6 and the graphs that the effects of the factors T, F and S are reflected more distinctly and strongly in the changes in mechanical properties (E and μ) than in the fatigue lives (SN data).

Table 5 Percentages of Modulus Retained for Numbers of Cycles N

		Max. stress 40% ult.				Max. stress 60% ult.				Max. stress 80% ult.			
		56% fg.		42% fg.		56% fg.		42% fg.		56% fg.		42% fg.	
Cycles	Min. stress % ult.	Tension	Flexure	Tension	Flexure	Tension	Flexure	Tension	Flexure	Tension	Flexure	Tension	Flexure
10	0	94.0	99.0	96.0	98.0	91.0	95.0	88.0	96.0	86.0	95.0	84.0	95.0
	20	97.0	99.0	97.0	99.0	96.0	97.0	94.5	97.0	95.0	97.0	92.0	96.5
50	0	89.0	97.0	84.0	98.0	81.0	87.0	70.0	92.0	-	87.0	-	86.0
	20	95.0	98.0	91.0	98.5	92.0	94.0	84.0	93.5	87.0	92.5	77.0	91.0
100	0	85.0	96.0	77.0	98.0	75.0	80.0	61.0	88.0	-	80.0	-	78.0
	20	93.0	97.5	89.0	98.0	88.0	93.0	77.0	91.0	-	88.0	(67.0)	87.0
500	0	70.0	88.0	56.0	94.0	57.0	60.0	(34.0)	66.0	-	60.0	-	-
	20	87.0	96.0	85.0	97.0	73.0	89.0	43.0	81.0	-	69.0	-	69.0
1000	0	60.0	84.0	47.0	88.0	-	50.0	-	-	-	50.0	-	-
	20	84.0	95.0	84.0	96.0	65.0	86.0	-	(75.0)	-	-	-	-
5000	0	47.0	69.0	(27.0)	67.0								
	20	75.0	94.0	80.0	94.0		85.0						
10000	0	46.5	66.0	-	(61.0)								
	20	68.0	93.0	77.0	93.5								

Table 6 Percentages of Poisson's Ratio Retained for Numbers of Cycles N

		Max. stress 40% ult.				Max. stress 60% ult.				Max. stress 80% ult.			
		56% fg.		42% fg.		56% fg.		42% fg.		56% fg.		42% fg.	
Cycles	Min. stress % ult.	Tension	Flexure	Tension	Flexure	Tension	Flexure	Tension	Flexure	Tension	Flexure	Tension	Flexure
10	0	94.5	98.0	90.5	98.0	90.0	97.0	81.5	95.0	87.0	93.5	81.0	93.5
	20	94.0	98.0	92.5	98.5	94.0	97.0	91.0	96.5	94.0	95.5	83.0	96.5
50	0	88.0	96.0	76.5	98.0	78.0	88.0	62.5	88.0	(61.0)	82.5	(63.0)	82.5
	20	90.0	96.5	85.0	96.5	87.0	92.0	75.0	93.0	80.0	89.0	63.0	92.0
100	0	83.0	93.5	69.0	97.5	91.0	81.0	53.0	83.0	47.0	74.0	(40.0)	73.0
	20	88.0	95.5	83.5	93.5	83.0	89.0	65.0	91.0	70.0	84.0	52.0	87.0
500	0	63.5	86.0	59.5	93.0	(51.0)	59.0	(27.0)	61.5	-	-	-	-
	20	83.0	92.0	80.0	83.0	66.5	85.0	39.0	80.0	-	(63.0)	-	67.5
1000	0	54.0	81.0	40.0	87.0	-	47.0	-	(50.0)				
	20	79.0	89.5	78.5	81.0	58.0	83.5	-	73.5				
5000	0	39.0	66.0	(24.5)	68.0								
	20	69.0	87.0	75.0	80.0	-	80.0	-	-				
10000	0	(38.0)	60.0	(20.0)	(62.0)								
	20	63.0	86.5	73.0	79.5								

Based on the graphical analysis of the ratios of "% modulus retained" for the effects of changes in test mode (T), minimum stress level (S) and fiberglass content (F), the following observations may be made:

(1) For any number of cycles, the % modulus retained in flexure was greater than that in tension (i.e. less degradation was apparent in flexure). This difference was more marked at higher values of N, the ratio reaching a maximum of about 2.5 in the F = 42, S = 0 case at 40% maximum stress and 5000 cycles. At the 40% max. level, the ratios for 0% minimum were consistently higher than those for the 20% minimum level. At the 60% maximum level, the tests with the 42% fiberglass material produced higher ratios than the tests with the 56% fiberglass content. This suggests the presence of both T x S and T x F interactions (see Figs. 57 and 58). The effect of amplitude and interactions will be discussed in sec. 5.

(2) For any number of cycles, the % modulus retained in tests with a minimum stress of 20% of ultimate was greater than the % retained in the tests with the 0% minimum stress level. At the 40% max. stress level this effect was not as apparent as the T effect at low values of N, but it was slightly more pronounced approaching the 10,000 cycle mark. The T effect was generally greater than the S effect at the 60% maximum stress level, i.e. when the amplitude increased. At the lesser amplitude (40% max.) a T x S interaction was apparent from the tensile tests (i.e. tensile tests yielded much higher ratios), but this trend was not manifested at the 60% maximum level. (See Figures 59 and 60.)

(3) The effect of fiberglass content was the least pronounced, although generally higher %'s of modulus were retained for the FRP with more reinforcement. The trends were mixed at the 40% maximum level, but T x F interaction became apparent from tensile tests in the plots with the 60% maximum stress

(tensile series again produced consistently higher ratios). (See Figs. 61 and 62.)

From individual stress-strain recordings, it was observed that the changes in Poisson's ratios were almost entirely a function of the changes in the longitudinal strains which naturally increased with N. Lateral strains reached peak values within the first few cycles and remained at almost constant values thereafter. Thus the plots of the T, F, and S effects, as determined by ratios of % μ retained for the two levels of these factors, reflect the same basic trends as the analysis for moduli at any particular constant amplitude of stress, i.e. less degradation is apparent in flexure, at a minimum stress level of 20% of ultimate, and generally for the material with the higher % of fiberglass reinforcement, all effects being generally greater at higher N values. In particular the following observations were made:

(1) The 0% minimum stress series produced a much greater T effect than the 20% minimum levels at the lesser stress amplitude, as was the case with the T effect on modulus ratios. The T effect was also similarly accentuated by the lower fiberglass content at the 60% maximum stress, i.e. greater amplitude. (See Figs. 63 and 64.)

(2) The S effect was less significant than the T effect at low N for both lesser and greater stress amplitudes. It was considerably greater coupled with the tensile mode at 40% maximum stress, and generally greater in tension at the 60% maximum stress. This parallels the trend in the analysis of modulus ratios. (See Figs. 65 and 66.)

(3) The 56% fiberglass content generally showed greater %'s of Poisson's ratio retained, but trends were somewhat mixed at the 40% maximum stress level and only one series produced consistently higher ratios with increasing N. At the 60% maximum stress level, tensile series yielded a much greater F

effect than did the flexural series, and an increase in ratios at higher N values became more apparent. Again the correspondence to the modulus ratio graphs is obvious. (See Figs. 67 and 68.)

This concludes the formal analysis of experimental results. The final chapter examines the observations made in sec. 4 in light of the FRPs material properties and fatigue behavior as discussed in sec. 2, and primary conclusions about the main effects and interactions are made.

4.4 Failure Modes

Figures 69 and 70 show typical failure modes in tension and flexure respectively. The predominant pattern in tension was that of brittle fracture more or less at right angles to the longitudinal axis, with gross delamination and pulling out of fibers being evident in many specimens. The flexural failures were characterized by local buckling of the layers under the loading nose and internal delaminations spreading from this region, as evidenced by development of a very noticeable color change.

5. Conclusions and Recommendations

5.1 Conclusions

For the FRP laminates tested, and within the limits of the experimental variables, the conclusions supported by the work carried out in this project may be summarized in the following paragraphs.

(A) Quasi-static properties:

(i) Lowering the percentage of fiberglass reinforcement produced highly significant reductions of modulus, with the test mode in an important but secondary role. Introduction of a greater volume of the weaker matrix material into a composite material leads to this result since a greater amount of structural integrity is lost due to microcracking before effective stress transfer to the reinforcing fabric is completed.

(ii) The effect of the test mode on ultimate strength was more significant than that of fiberglass content. The flexural stress distribution, keeping in mind the dimensions of bending specimens relative to tensile specimens, produced higher ultimate strengths because it exposed a relatively larger volume of material to a lesser average tensile stress, which is the controlling factor in determining flexural behavior. For such a brittle material, a critical stress is required to initiate or propagate a critical flaw, culminating in failure.

(iii) The variations in Poisson's ratios were generally random and may be caused by local strain amplification in the resin due to fiber spacings or material flaws.

(iv) No interactions were found to be significant in the quasi-static tests.

(B) Fatigue Lives and Allowable Stresses

Whereas material properties generally determined the short-term static behavior, fatigue characteristics were predominantly influenced by the stress or energy input (distribution and amplitude).

(i) In general, the % of ultimate stress allowable in flexure was greater than that in tension for any specified life N. The rationale would be similar to the one given in (A)(ii) above.

(ii) The stress allowable when a minimum level of 20% of ultimate was imposed was invariably greater than that when cyclic stress alternated between 0 and maximum. This may be related to the phenomenon of fracture surface work discussed in sec. 2.2. A constant positive level of stress in a crazed specimen may keep open many of the microcracks, which would act as crack arrestors and absorb considerable mechanical energy. Furthermore, introducing the minimum stress level reduces the stress amplitude and hence the fluctuating energy input. This appears to be more significant than the corresponding increase in static mean stress level.

(iii) While the effect of fiberglass content on fatigue properties was less marked than the effects of the other variables, it was in general more apparent early in the fatigue life, the greater reinforcement yielding greater allowable stresses as expected.

(iv) The presence of second-order interactions was noted in sec. 4. Their influence and interpretation bear further study, but it may be said that interactions seem more significant at early stages in fatigue life probably due to the general tendency of the F factor (i.e. the ratio of fiberglass to resin), and hence the associated interactions, to play a lesser role at higher values of N. This may be expected from the relatively extensive degradation of the resin fraction early in life and the progressive nature of the mechanisms which operate to propagate and/or generate critical flaws in the fiberglass phase (see sec. 2.2).

(v) The influence of the main factors on fatigue life (N cycles to failure) was notably less than similar effects on mechanical properties in fatigue.

(C) Changes in Mechanical Properties in Fatigue

The strength retention properties, characterized by %'s of modulus and Poisson's ratio retained with increasing N, reflect the same basic correlations between flexure/tension, 20%/0% minimum stress and 56%/42% fiberglass content as do the fatigue life properties discussed in (B). The tendency of any particular effect to be greater at higher N values was more clearly manifested here than in the fatigue life analysis. This trend may be due partly to the concept of increased energy input with time (e.g. total time spent at maximum stress level) and partly to the lessened influence of the F factor and certain interactions at later stages of fatigue life.

5.2 Recommendations

Recommendations for further research into the fatigue performance of FRPs should include:

1. Investigation of a wider range of the test variables chosen to establish trends more clearly.

2. Development of testing equipment, such as a multiple-head unit, that would enable several specimens to be stressed simultaneously. The consequent savings in total machine time would permit more replicates to be run, resulting in a broader statistical foundation for analysis, and lead to more extensive investigation of important material and test variables.

Bibliography

1. Prosen S.P., Simon R.A., "Carbon Fiber Composites for Hydrospace/Aerospace Applications", Plastics and Polymers, J. Plastics Institute, June 1968.
2. Welch R.G., "Reinforced Plastics in Transportation Vehicles", Proceedings, Society of the Plastics Industry (SPI), Inc., 19th Conference, Reinforced Plastics (RP) Division, 1964.
3. Lindstrom R.S., Heitman R.E., "Method for Predicting the Strength Degradation in an Underground Environment of Polyester Fiberglass Laminates", Proc. SPI, 19th Conf. RP Division, 1964.
4. Benjamin B.S., "Structural Design with Plastics", Van Nostrand - Reinhold, New York, 1969.
5. Skeist I., ed., "Plastics in Building", Reinhold, New York 1966.
6. Broutman L.J., Krock R.H., eds., "Modern Composite Materials", McGraw-Hill, New York, 1968.
7. Holliday L., ed., "Composite Materials", Elsevier, London, 1966.
8. Boller K.H., "Fatigue Characteristics of RP Laminates Subjected to Axial Loading", Modern Plastics, June 1964.
9. Boller K.H., "Fatigue Properties of Fibrous Glass-Reinforced Laminates Subjected to Various Conditions", Modern Plastics, June 1957.
10. Thompson A.W., "The Fatigue and Creep Properties of Reinforced Plastics", J. Plastics Institute, February 1962.
11. Lazar L.S., "Accelerated Fatigue of Reinforced Plastics", Proc. SPI, 12th Conf. RP Division, 1957.
12. Carswell W.S., Borwick G.R., "Repeated Loading of Chopped-Mat Polyester Sheet", Trans. and J. Plastics Institute, October 1965.

13. James T.K., Appl F.J., Bert C.W., "Low-cycle Fatigue of a Glass-fabric-reinforced Plastic Laminate", Experimental Mechanics, July 1968.

14. Owen M.J., Smith T.R., "Some Fatigue Properties of Chopped-Strand-Mat/Polyester-Resin Laminates", Plastics and Polymers, J. Plastics Institute, February 1968.

15. Owen M.J., Smith T.R., Dukes R., "Failure of Glass-Reinforced Plastics, with Special Reference to Fatigue", Plastics and Polymers, J. Plastics Institute, June 1969.

16. Dally J.W., Carrillo D.H., "Fatigue Behavior of Glass-Fiber Fortified Thermoplastics", Polymer Engineering and Science, November 1969.

17. Cessna L.C., Levens J.A., Thomson J.B., "Flexural Fatigue of Glass-Reinforced Thermoplastics", Polymer Engineering and Science, September 1969.

18. Dally J.W., Broutman L.J., "Frequency Effects on the Fatigue of Glass-Reinforced Plastics", J. Composite Materials, Vol. 1 (1967), p.424-442.

19. Boller K.H., "Effect of Pre-cyclic stresses on Fatigue Life of RP Laminates", Modern Plastics, April 1965.

20. Freund J.F., Silvergleit M., "Fatigue Characteristics of Glass-Filament Reinforced Plastic Material", Proc. SPI, 21st Conf. RP Division, 1966.

21. Fujii T., Mizukawa K., "The Effect of the Combination of Roving Glass Cloth and Mat upon the Fatigue Strength of Reinforced Polyester Laminates", Proc. SPI, 24th Conf., RP/Composites Division, 1969.

22. McAbee E., Chmura M., "Effects of High Rates Compared with Static Rates of Loading on the Mechanical Properties of Glass Reinforced Plastics", Proc. SPI, 16th Conf. RP Division, 1961.

23. Lavengood R.E., Anderson R.M., "Matrix Properties Controlling Torsional Fatigue Life of Fiber Reinforced Composites", Proc. SPI, 24th Conf., RP/Composites Division, 1969.

24. Hagerup E., "Flexural Fatigue Testing of Polyesters", Proc. SPI, 17th Conf. RP Division, 1962.

25. Opp D.A., Skinner D.W., Wiktorek R.J., "A Model for Polymer Fatigue", Polymer Engineering and Science, March 1969.

26. Scop P.M., Argon A.S., "Statistical Theory of Strength of Laminated Composites", J. Composite Materials, Vol. 1 (1967), p. 92-99.

27. Gotham K.V., "A Formalized Experimental Approach to the Fatigue of Thermo plastics", Plastics and Polymers, J. Plastics Institute, August 1969.

28. Boller K.H., "Effect of Moisture Absorption on Flexural Properties of a Glass-Fabric-Polyester Laminate", Forest Products Laboratory (FPL) Report 1819, U.S. Department of Agriculture, Forest Service, Wisconsin, 1962.

29. King A., "Ultraviolet Light: its Effects on Plastics", Plastics and Polymers, J. Plastics Institute, June 1968.

30. James D.I., Norman R.H., Stone M.H., "Water Attack on the Glass-Resin Bond on GRP", Plastics and Polymers, J. Plastics Institute, February 1968.

31. Rawe A.W., "Environmental Behavior of Glass-Fibre Reinforced Plastics", J. Plastics Institute, February 1962.

32. Werren F., "Effect of Span-Depth Ratio and Thickness on the Mechanical Properties of a Typical Glass-Fabric-Base Plastic Laminate as Determined by Bending Tests", FPL Report 1807, U.S. Dept. of Agriculture, Forest Service, Wisconsin, 1955 (reissued 1960).

33. Youngs R.L., "Effect of Thickness on the Mechanical Properties of Glass-Fabric-Base Plastic Laminates", FPL Report 1873, U.S. Dept. of Agriculture, Forest Service, Wisconsin, 1960.

34. Werren F., Heebink B.G., "Effect of Defects on the Tensile and Compressive Properties of a Glass-Fabric-Base Plastic Laminate", FPL Report 1814, U.S. Dept. of Agriculture, Forest Service, Wisconsin, 1955 (reissued 1960).

35. Steel D.J., "The Creep and Stress-Rupture of Reinforced Plastics", Trans. and J. Plastics Institute, October 1965.

36. Chambers R.E., McGarry F.J., "Tensile and Compressive Properties of Fiberglass Reinforced Laminates", American Society for Testing Materials (A.S.T.M.) Bulletin, October 1958.

37. Chambers R.E., McGarry F.J., "Shear Effects in Glass-Fiber Reinforced Plastics Laminates", A.S.T.M. Bulletin, May 1959.

38. Desai M.B., McGarry F.J., "Failure Mechanisms in Glass-Fiber Reinforced Plastics", A.S.T.M. Bulletin, July 1959.

39. Chambers R.E., "Laminate Behavior as Determined from Internal Strain Measurements", Proc. S.P.I., 13th Conf., RP Division, 1958.

40. McGarry F.J., Willner A.M., "Microcracking in Fibrous Glass Reinforced Resin Composites", Proc. SPI, 23rd Conf., RP/Composites Division, 1968.

41. McGarry F.J., "Microcracking in Fibrous Glass Reinforced Resin Composites", International Conference on Structure, Solid Mechanics, and Engineering Design in Civil Engineering Materials, Southampton, England, April 1969.

42. West D.C., Outwater J.O., "The Stress Distribution in the Resin of Reinforced Plastics", Proc. S.P.I., 16th Conf., RP Division, 1961.

43. Throckmorton P.E., Hickman H.M., Browne M.F., "Origin of Stress Failure in Glass Reinforced Plastics", Proc. SPI, 18th Conf. RP Division, 1963.

44. Broutman L.J., "Failure Mechanisms for Filament Reinforced Plastics", Modern Plastics, April 1965.

45. Owen M.J., Dukes R., Smith T.R., "Fatigue and Failure Mechanisms in GRP with Special Reference to Random Reinforcements", Proc. SPI, 23rd Conf., RP/Composites Division, 1968.

46. Broutman L.J., Sahu S., "Progressive Damage of a Glass Reinforced Plastic During Fatigue", Proc., SPI, 24th Conf., RP/Composites Division, 1969.

47. Kies J.A., "Maximum Strains in Resin of Fiberglass Composites", Naval Research Laboratory (NRL) Report 5752, Washington, D.C., 1962.

48. Zimmer J.E., Cost J.R., "Determination of the Elastic Constants of a Fiber Composite Using Ultrasonic Velocity Measurements", McDonnell Douglas Astronautics Co., Douglas Paper 10181, Huntington Beach, California, June 1969.

49. Cochran W.G., Cox G.M., "Experimental Designs", 2nd ed., Wiley, New York, 1957: Chap. 5, Factorial Experiments, pp. 148-188.

50. Freund J.E., "Mathematical Statistics", Prentice-Hall, New York, 1962. Chap. 13, Regression and Correlation, Chap. 14, Introduction to Analysis of Variance, pp. 295-350.

51. Hicks C.R., "Fundamental Concepts in the Design of Experiments", Holt, Rinehart and Winston, New York 1964. Chapter 6, Factorial Experiments, Chap. 7, 2^n Factorial experiments, pp. 75-108; Chap. 12, Experiments of Two or More Factors - Restrictions on Randomization, pp. 179-188; Chap. 14, Factorial Experiment - Confounding in

Blocks, pp. 201-219.

Appendix A

Figures

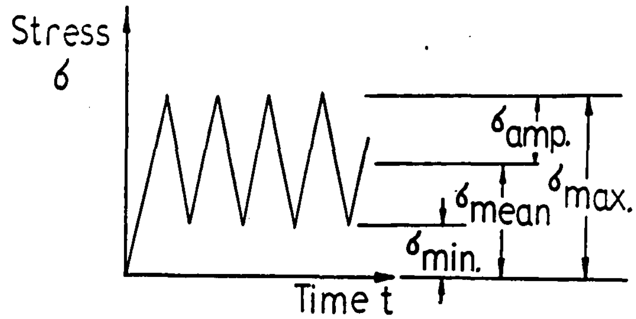

$$\sigma_{max} = \sigma_{mean} + \sigma_{amp} = \sigma_{min} + 2\sigma_{amp}$$

$$\sigma_{mean} = \sigma_{min} + \sigma_{amp} = \frac{\sigma_{max} + \sigma_{min}}{2}$$

$$\sigma_{amp} = \frac{\sigma_{max} - \sigma_{min}}{2}$$

FIG.1. STRESS VARIABLES

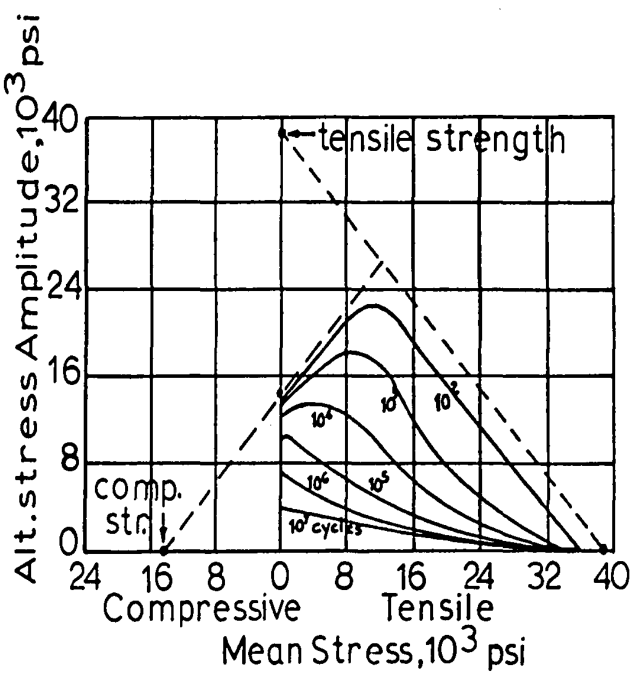

FIG.2. TYPICAL 'GOODMAN' DIAGRAM
(after Boller, (8))

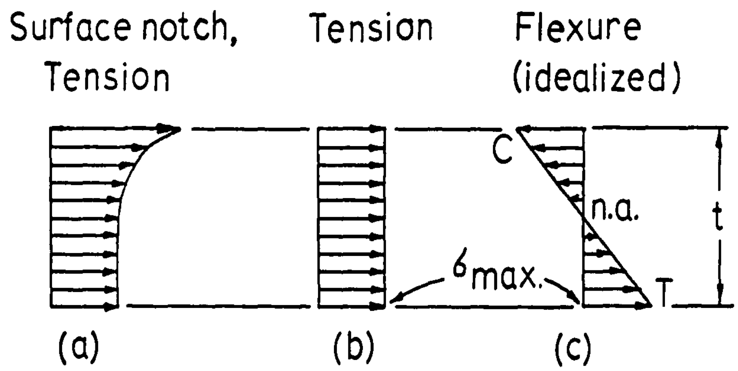

FIG.3. STRESS DISTRIBUTIONS

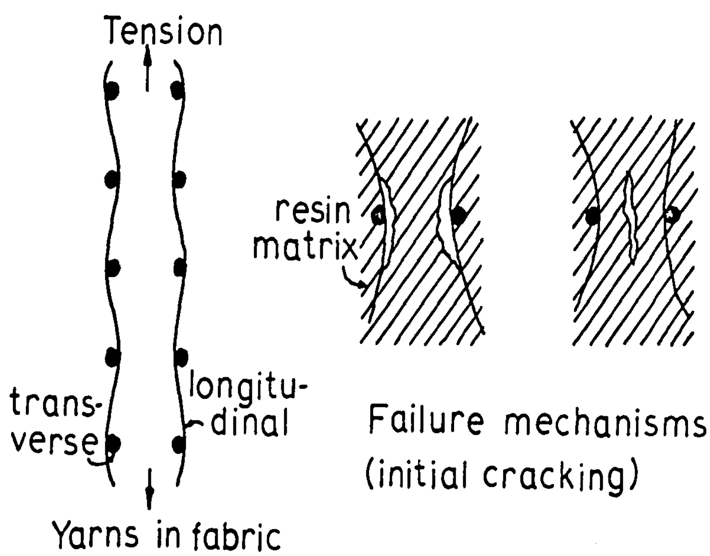

FIG.4. FAILURE MECHANISMS
(after Desai & McGarry,(38))

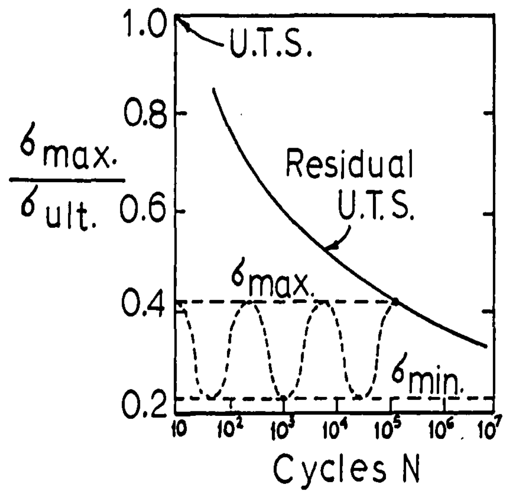

FIG.5. RESIDUAL STRENGTH AT FATIGUE LIFE
(after Broutman & Sahu,(46))

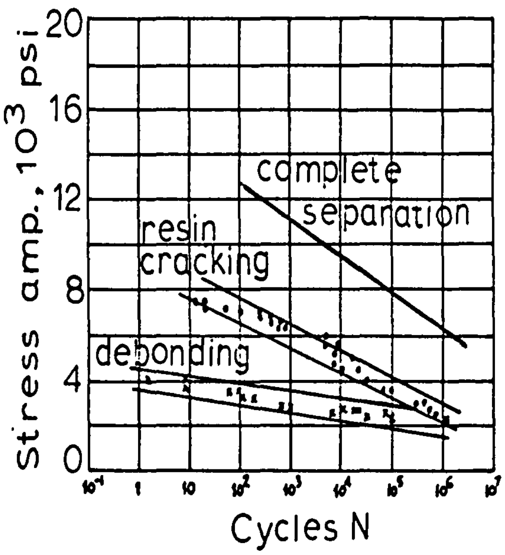

FIG.6. BANDED SN DIAGRAM
REFLECTING INTERNAL DAMAGE
(after Owen, Dukes & Smith,(45))

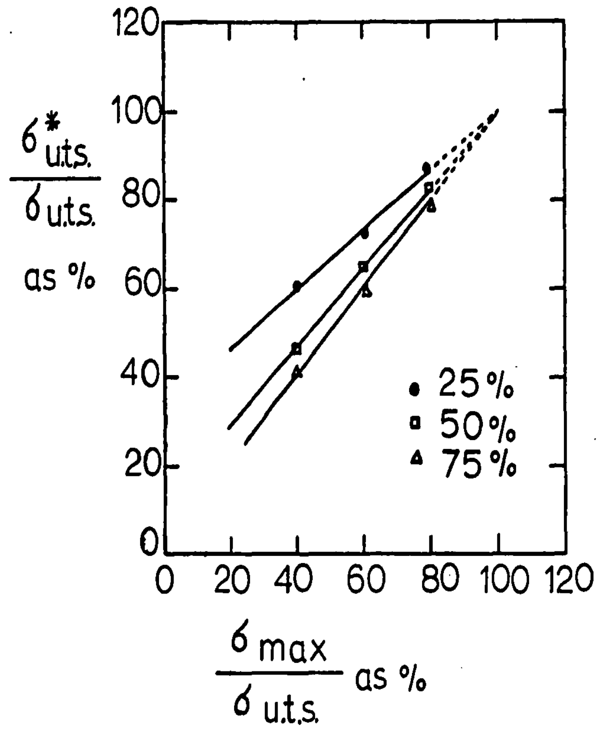

FIG.7. RESIDUAL STRENGTH RELATED TO STRESS AND FATIGUE LIFE

(after Broutman & Sahu,(46))

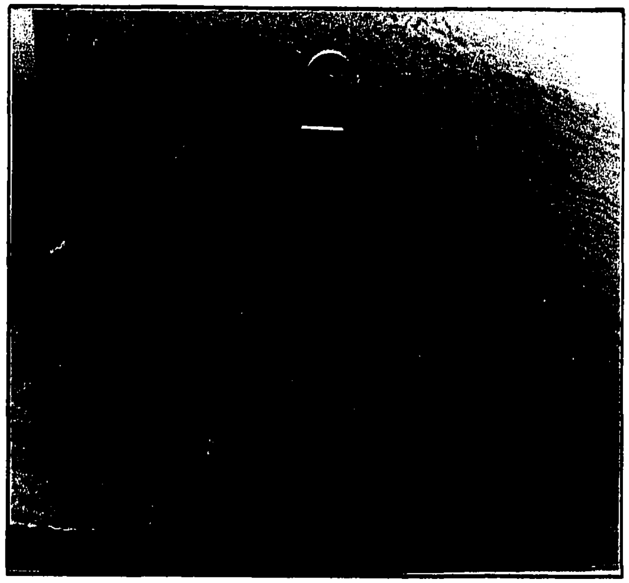

FIG.8. TensiHKut Machine & Templates

FIG.10. Instron TK50 Testing Machine
(Recording equipment at right)

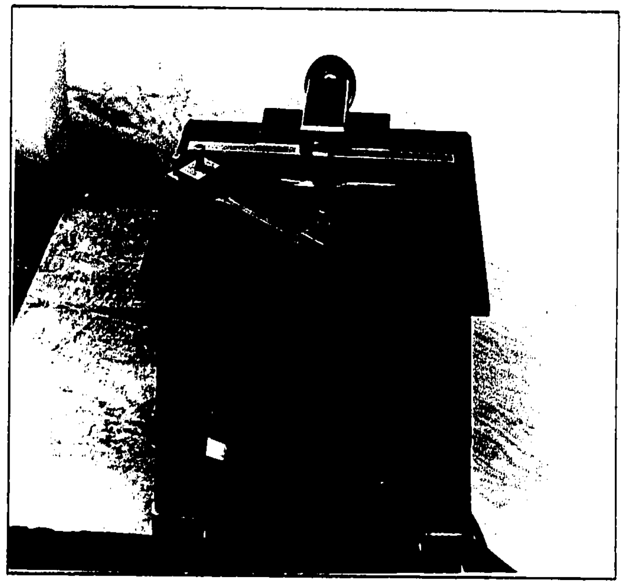

FIG.8. TensiHKut Machine & Templates

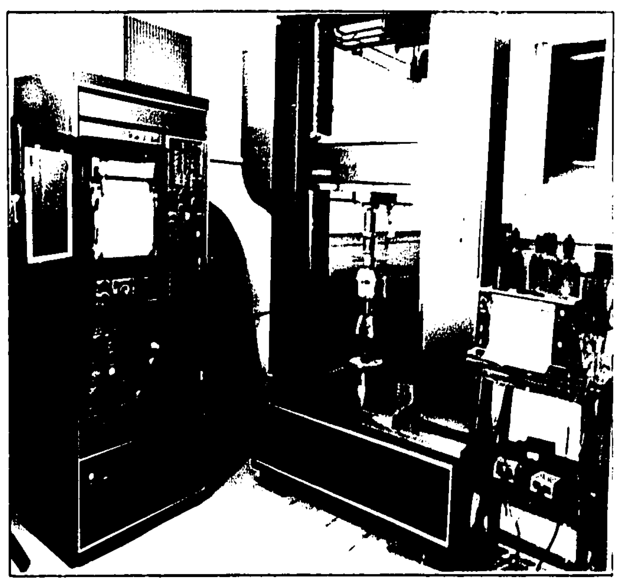

FIG.10. Instron [illegible] Testing Machine

Recording equipment at right

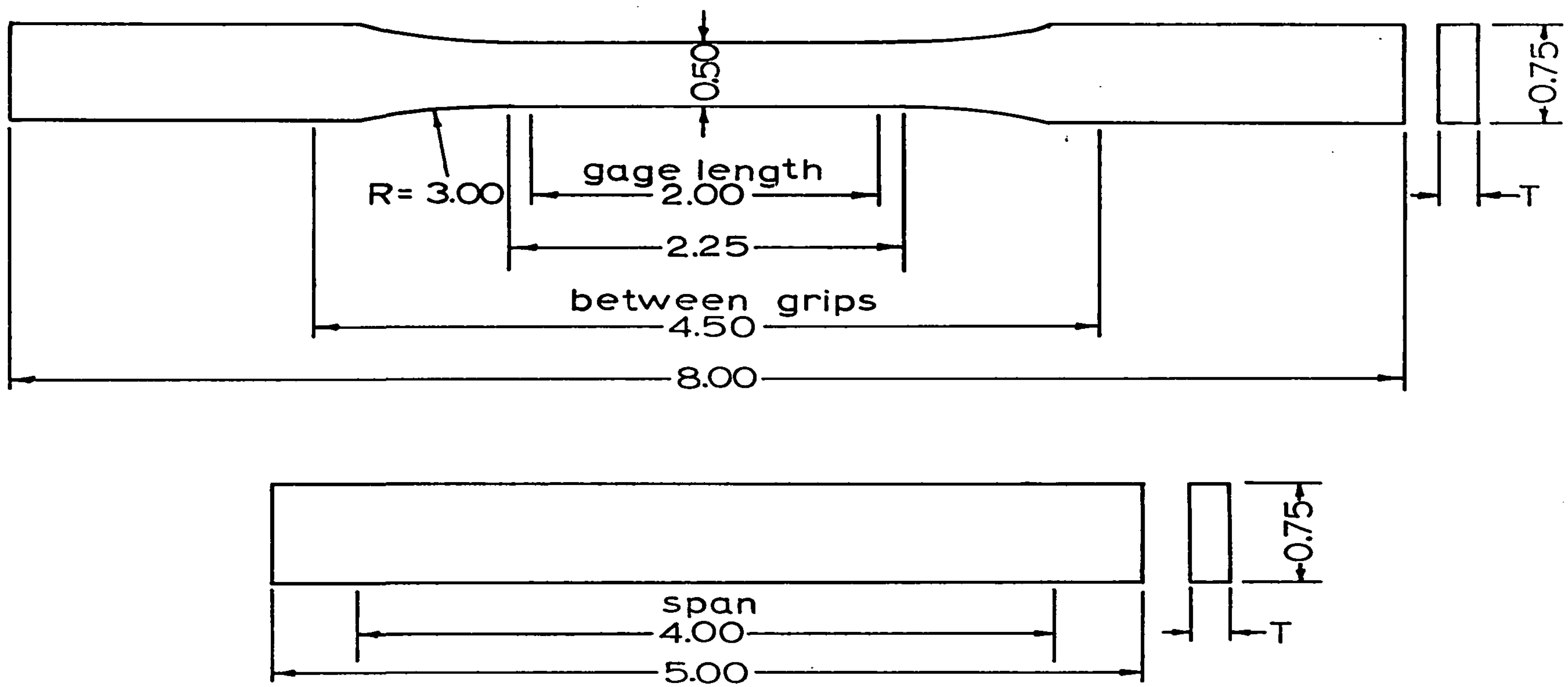

FIG. 9. TENSION & FLEXURE SPECIMENS (F.S.)

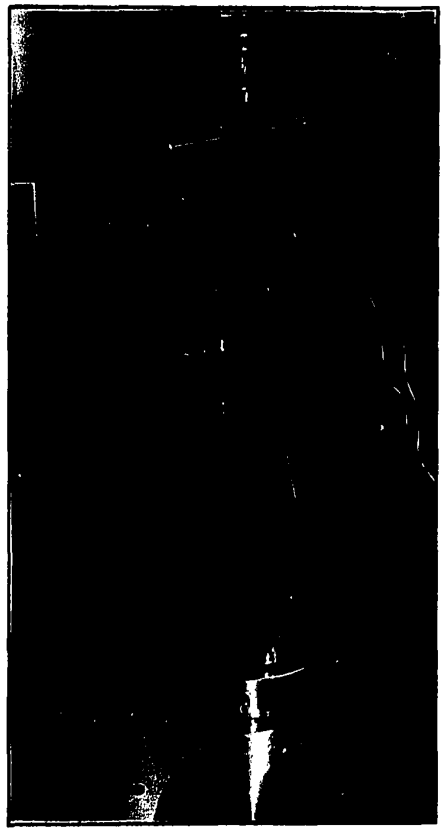

FIG.11. Tensile Test Apparatus

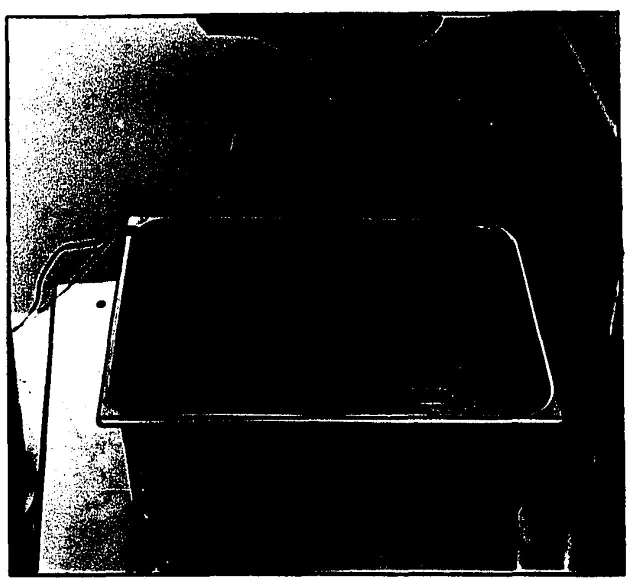

FIG.12. Flexure Test Apparatus

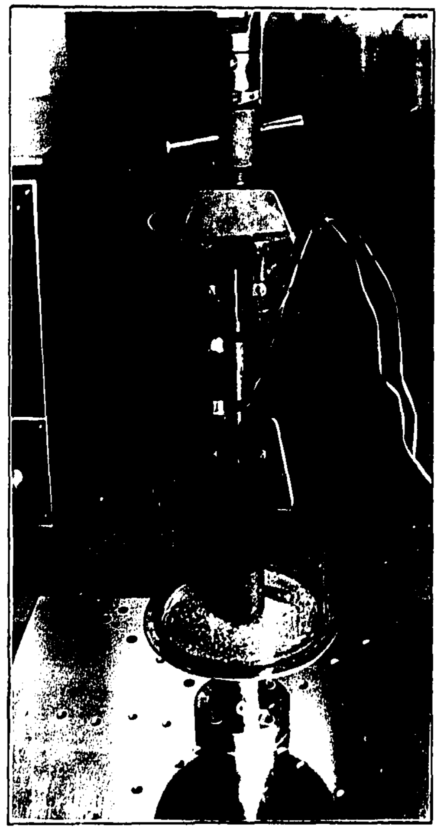

FIG.11. Tensile Test Apparatus

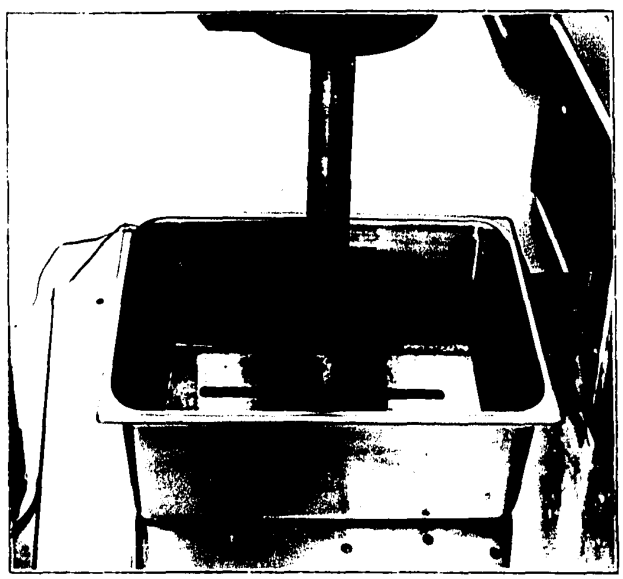

FIG.12. Flexure Test Apparatus

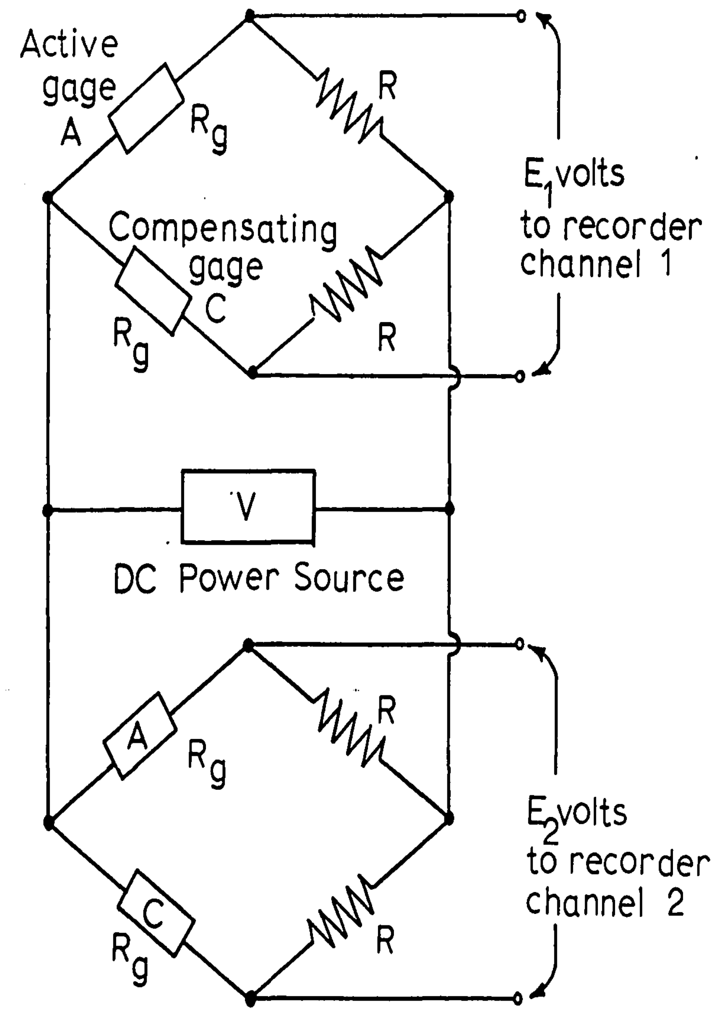

$R = R_g = 120.0 \pm 0.03\Omega$, $V = 4.0v$

$$E = \frac{R_g \cdot R}{R_g + R} \cdot I \cdot K \cdot S \quad \begin{cases} K = \text{strain gage factor} \\ S = \text{strain, in./in.} \end{cases}$$

$$I = \frac{V}{R_g + R}$$

$$E = \frac{R \cdot R}{2 \cdot R} \cdot \frac{V}{2 \cdot R} \cdot K \cdot S = \frac{V \cdot K \cdot S}{4}$$

$$\therefore S = \frac{E}{K}$$

FIG.13. STRAIN GAGE CIRCUIT

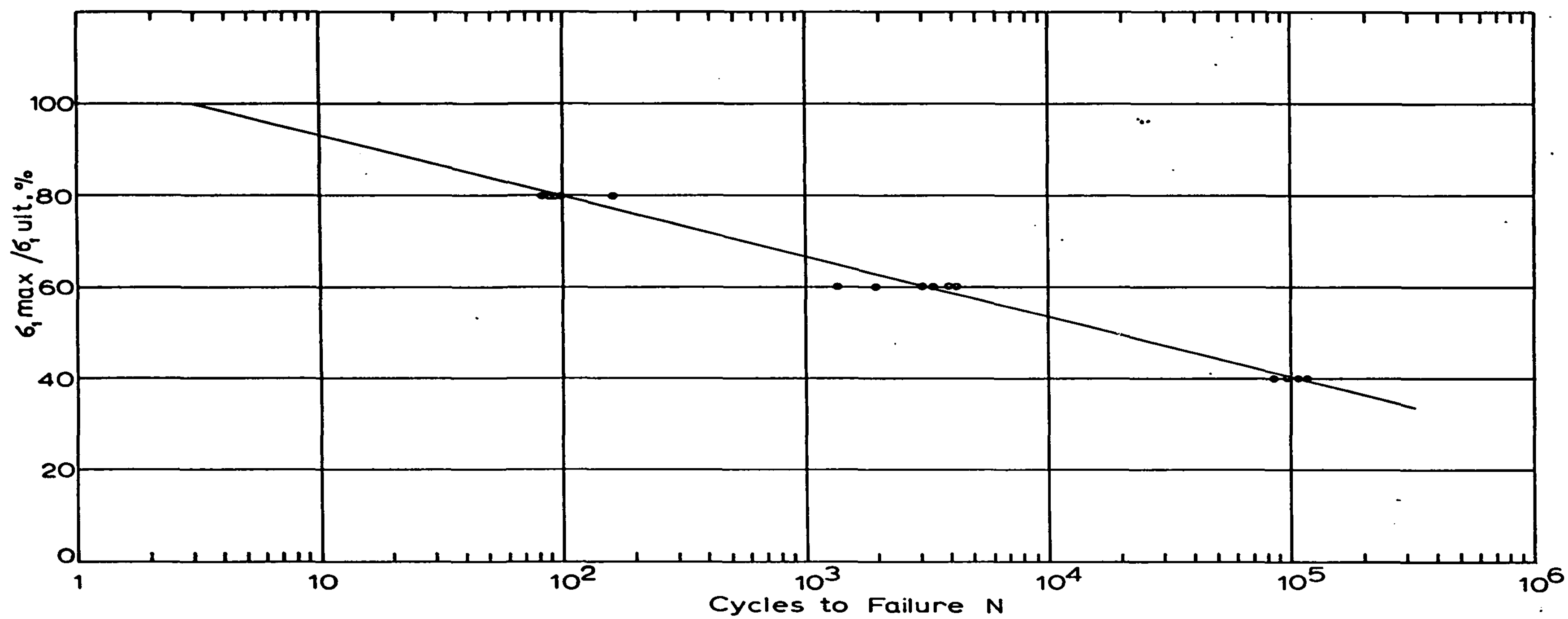

FIG.14. SN CURVE - Tension 56% Fiberglass 0 Min.Stress

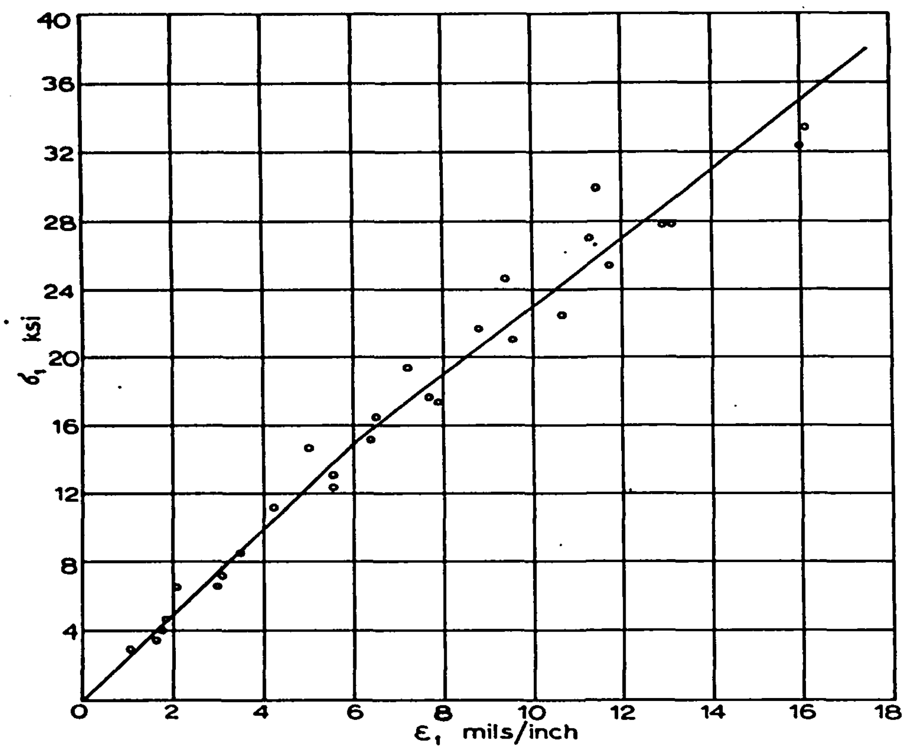

FIG.15. STRESS-STRAIN CURVE
Tension 56% Fiberglass Replicate 1

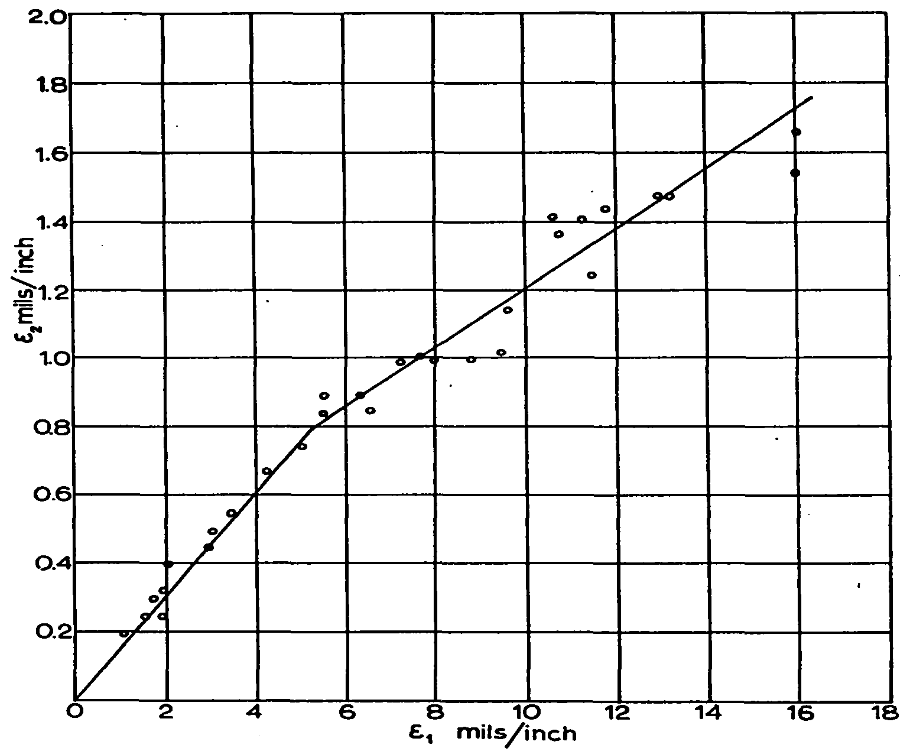

FIG.16. POISSON'S RATIOS
Tension 56% Fiberglass Replicate 1

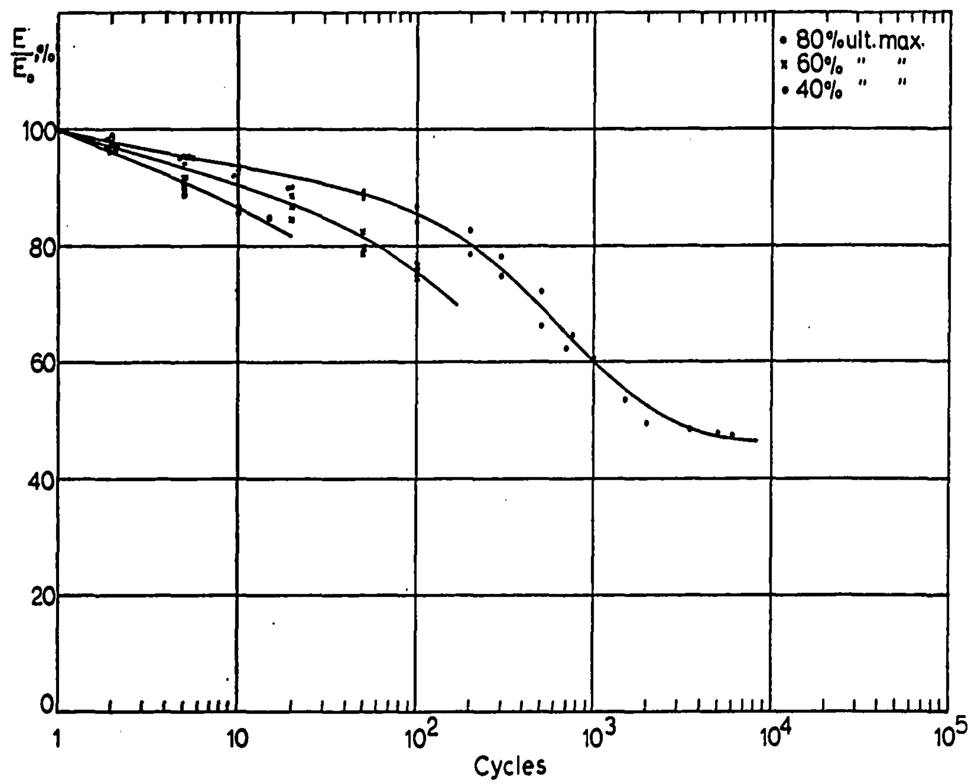

FIG.17. MODULUS RETENTION - Tension 56% F.g. 0 Min. Stress

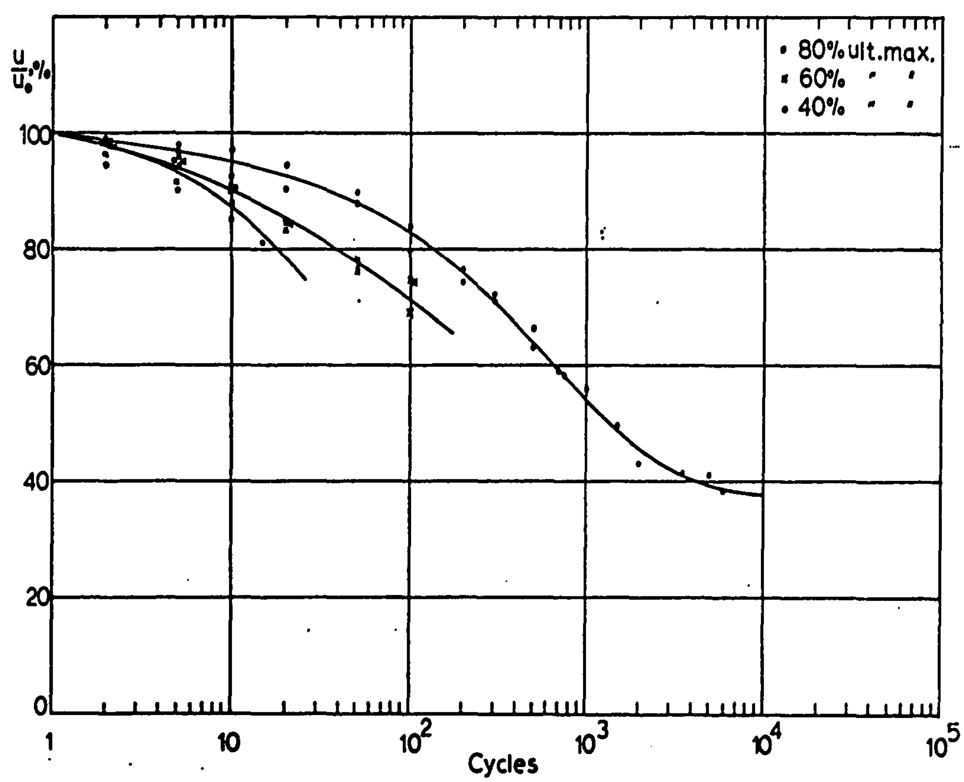

FIG.18. POISSON'S RATIO RETENTION

Tension 56% Fg. 0 Min. Stress

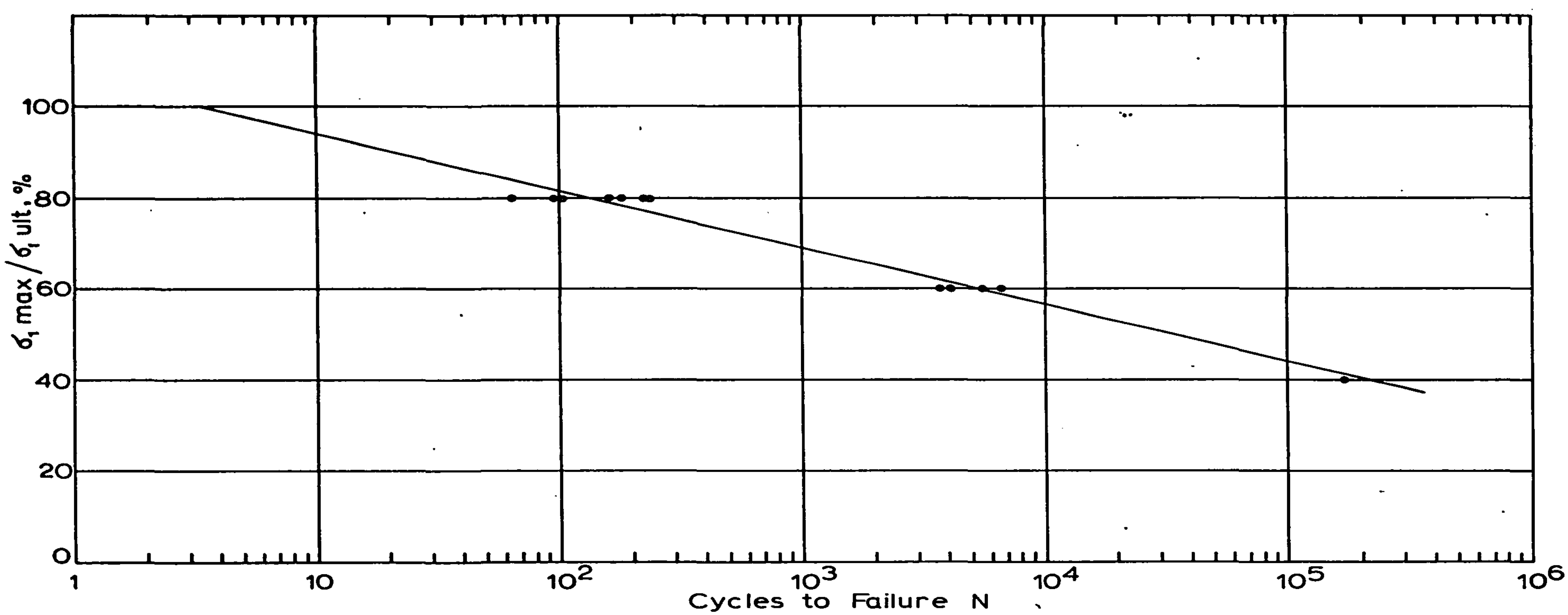

FIG.19. SN CURVE - Flexure 56% Fiberglass 0 Min. Stress

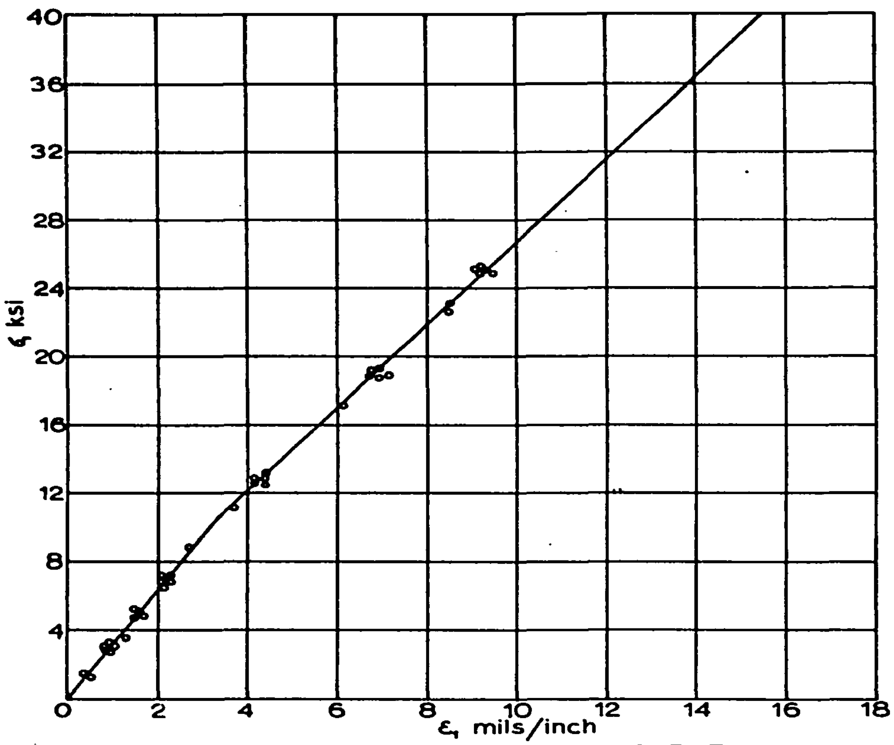

FIG. 20. STRESS-STRAIN CURVE

Flexure 56% Fiberglass Replicate 1

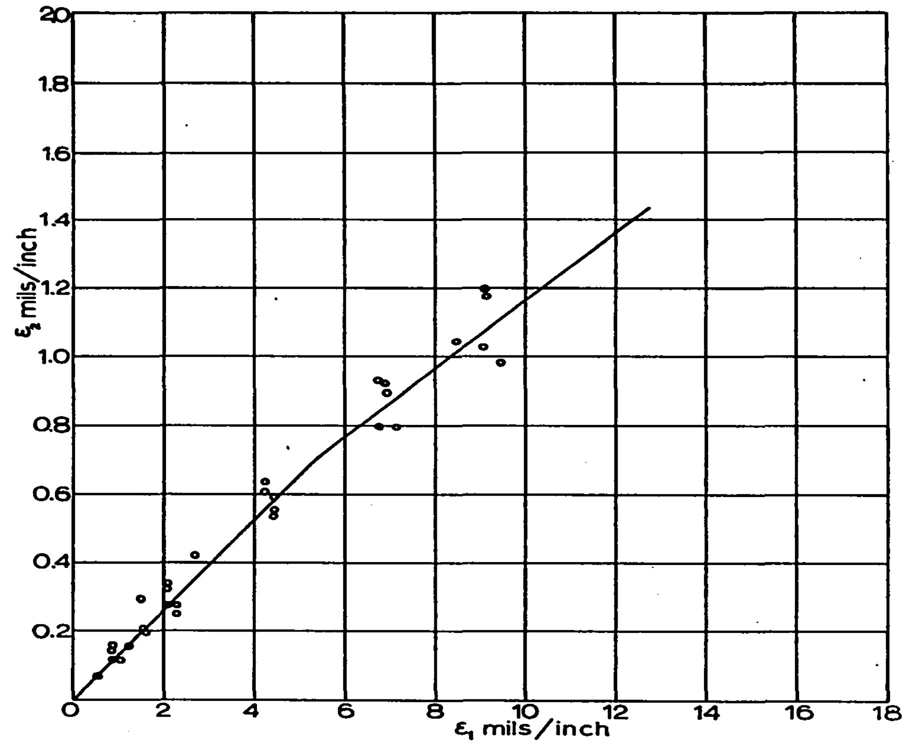

FIG. 21. POISSON'S RATIOS

Flexure 56% Fiberglass Replicate 1

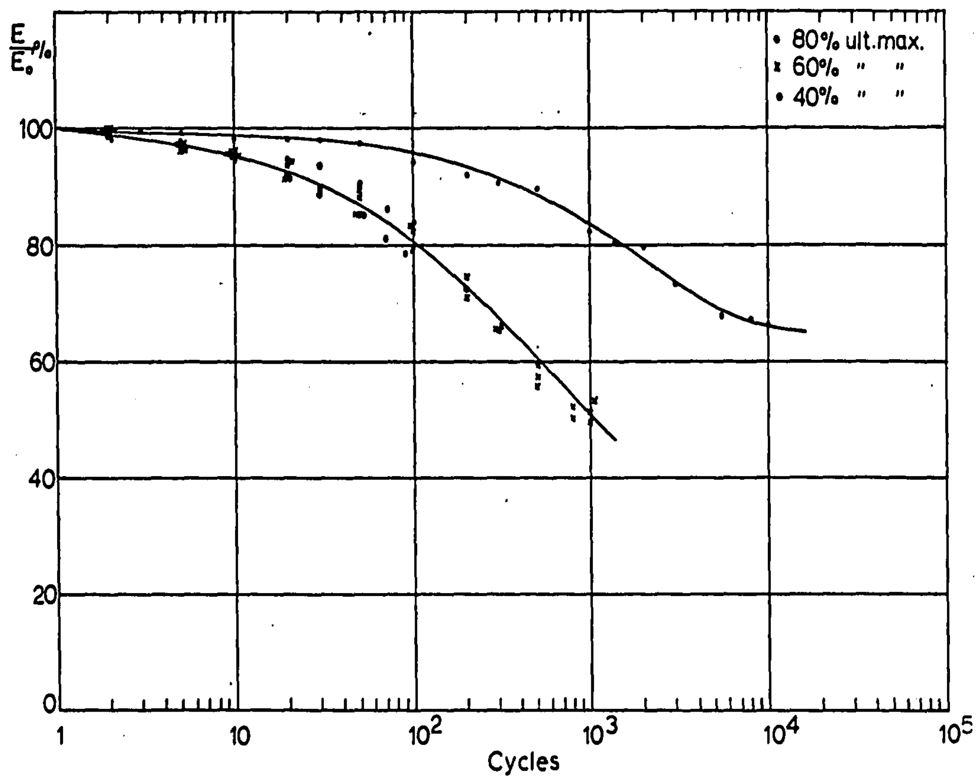

FIG.22. MODULUS RETENTION - Flexure 56% F.g. 0 Min. Stress

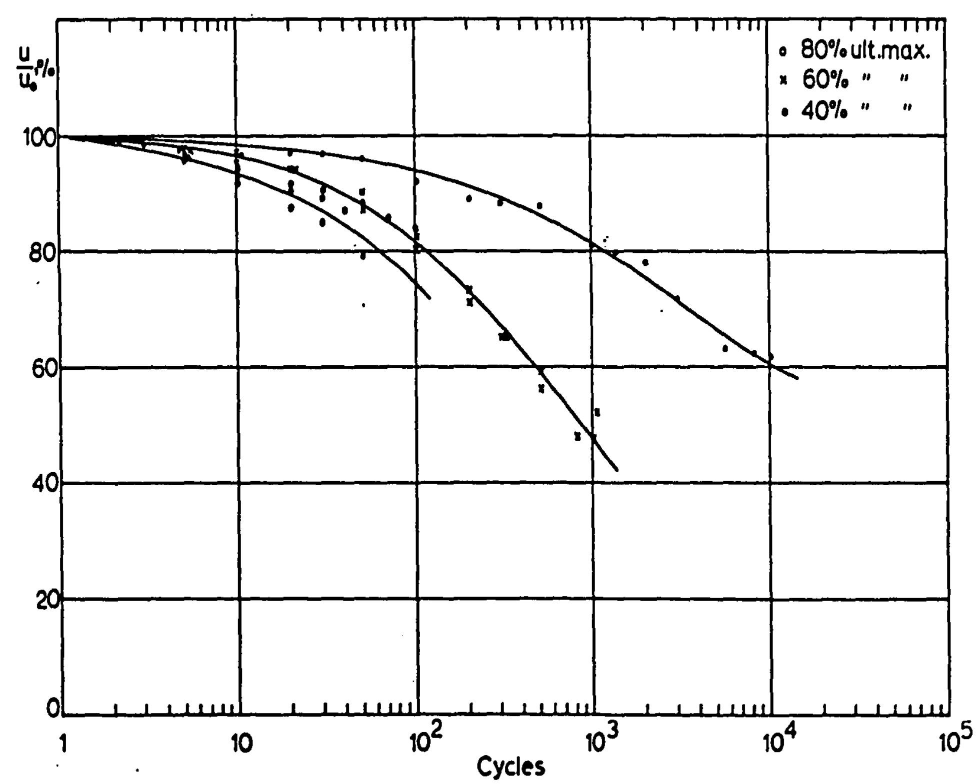

FIG.23. POISSON'S RATIO RETENTION

Flexure 56% Fg 0 Min Stress

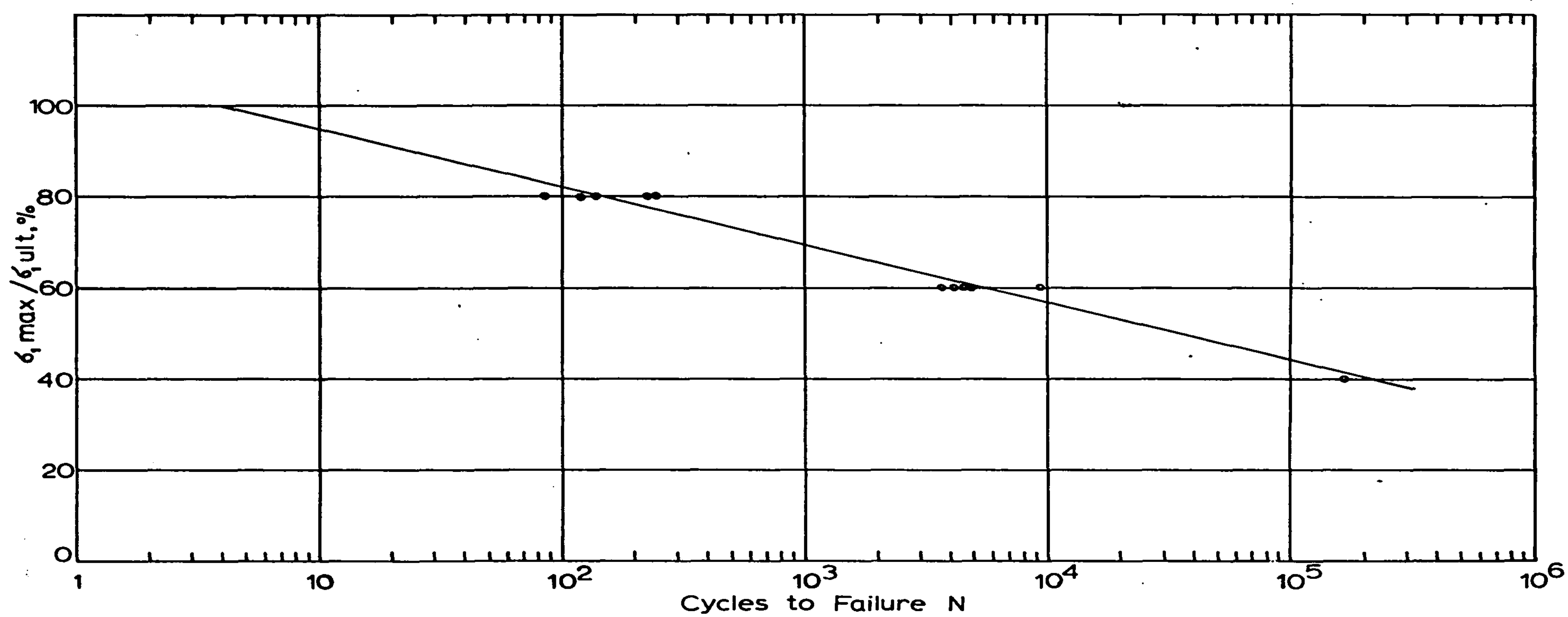

FIG.24. SN CURVE - Tension 56% Fiberglass 20% ult. Min. Stress

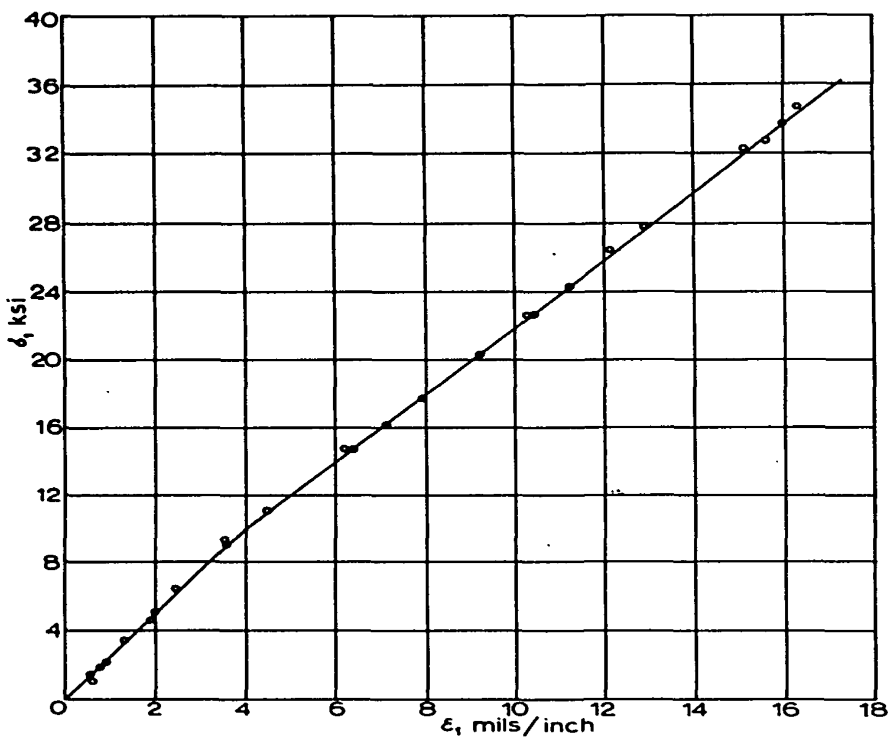

FIG.25. STRESS-STRAIN CURVE

Tension 56% Fiberglass Replicate 2

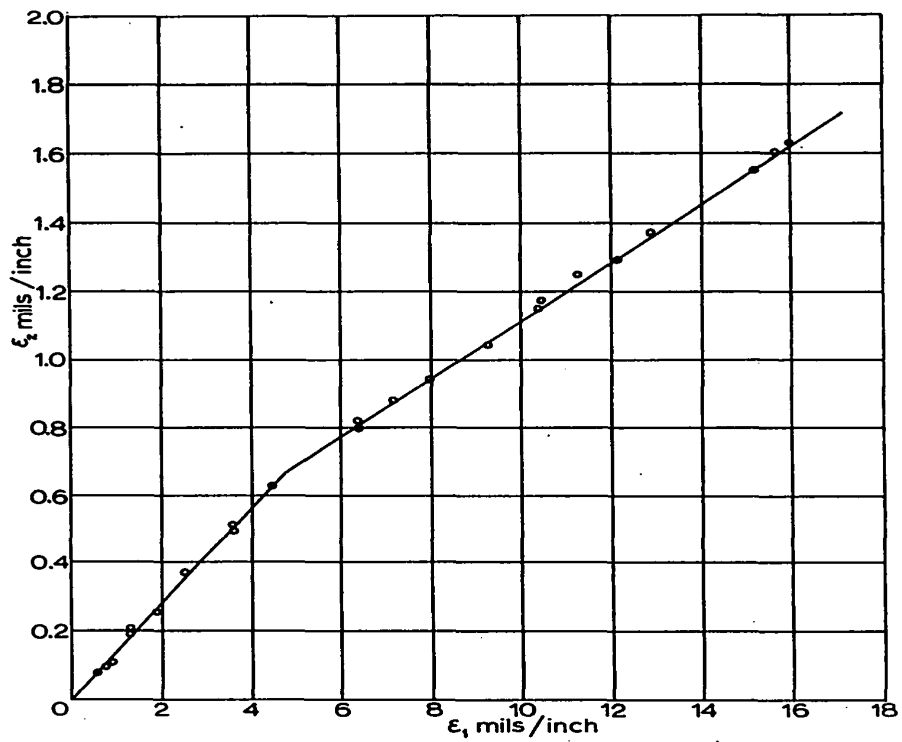

FIG.26. POISSON'S RATIOS

Tension 56% Fiberglass Replicate 2

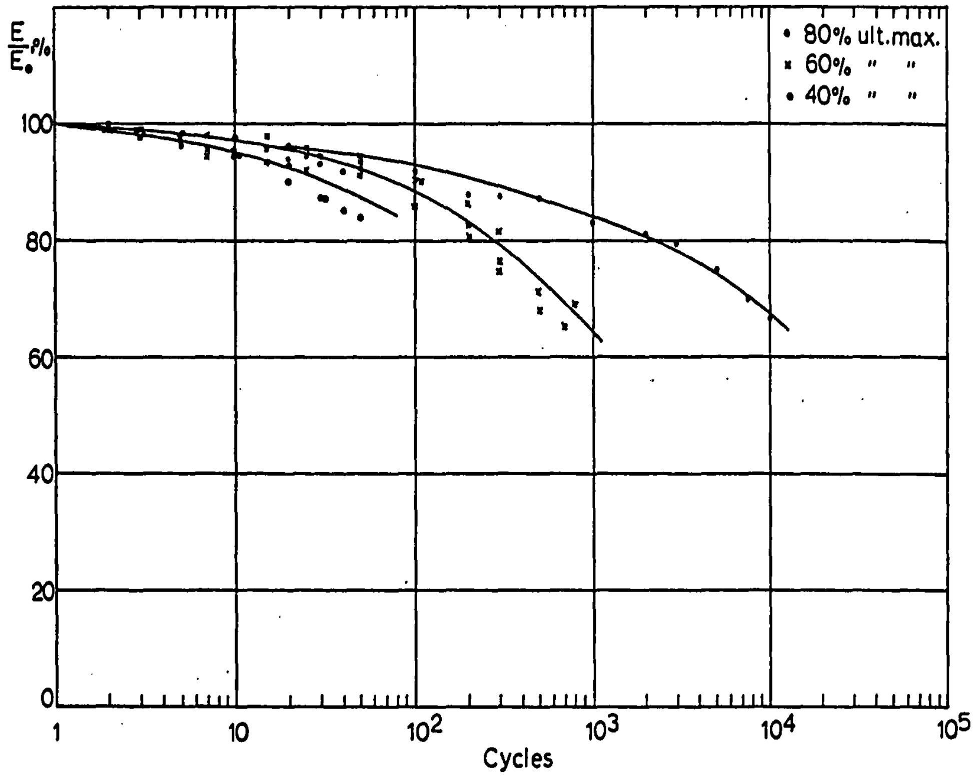

FIG.27. MODULUS RETENTION – Tension 56%F.g. 20%ult.Min.Stress

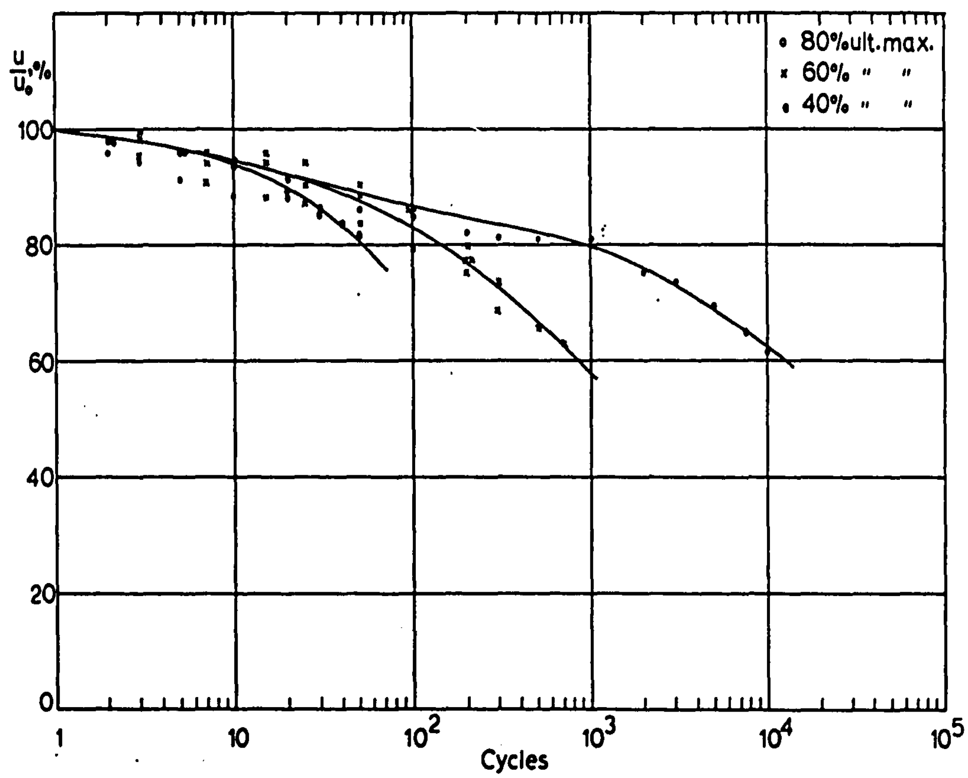

FIG.28. POISSON'S RATIO RETENTION

Tension 56%F.g. 20%ult.Min.Stress

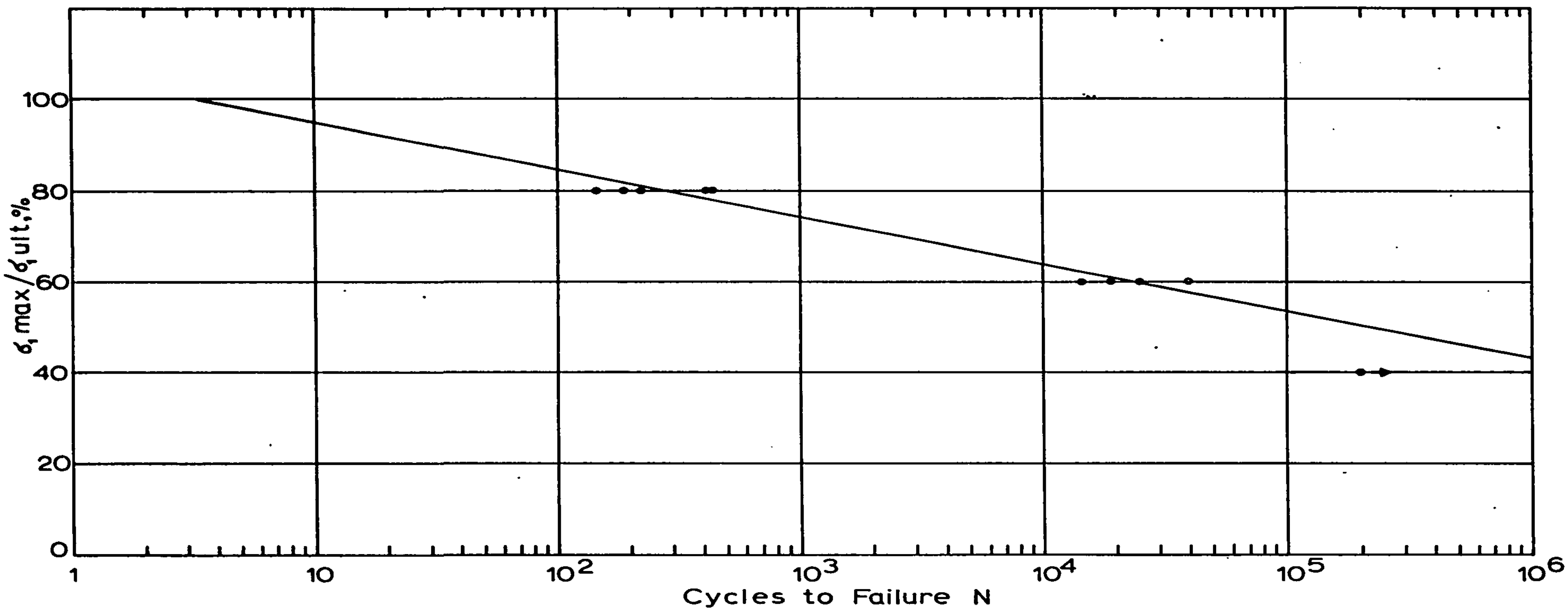

FIG.29. SN CURVE - Flexure 56% Fiberglass 20% ult. Min. Stress

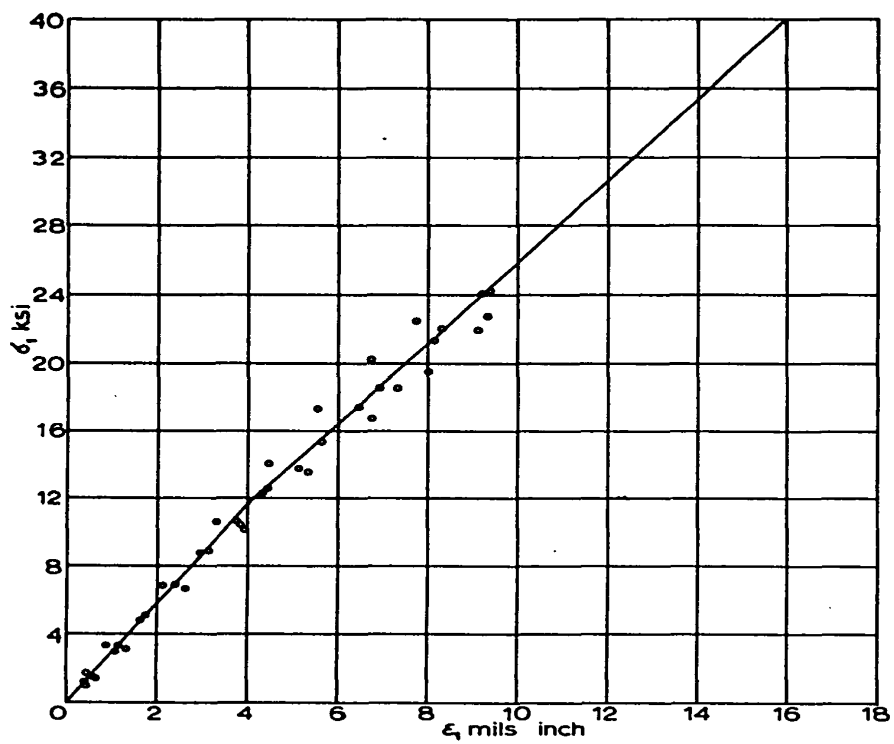

FIG. 30. STRESS-STRAIN CURVE

Flexure 56% Fiberglass Replicate 2

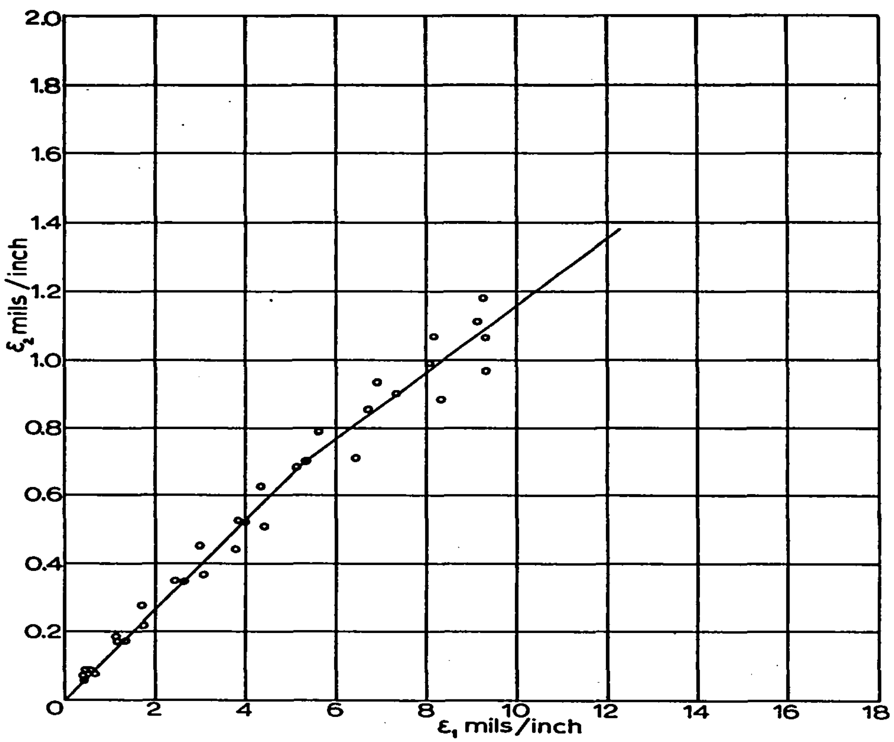

FIG. 31. POISSON'S RATIOS

Flexure 56% Fiberglass Replicate 2

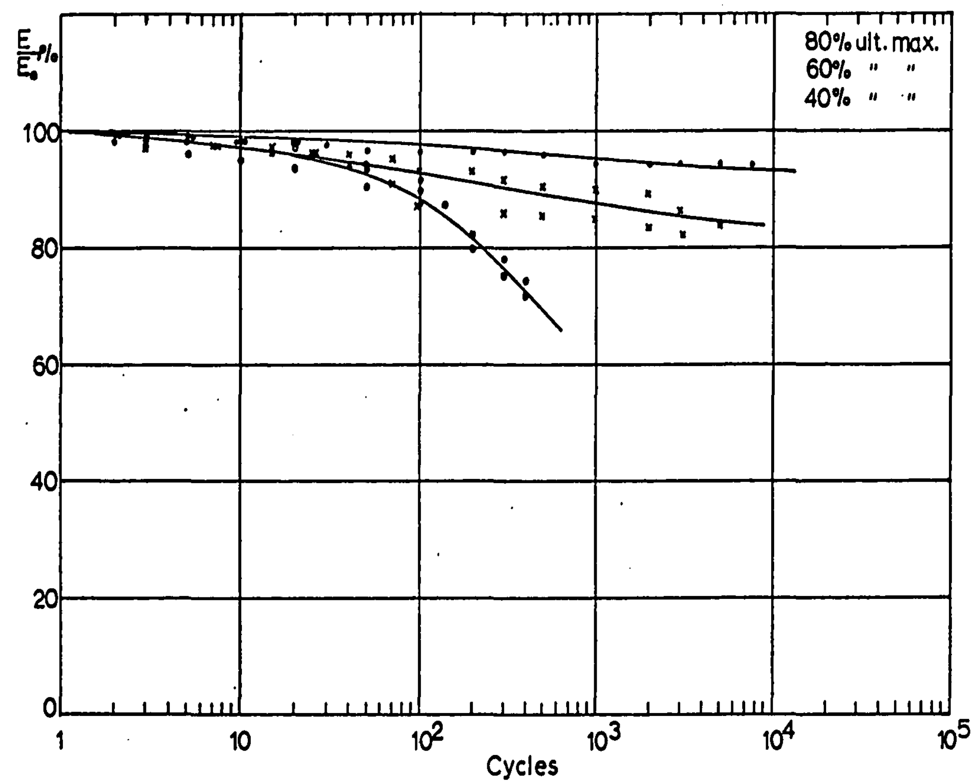

FIG.32. MODULUS RETENTION - Flexure 56% F.g. 20% ult. Min. Stress

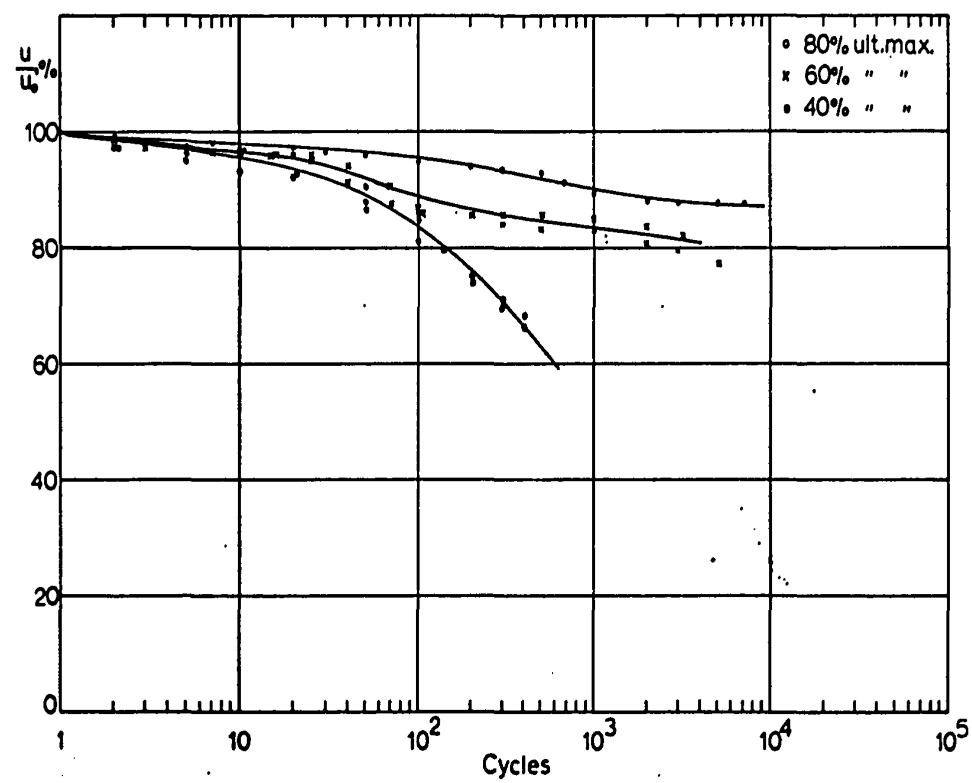

FIG.33. POISSON'S RATIO RETENTION

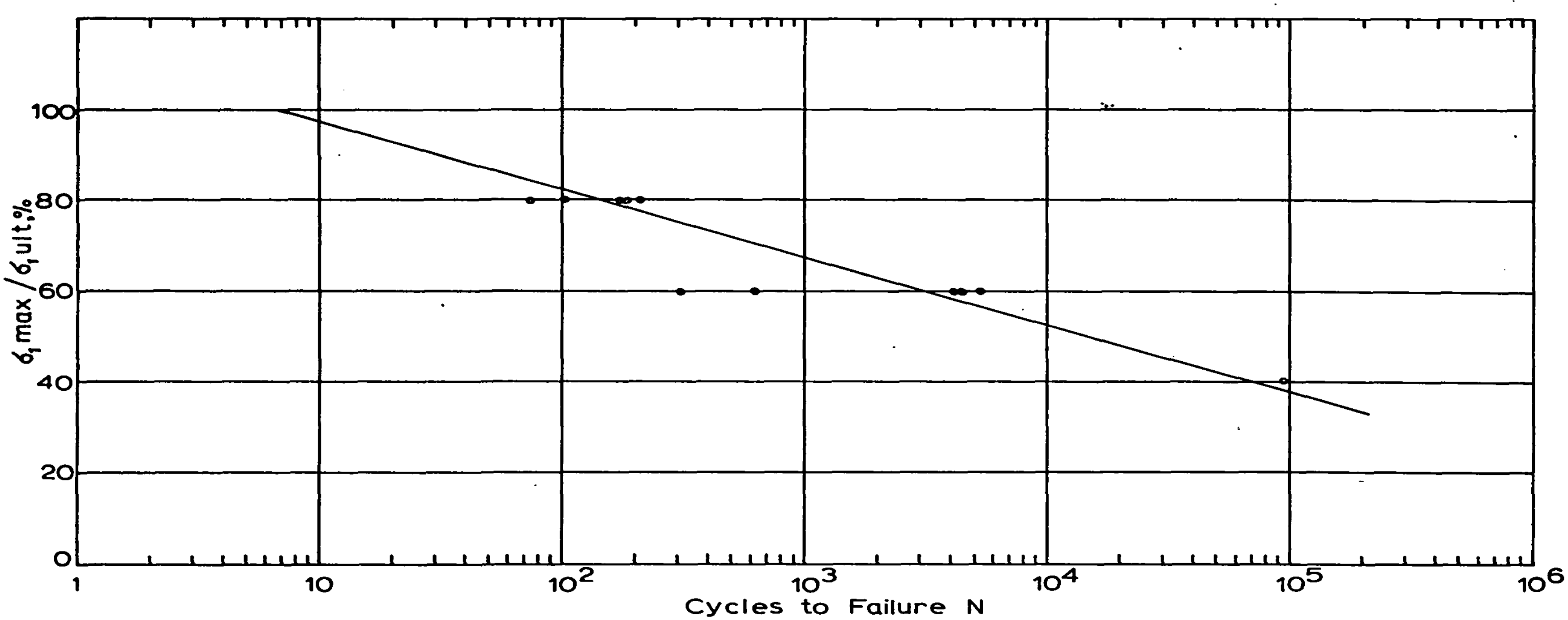

FIG.34. SN CURVE - Tension 42% Fiberglass 0 Min.Stress

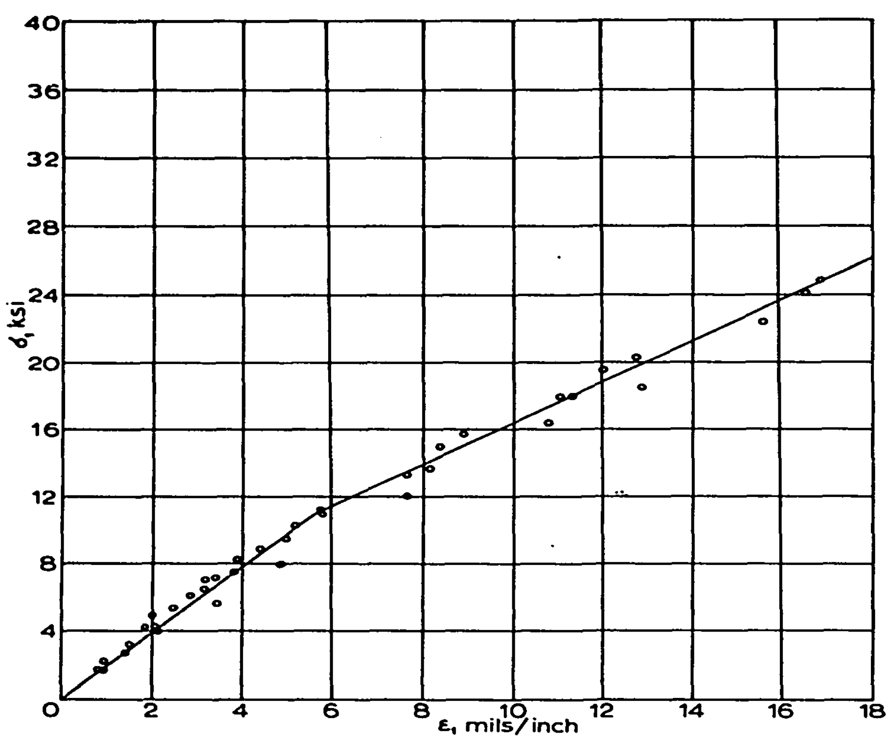

FIG. 35. STRESS-STRAIN CURVE

Tension 42% Fiberglass Replicate 1

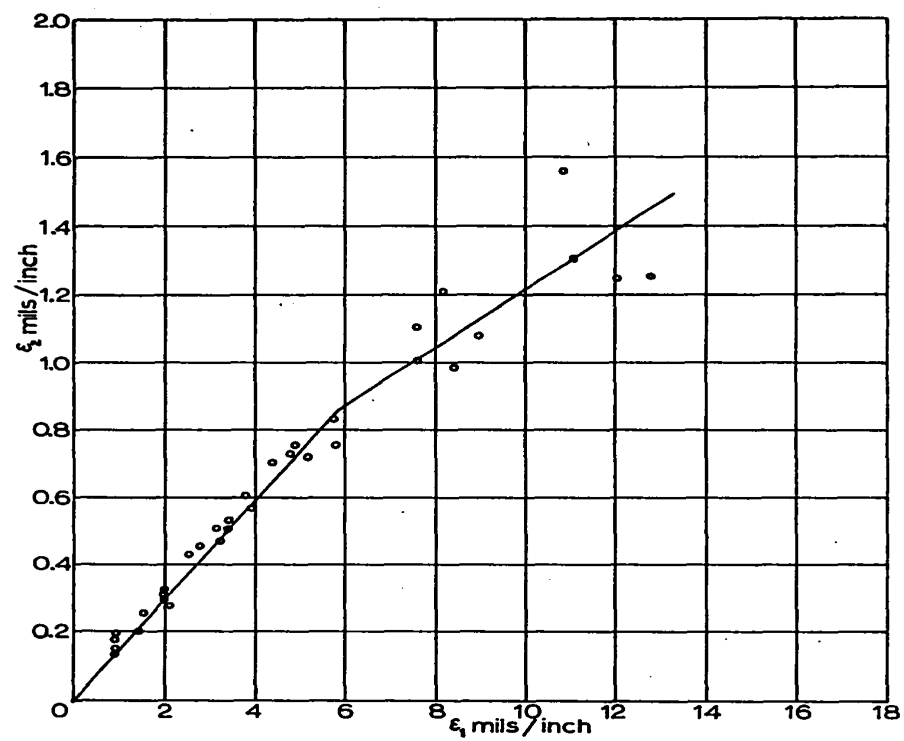

FIG. 36. POISSON'S RATIOS

Tension 42% Fiberglass Replicate 1

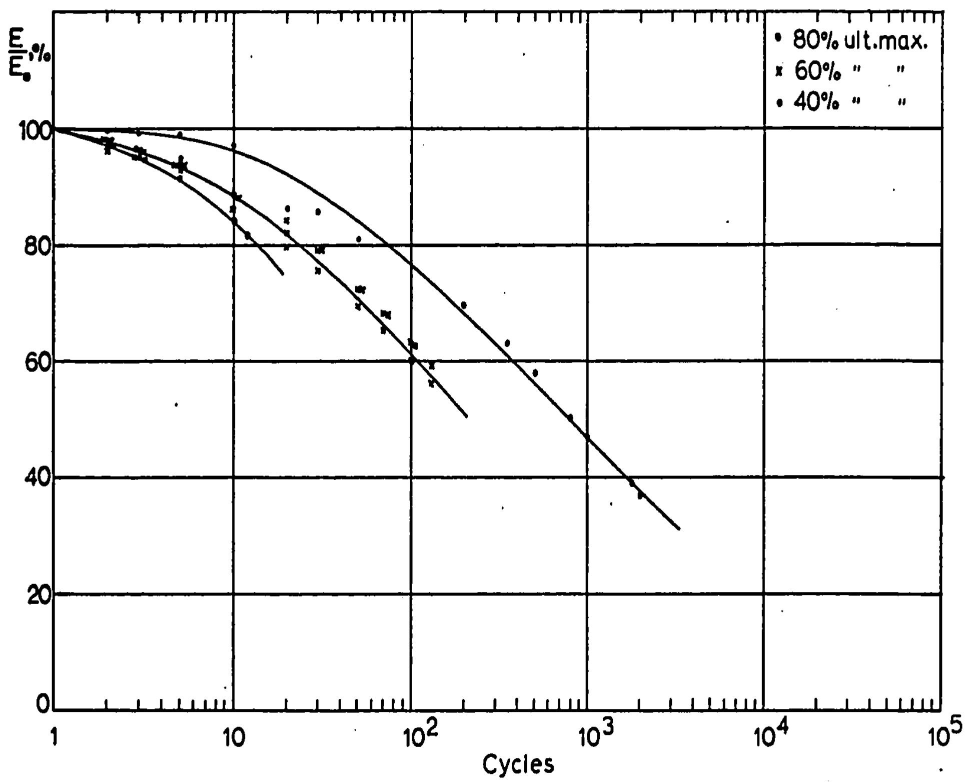

FIG.37. MODULUS RETENTION - Tension 42%F.g. 0 Min.Stress

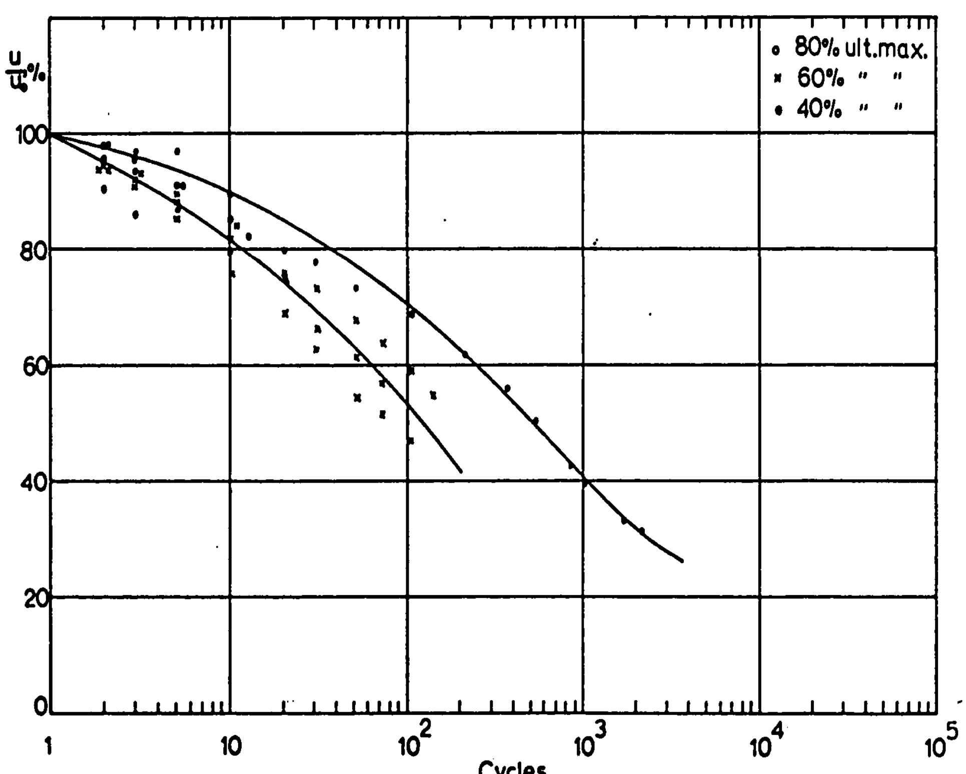

FIG.38. POISSON'S RATIO RETENTION

Tension 42% F.g. 0 Min.Stress

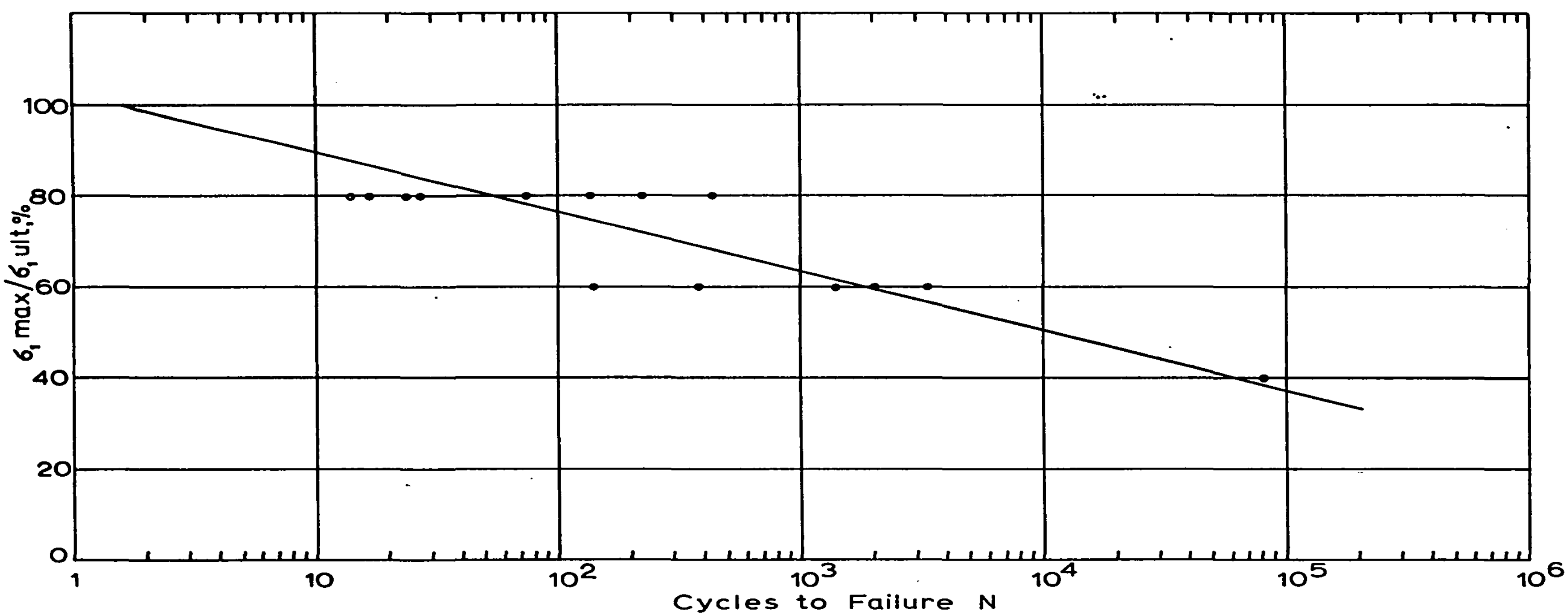

FIG.39. SN CURVE - Flexure 42% Fiberglass 0 Min. Stress

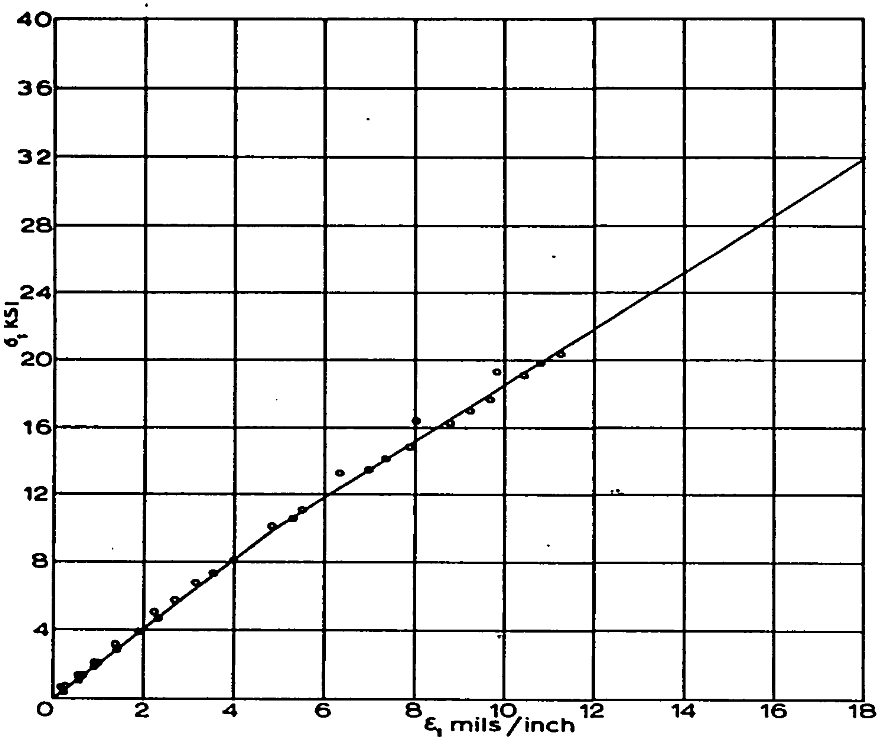

FIG.40. STRESS-STRAIN CURVE

Flexure 42% Fiberglass Replicate 1

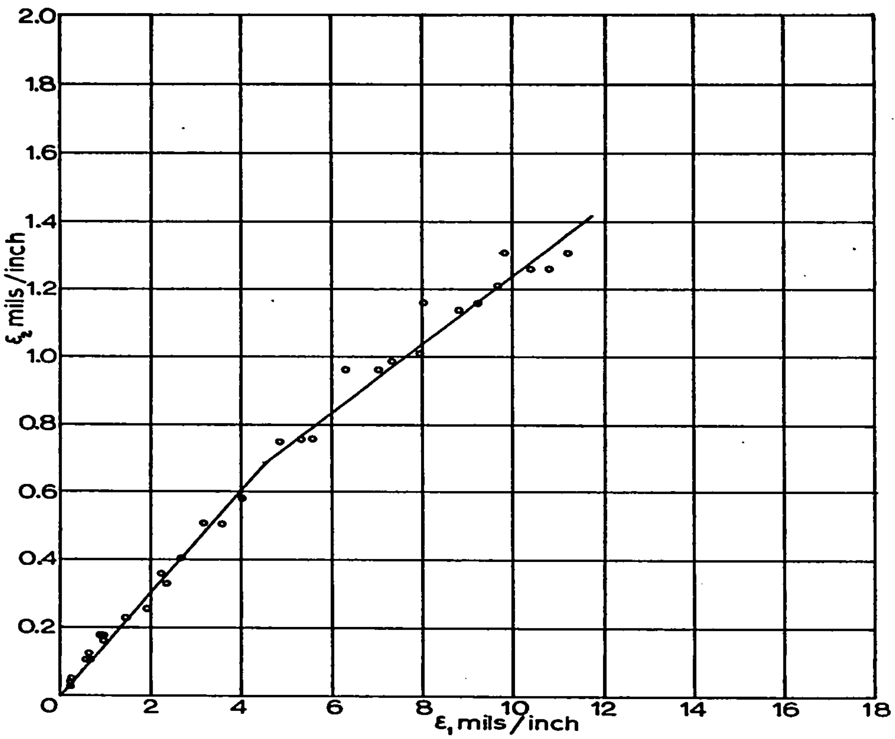

FIG.41. POISSON'S RATIOS

Flexure 42% Fiberglass Replicate 1

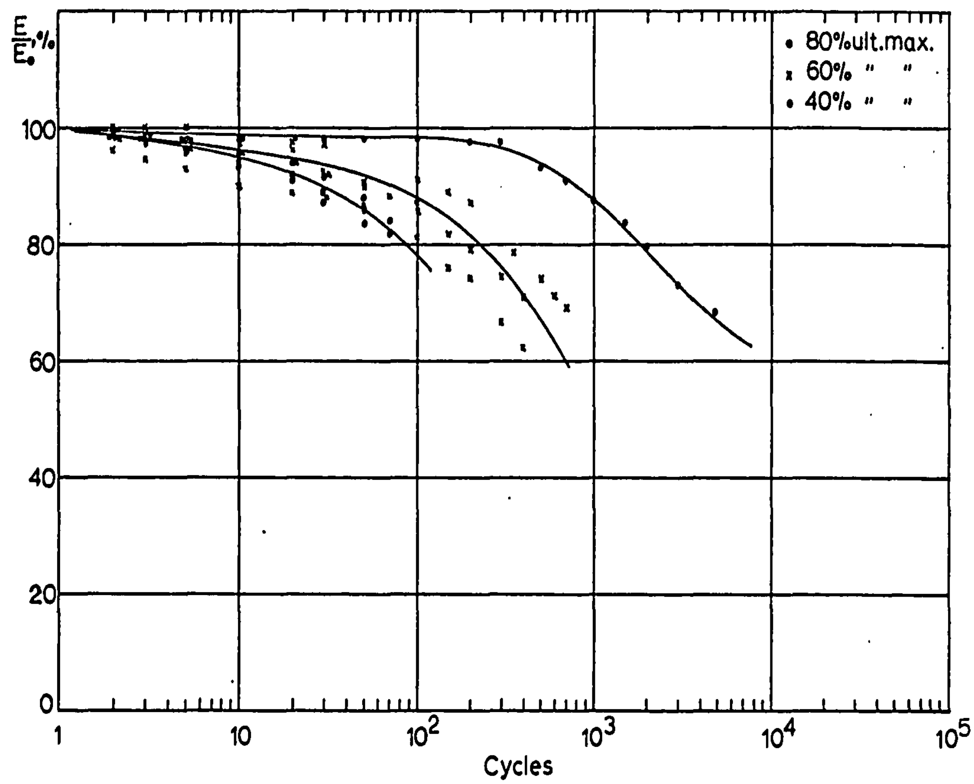

FIG.42. MODULUS RETENTION - Flexure 42%F.g. 0 Min.Stress

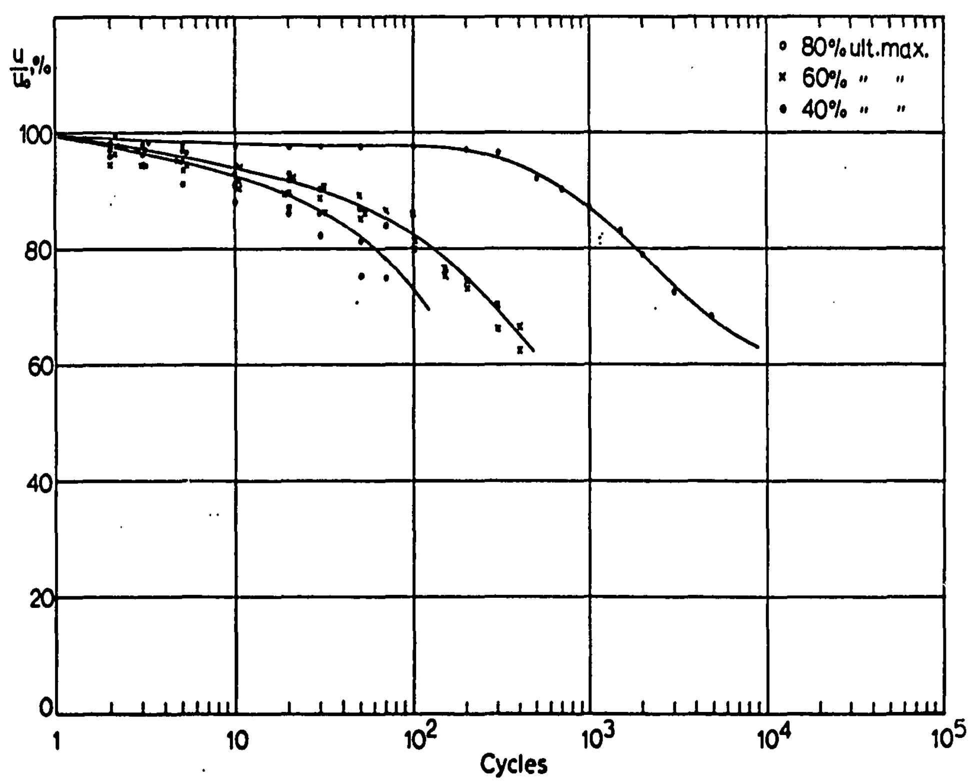

FIG.43. POISSON'S RATIO RETENTION

Tension 42%F.g. 0 Min.Stress

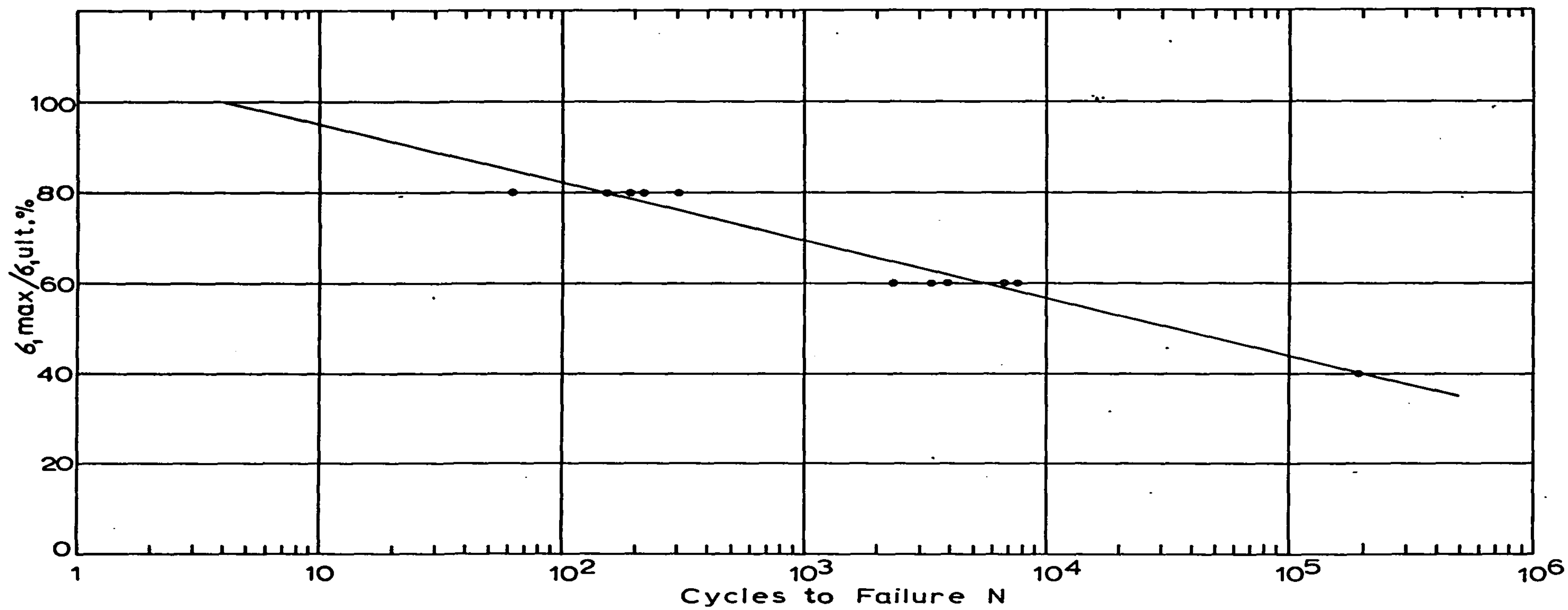

FIG.44. SN CURVE - Tension 42% Fiberglass 20% ult. Min. Stress

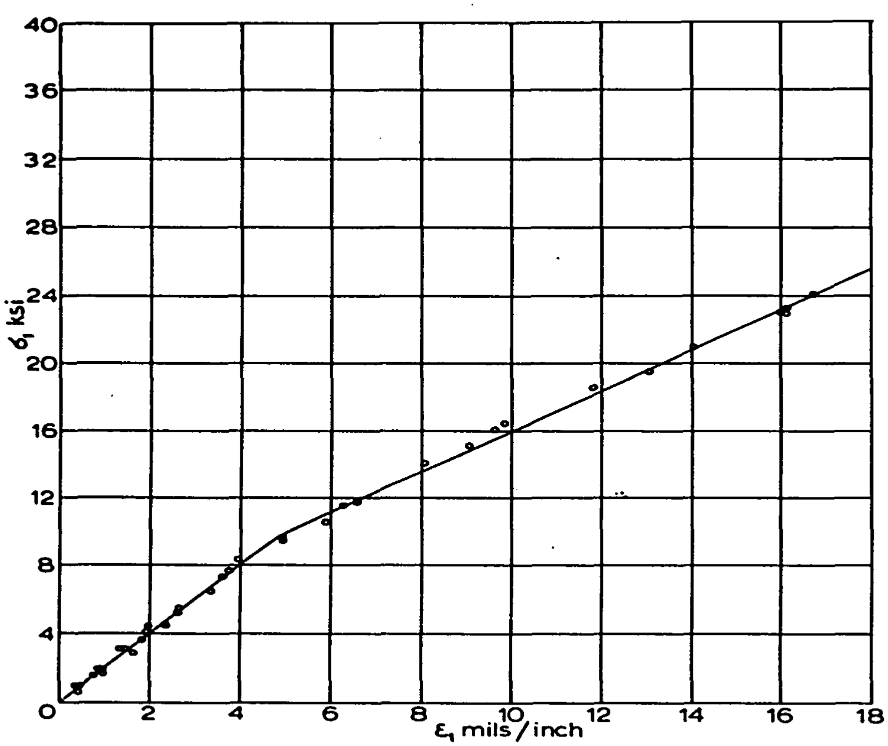

FIG.45. STRESS-STRAIN CURVE

Tension 42% Fiberglass Replicate 2

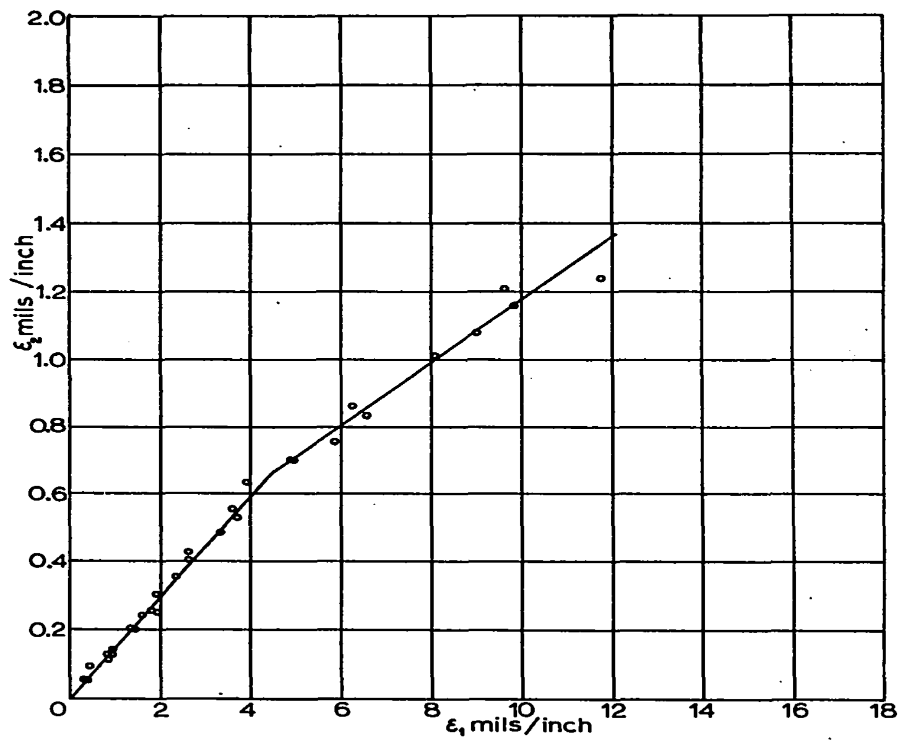

FIG.46. POISSON'S RATIOS

Tension 42% Fiberglass Replicate 2

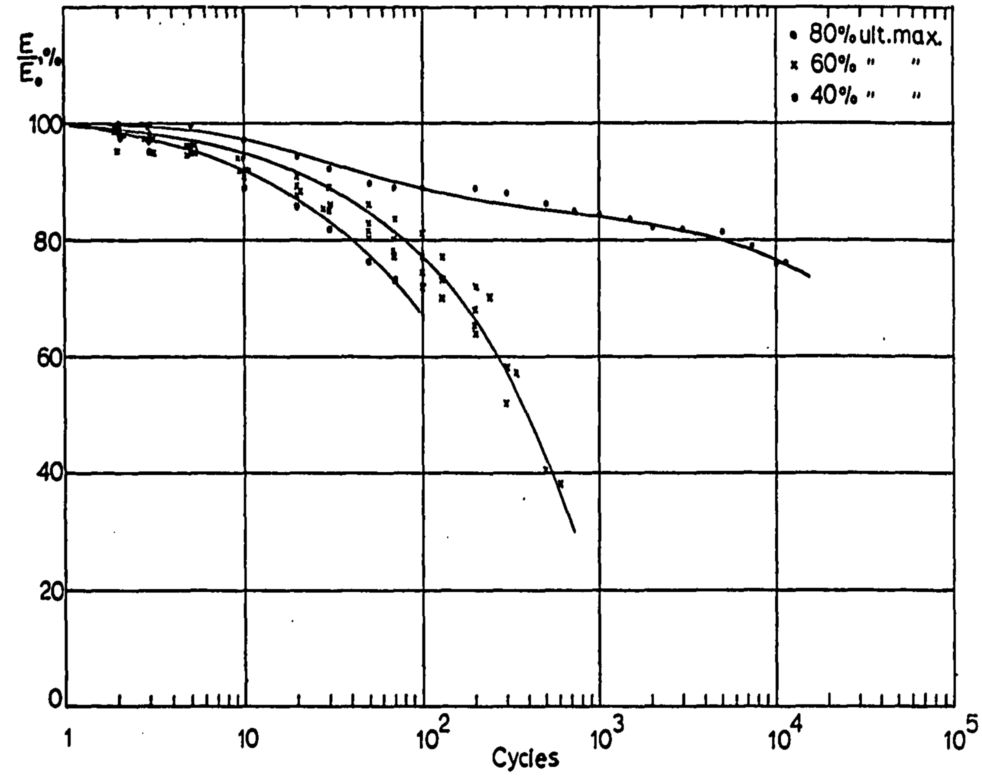

FIG.47. MODULUS RETENTION - Tension 42% F.g. 20% ult. Min.Stress

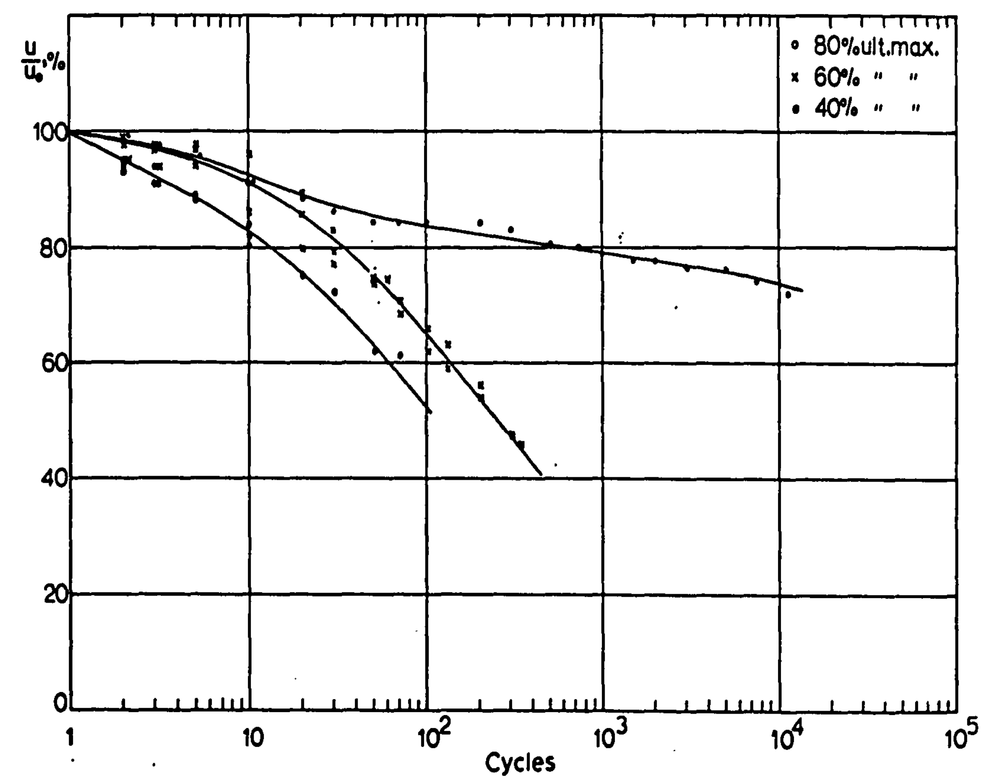

FIG.48. POISSON'S RATIO RETENTION

Tension 42% F.g. 20% ult Min.Stress

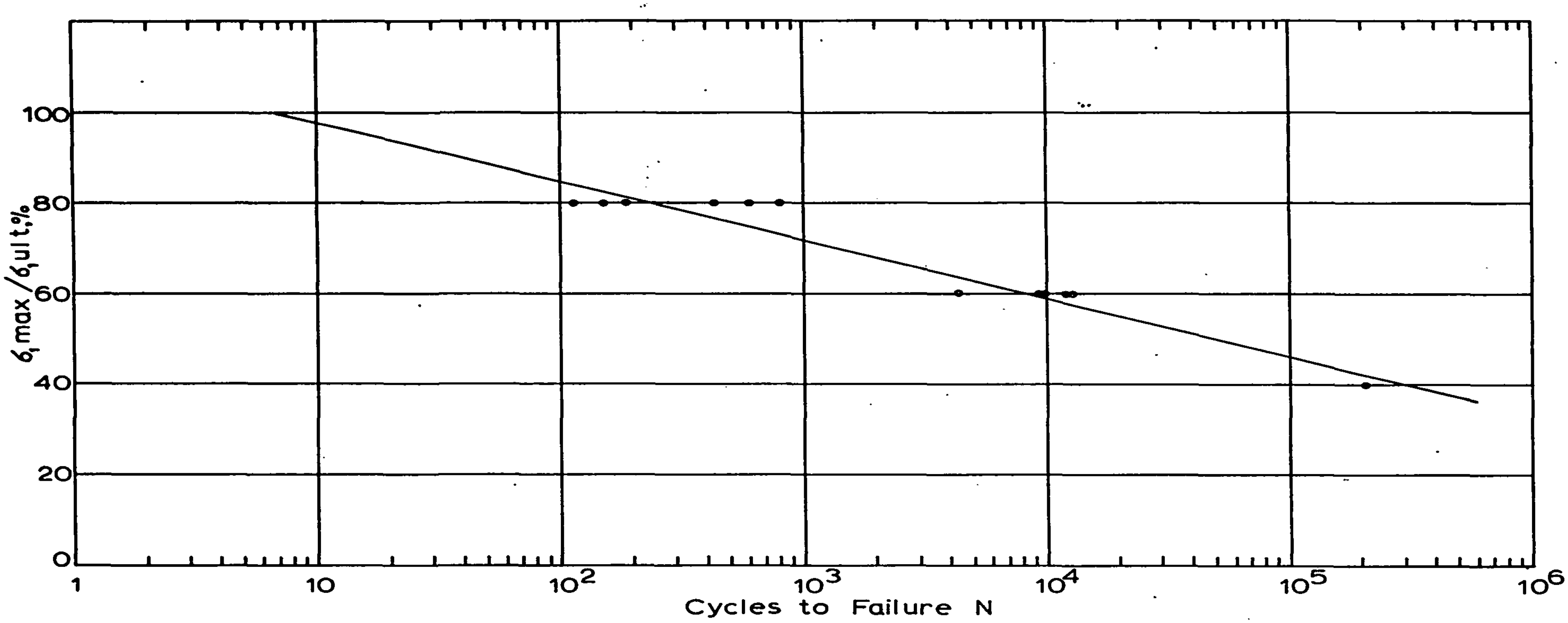

FIG.49. SN CURVE - Flexure 42% Fiberglass 20% ult. Min. Stress

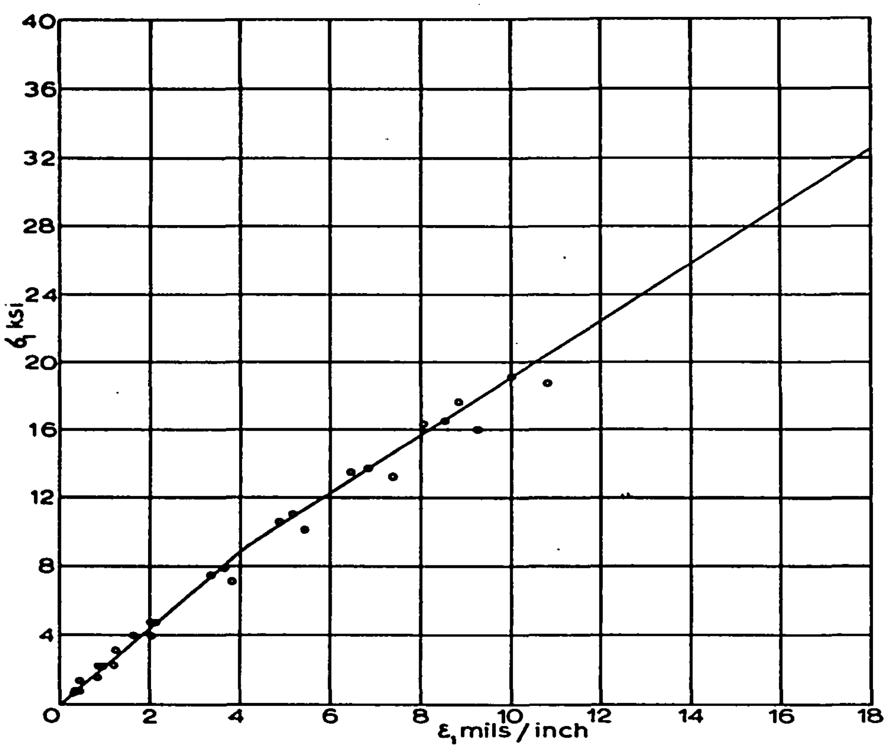

FIG.50. STRESS-STRAIN CURVE

Flexure 42% Fiberglass Replicate 2

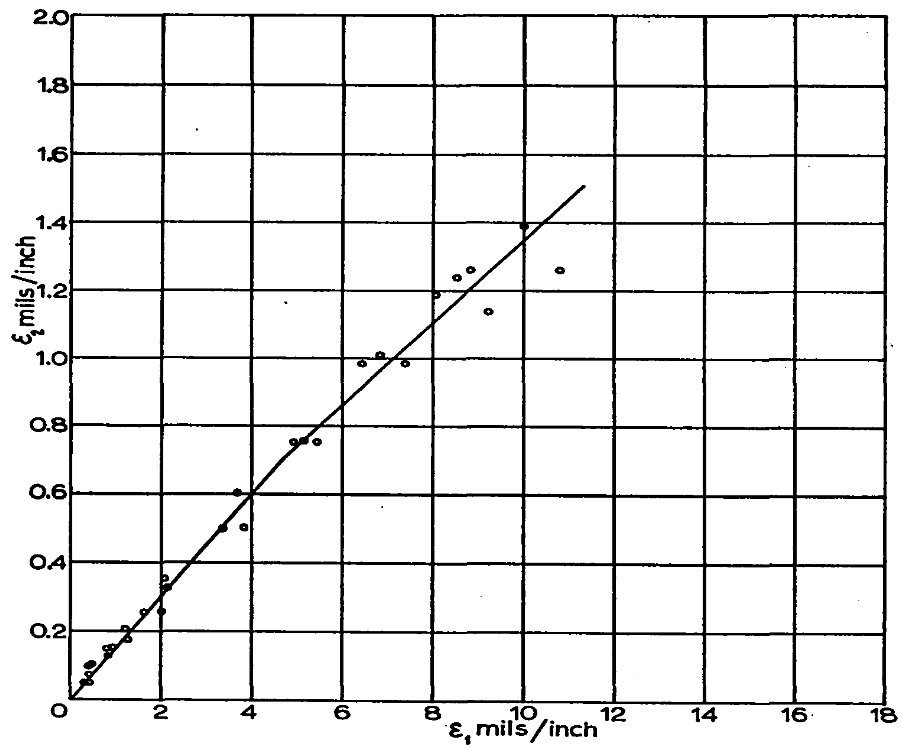

FIG.51. POISSON'S RATIOS

Flexure 42% Fiberglass Replicate 2

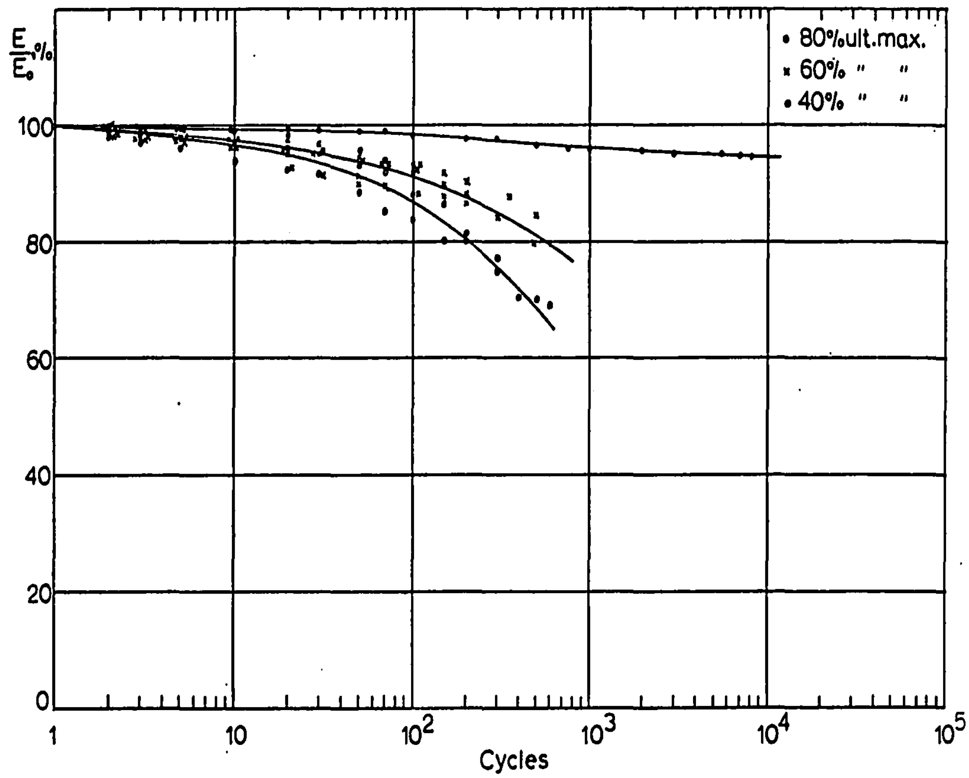

FIG.52. MODULUS RETENTION – Flexure 42% F.g. 20% ult. Min. Stress

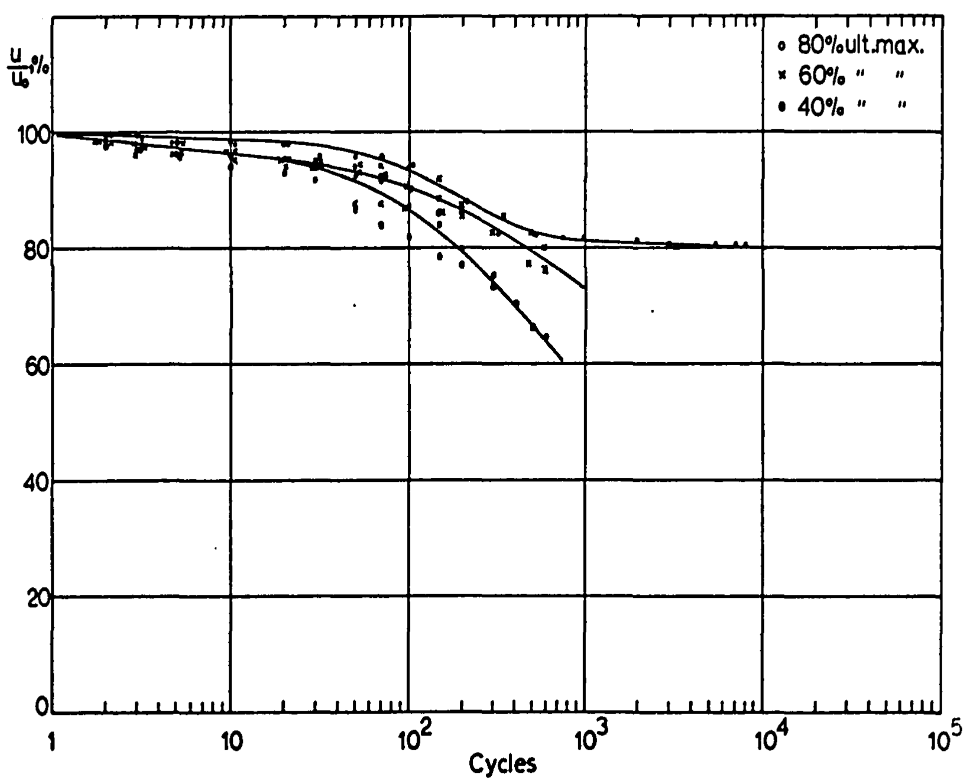

FIG.53. POISSON'S RATIO RETENTION
Flexure 42% F.g. 20% ult. Min. Stress

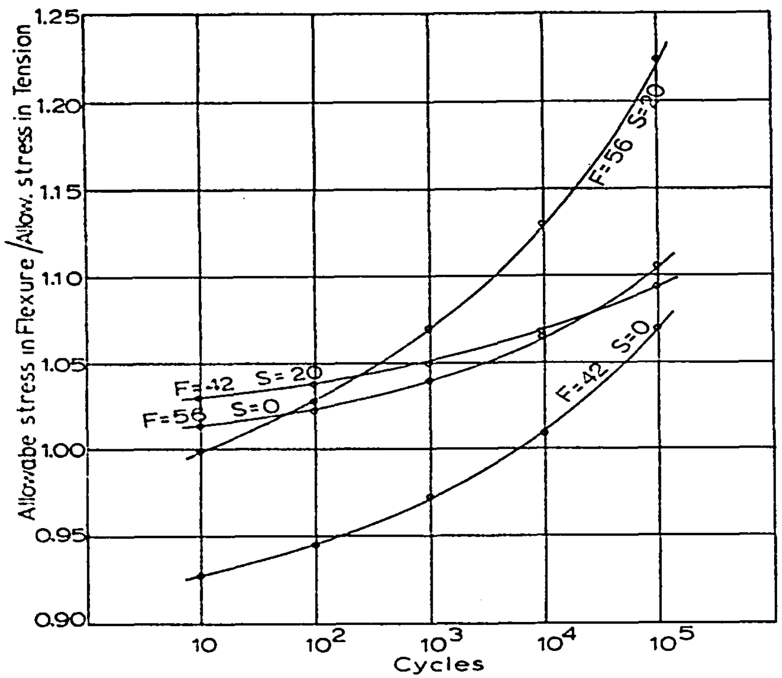

FIG.54. Effect of Test Mode on Fatigue Life Stresses

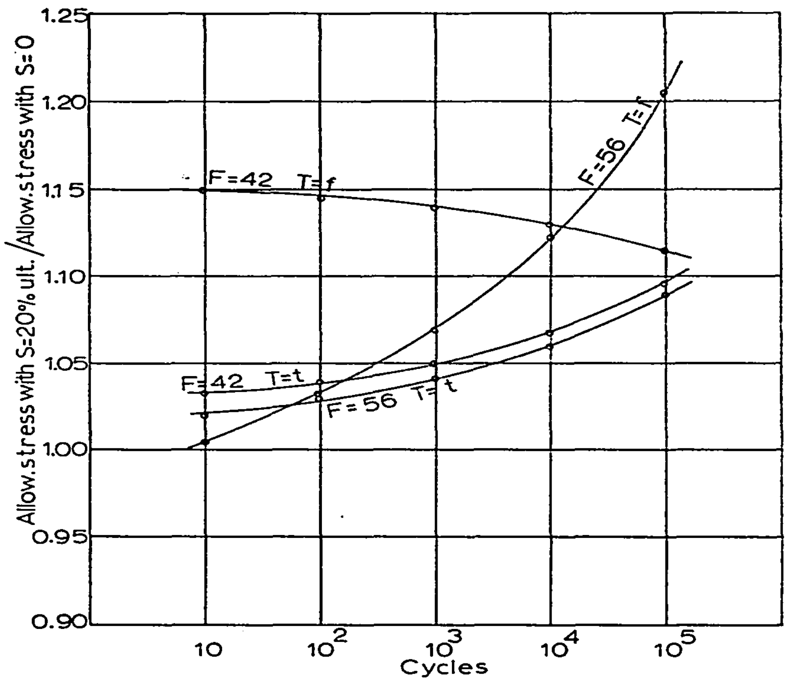

FIG.55. Effect of Min. Stress on Fatigue Life Stresses

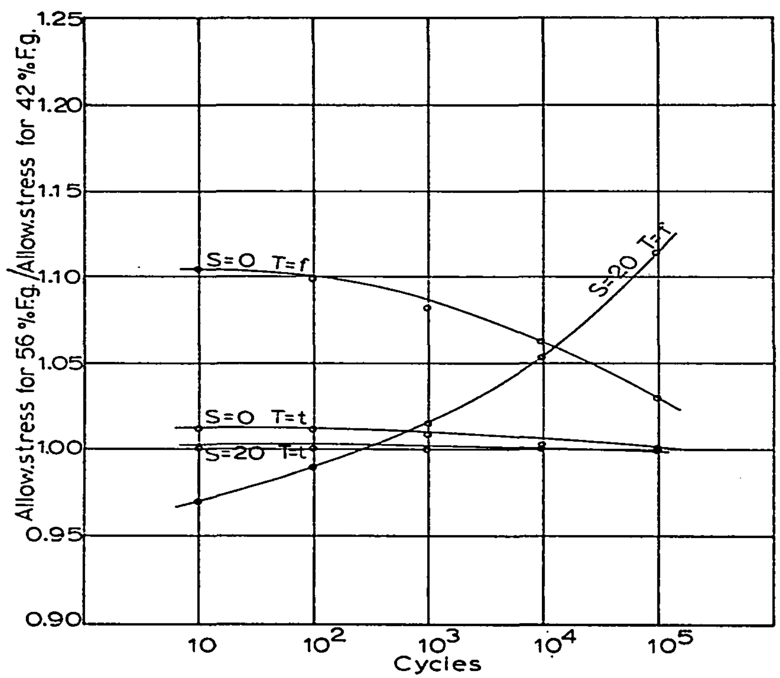

FIG.56. Effect of Fiberglass % on Fatigue Life Stresses

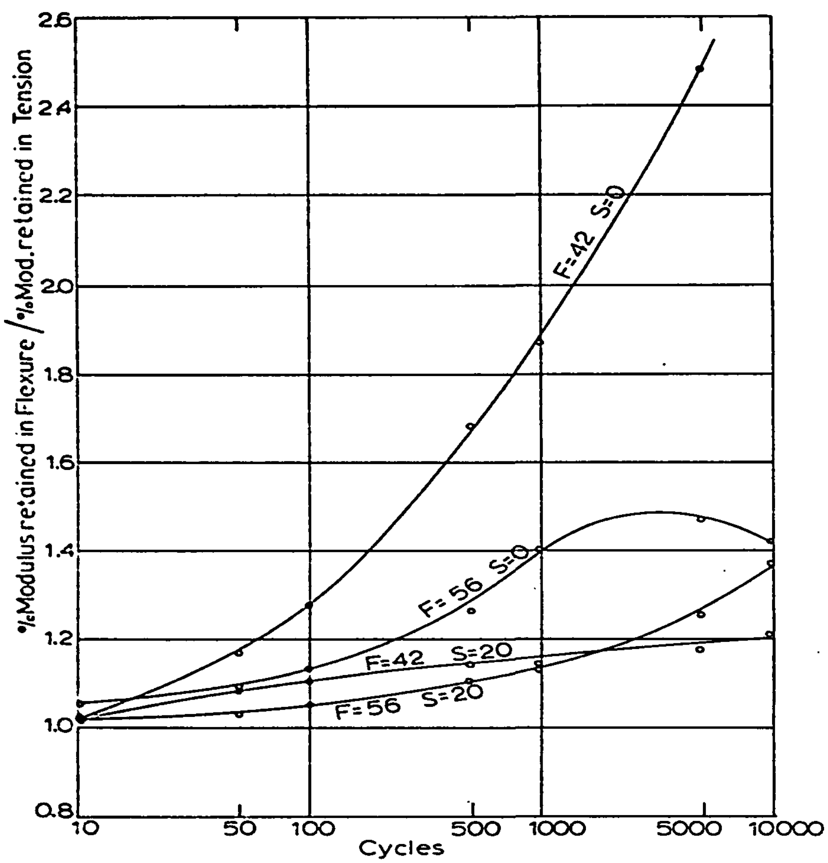

FIG. 57. Effect of Test Mode on Modulus Retention
40% ult. Max Stress

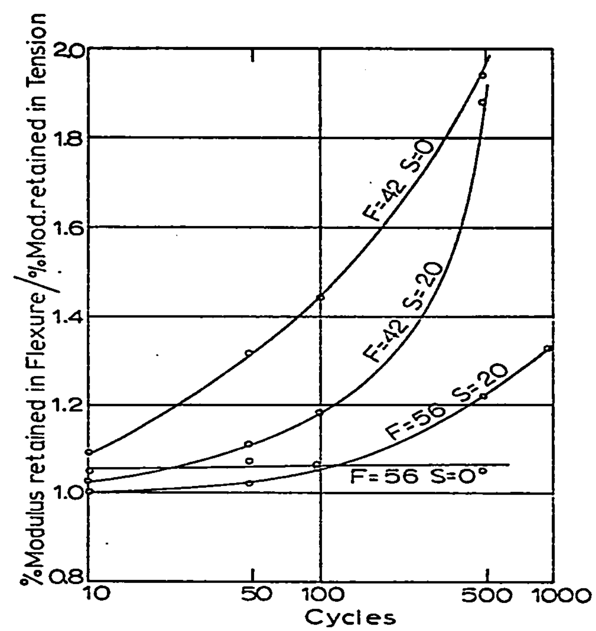

FIG. 58. Effect of Test Mode on Modulus Retention
60% ult. Max. Stress

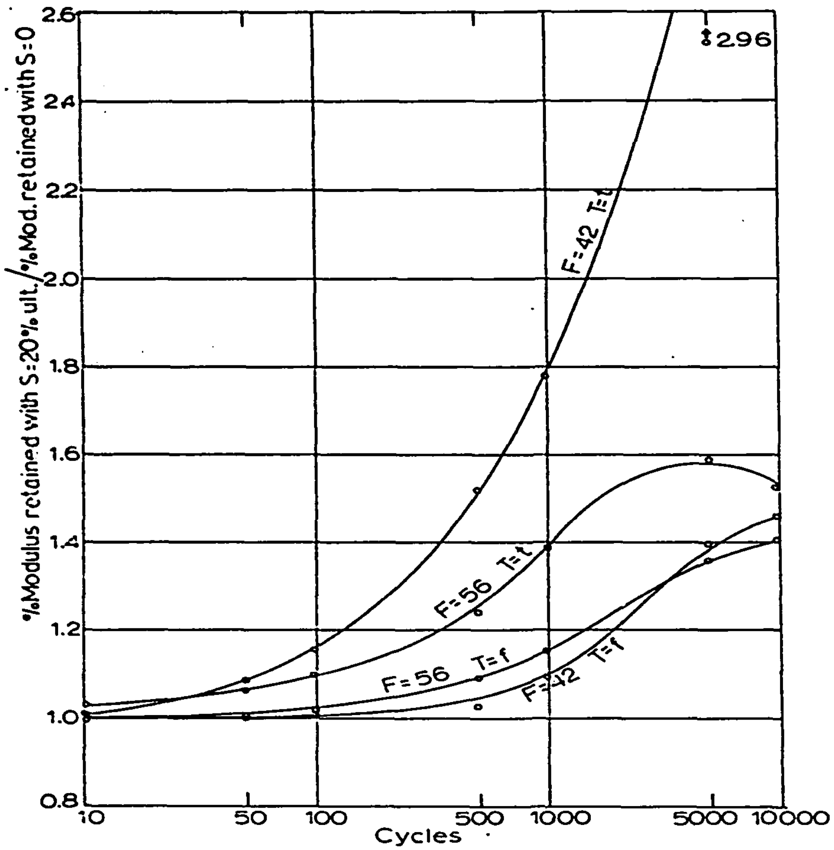

FIG.59. Effect of Min.Stress on Modulus Retention
40% ult. Max. Stress

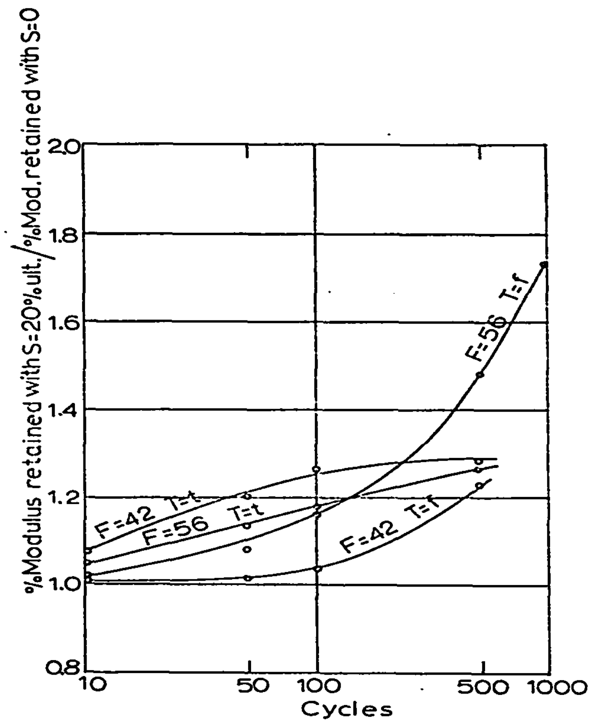

FIG.60. Effect of Min.Stress on Modulus Retention
60% ult. Max. Stress

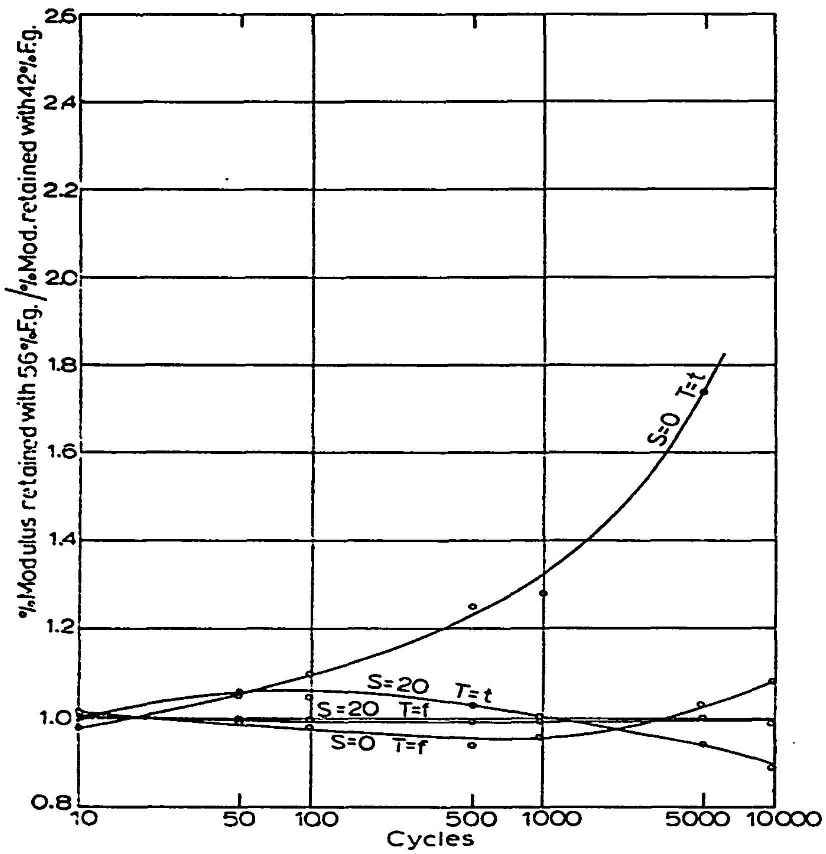

FIG.61. Effect of Fiberglass % on Modulus Retention
40% ult. Max. Stress

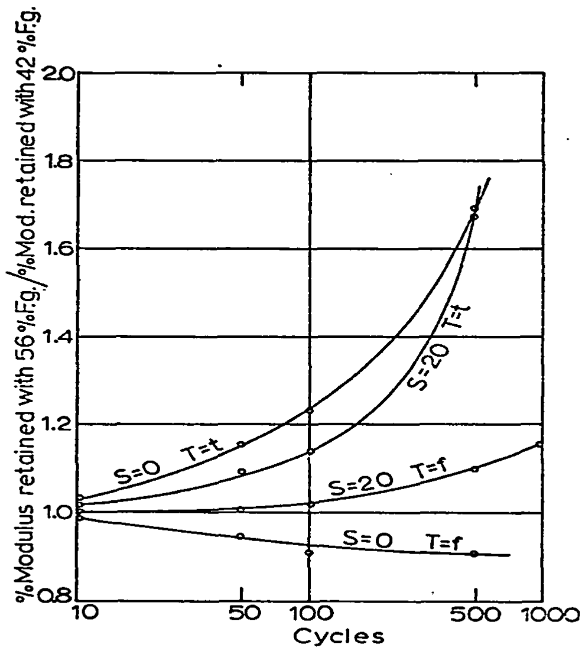

FIG.62. Effect of Fiberglass % on Modulus Retention
60% ult. Max. Stress

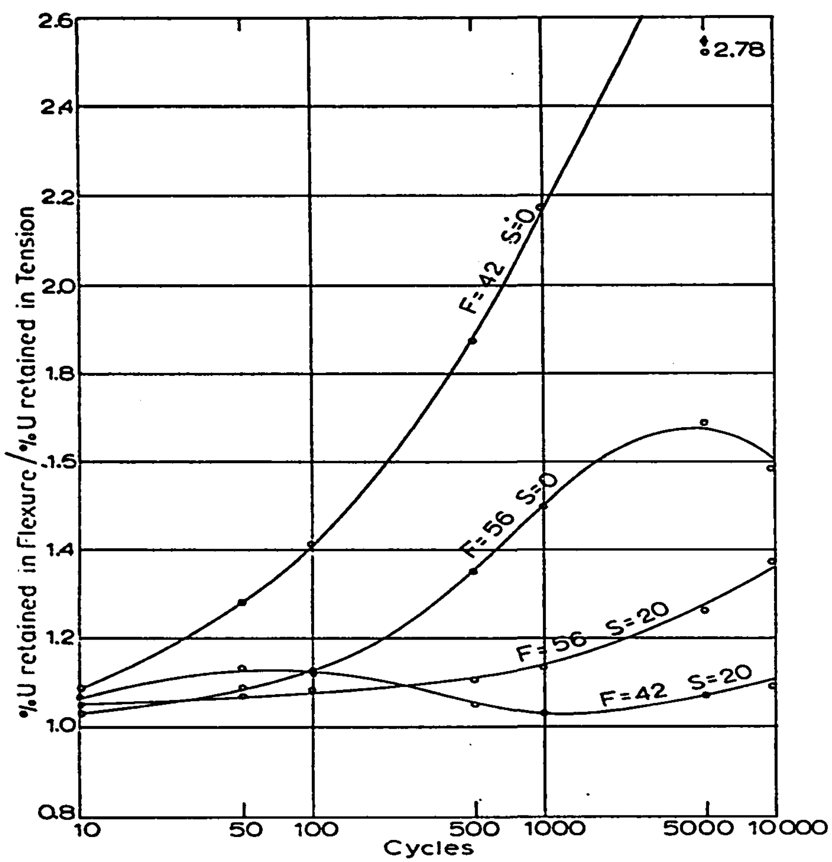

FIG.63. Effect of Test Mode on U Retention
40% ult. Max. Stress

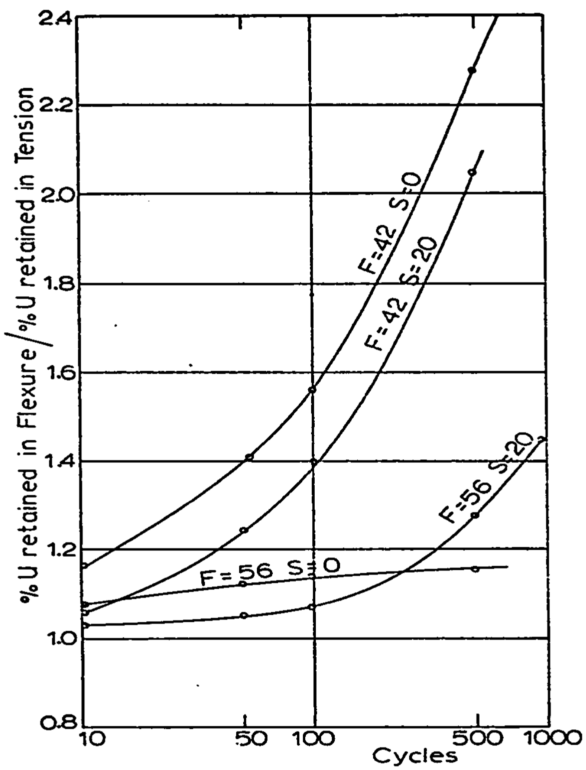

FIG.64. Effect of Test Mode on U Retention
60% ult. Max. Stress

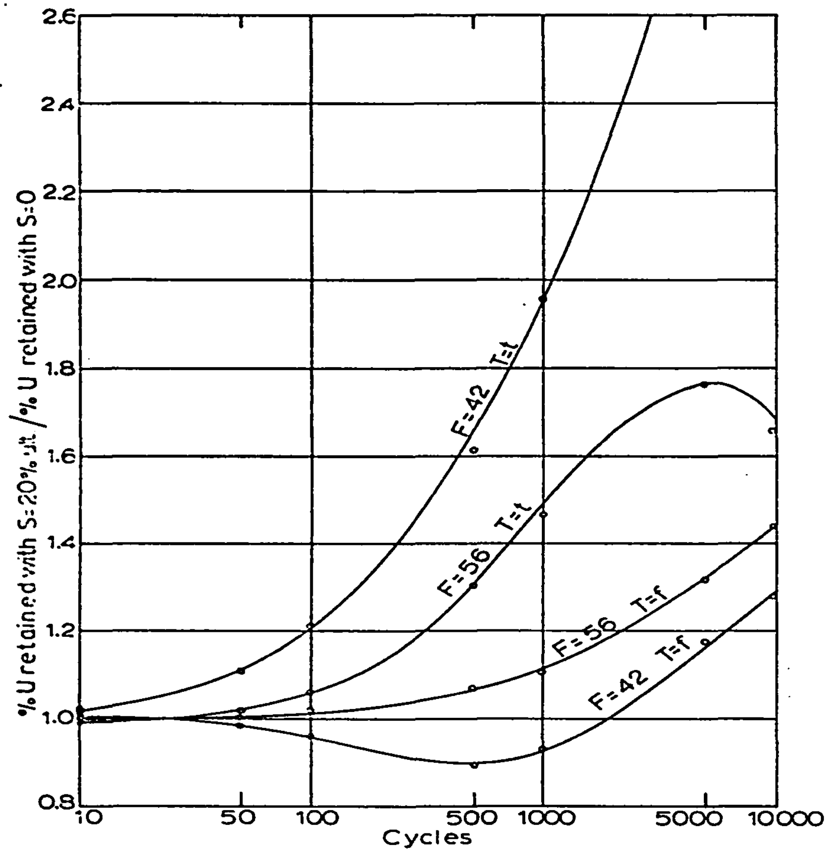

FIG. 65. Effect of Min. Stress on U Retention
40% ult Max. Stress

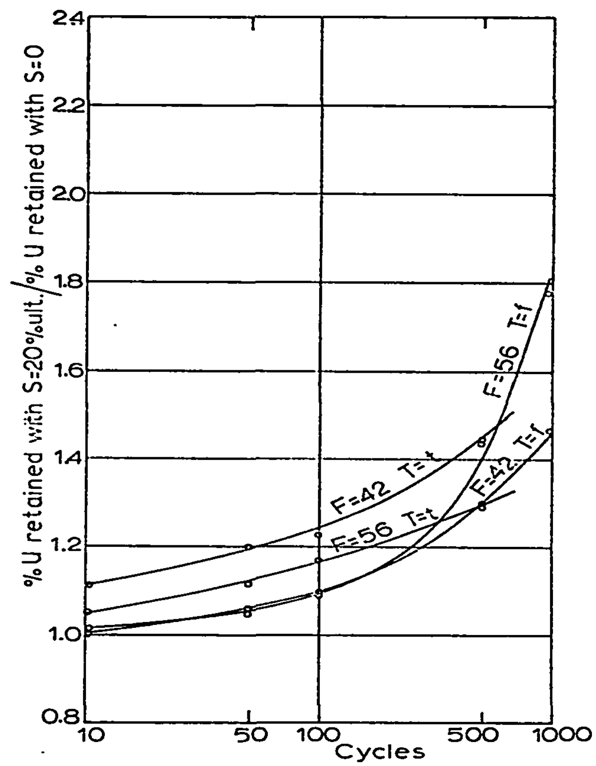

FIG. 66. Effect of Min. Stress on U Retention
60% ult. Max. Stress

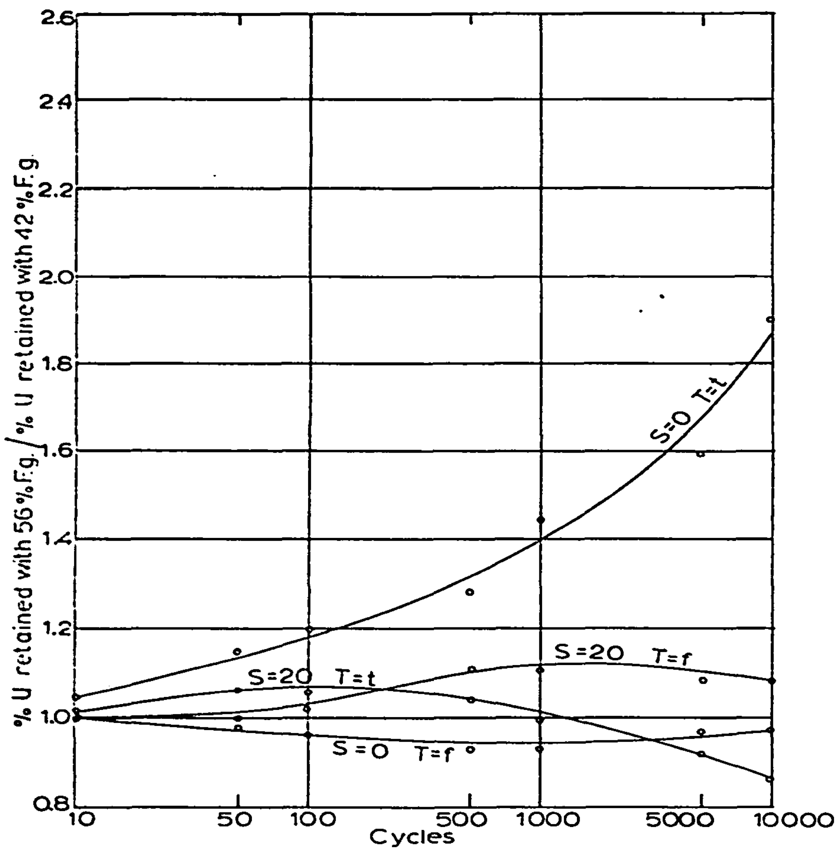

FIG.67. Effect of Fiberglass % on U Retention
40% ult. Max. Stress

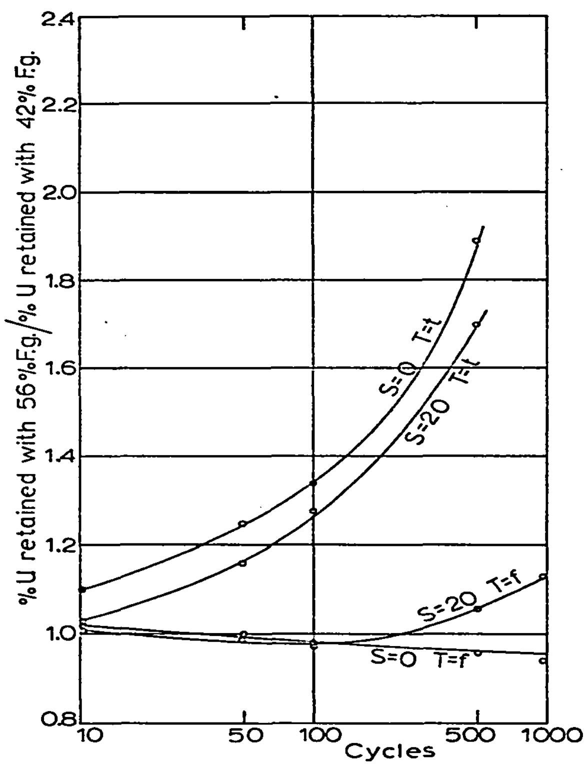

FIG.68. Effect of Fiberglass % on U Retention
60% ult. Max. Stress

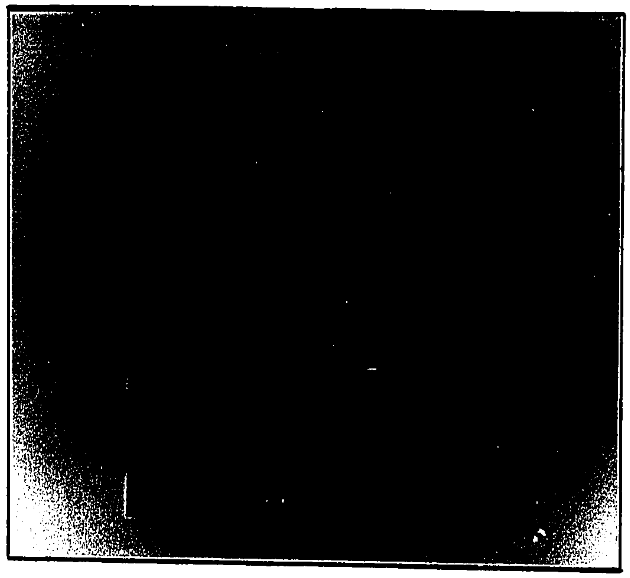

FIG.69. Typical Tensile Failures

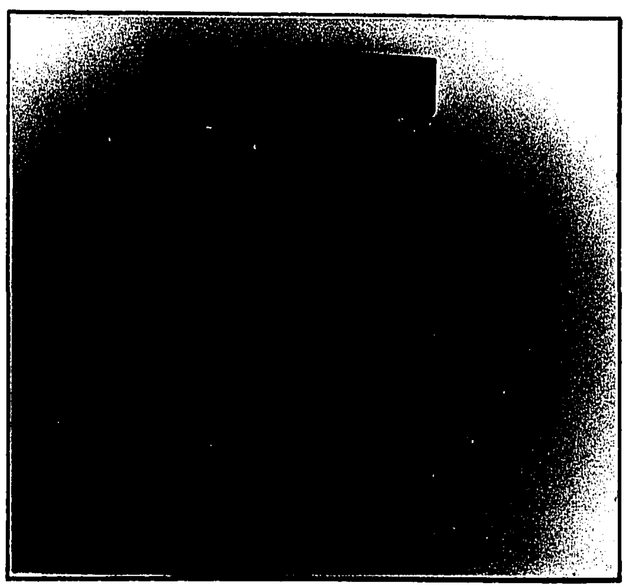

FIG.70. Typical Flexural Failures

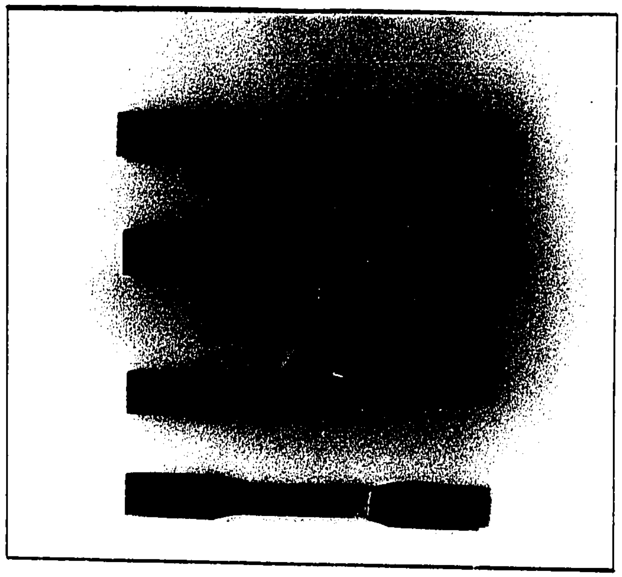

FIG.69. Typical Tensile Failures

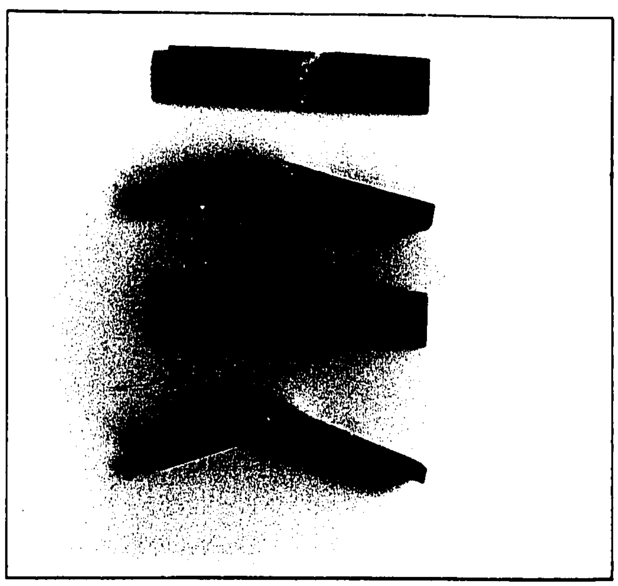

FIG.70. Typical Flexural Failures

Appendix B

Computer Programs

```
C
C     ..................................................................
C
C        SAMPLE MAIN PROGRAM FOR POLYNOMIAL REGRESSION - POLRG
C
C        PURPOSE
C           (1) READ THE PROBLEM PARAMETER CARD FOR A POLYNOMIAL REGRES-
C           SION, (2) CALL SUBROUTINES TO PERFORM THE ANALYSIS, (3)
C           PRINT THE REGRESSION COEFFICIENTS AND ANALYSIS OF VARIANCE
C           TABLE FOR POLYNOMIALS OF SUCCESSIVELY INCREASING DEGREES,
C           AND (4) OPTIONALLY PRINT THE TABLE OF RESIDUALS AND A PLOT
C           OF Y VALUES AND Y ESTIMATES.
C
C        REMARKS
C           THE NUMBER OF OBSERVATIONS, N, MUST BE GREATER THAN M+1,
C           WHERE M IS THE HIGHEST DEGREE POLYNOMIAL SPECIFIED.
C           IF THERE IS NO REDUCTION IN THE RESIDUAL SUM OF SQUARES
C           BETWEEN TWO SUCCESSIVE DEGREES OF THE POLYNOMIALS, THE
C           PROGRAM TERMINATES THE PROBLEM BEFORE COMPLETING THE ANALY-
C           SIS FOR THE HIGHEST DEGREE POLYNOMIAL SPECIFIED.
C
C        SUBROUTINES AND FUNCTION SUBPROGRAMS REQUIRED
C           GDATA
C           ORDER
C           MINV
C           MULTR
C           PLOT  (A SPECIAL PLOT SUBROUTINE PROVIDED FOR THE SAMPLE
C                 PROGRAM.)
C
C        METHOD
C           REFER TO B. OSTLE, 'STATISTICS IN RESEARCH', THE IOWA STATE
C           COLLEGE PRESS', 1954, CHAPTER 6.
C
C     ..................................................................
C
C     THE FOLLOWING DIMENSION MUST BE GREATER THAN OR EQUAL TO THE
C     PRODUCT OF N*(M+1), WHERE N IS THE NUMBER OF OBSERVATIONS AND M
C     IS THE HIGHEST DEGREE POLYNOMIAL SPECIFIED..
C
      DIMENSION X(1100)
C
C     THE FOLLOWING DIMENSION MUST BE GREATER THAN OR EQUAL TO THE
C     PRODUCT OF M*M..
C
      DIMENSION DI(100)
C
C     THE FOLLOWING DIMENSION MUST BE GREATER THAN OR EQUAL TO
C     (M+2)*(M+1)/2..
C
      DIMENSION D(66)
C
C     THE FOLLOWING DIMENSIONS MUST BE GREATER THAN OR EQUAL TO M..
C
      DIMENSION B(10),E(10),SB(10),T(10)
C
C     THE FOLLOWING DIMENSIONS MUST BE GREATER THAN OR EQUAL TO (M+1)..
C
```

```
      DIMENSION XBAR(11),STD(11),COE(11),SUMSQ(11),ISAVE(11)
C
C   THE FOLLOWING DIMENSION MUST BE GREATER THAN OR EQUAL TO 10..
C
      DIMENSION ANS(10)
C
C   THE FOLLOWING DIMENSION WILL BE USED IF THE PLOT OF OBSERVED DATA
C   AND ESTIMATES IS DESIRED.  THE SIZE OF THE DIMENSION, IN THIS
C   CASE, MUST BE GREATER THAN OR EQUAL TO N*3.  OTHERWISE, THE SIZE
C   OF DIMENSION MAY BE SET TO 1.
C
      DIMENSION P(300)
C
C   .............................................................
C
C      IF A DOUBLE PRECISION VERSION OF THIS ROUTINE IS DESIRED, THE
C      C IN COLUMN 1 SHOULD BE REMOVED FROM THE DOUBLE PRECISION
C      STATEMENT WHICH FOLLOWS.
C
C   DOUBLE PRECISION X,XBAR,STD,D,SUMSQ,DI,E,B,SB,T,ANS,DET,COE
C
C      THE C MUST ALSO BE REMOVED FROM DOUBLE PRECISION STATEMENTS
C      APPEARING IN OTHER ROUTINES USED IN CONJUNCTION WITH THIS
C      ROUTINE.
C
C      ..........................................................
C
    1 FORMAT(A4,A2,I5,I2,I1)
    2 FORMAT(2F6.0)
    3 FORMAT(27H1POLYNOMIAL REGRESSION......A4,A2/)
    4 FORMAT(23H0NUMBER OF OBSERVATIONS,I6//)
    5 FORMAT(32H0POLYNOMIAL REGRESSION OF DEGREE,I3)
    6 FORMAT(12H0  INTERCEPT,E20.7)
    7 FORMAT(26H0  REGRESSION COEFFICIENTS/(6E20.7))
    8 FORMAT(1H0/24X,24HANALYSIS OF VARIANCE FOR,I4,19H  DEGREE POLYNOMI
     1AL/)
    9 FORMAT(1H0,5X,19HSOURCE OF VARIATION,7X,9HDEGREE OF,7X,6HSUM OF,9X
     1,4HMEAN,10X,1HF,9X,20HIMPROVEMENT IN TERMS/33X,7HFREEDOM,8X,7HSQUA
     2RES,7X,6HSQUARE,7X,5HVALUE,8X,17HOF SUM OF SQUARES)
   10 FORMAT(20H0  DUE TO REGRESSION,12X,I6,F17.5,F14.5,F13.5,F20.5)
   11 FORMAT(32H   DEVIATION ABOUT REGRESSION   ,I6,F17.5,F14.5)
   12 FORMAT(8X,5HTOTAL,19X,I6,F17.5///)
   13 FORMAT(17H0  NO IMPROVEMENT)
   14 FORMAT(1H0//27X,18HTABLE OF RESIDUALS//16H OBSERVATION NO.,5X,7HX
     1VALUE,7X,7HY VALUE,7X,10HY ESTIMATE,7X,8HRESIDUAL/)
   15 FORMAT(1H0,3X,I6,F18.5,F14.5,F17.5,F15.5)
C
C   .............................................................
C
C   READ PROBLEM PARAMETER CARD
C
  100 READ (5,1) PR,PR1,N,M,NPLOT
C
C      PR....PROBLEM NUMBER (MAY BE ALPHAMERIC)
C      PR1...PROBLEM NUMBER (CONTINUED)
C      N.....NUMBER OF OBSERVATIONS
C      M.....HIGHEST DEGREE POLYNOMIAL SPECIFIED
C      NPLOT.OPTION CODE FOR PLOTTING
```

```
C              0  IF PLOT IS NOT DESIRED.
C              1  IF PLOT IS DESIRED.
C
C     PRINT PROBLEM NUMBER AND N.
C
      WRITE (6,3) PR,PR1
      WRITE (6,4) N
C
C     READ INPUT DATA
C
      L=N*M
      DO 110 I=1,N
      J=L+I
C
C        X(I) IS THE INDEPENDENT VARIABLE, AND X(J) IS THE DEPENDENT
C        VARIABLE.
C
  110 READ (5,2) X(I),X(J)
C
      CALL GDATA (N,M,X,XBAR,STD,D,SUMSQ)
C
      MM=M+1
      SUM=0.0
      NT=N-1
C
      DO 200 I=1,M
      ISAVE(I)=I
C
C     FORM SUBSET OF CORRELATION COEFFICIENT MATRIX
C
      CALL ORDER (MM,D,MM,I,ISAVE,DI,E)
C
C     INVERT THE SUBMATRIX OF CORRELATION COEFFICIENTS
C
      CALL MINV (DI,I,DET,B,T)
C
      CALL MULTR (N,I,XBAR,STD,SUMSQ,DI,E,ISAVE,B,SB,T,ANS)
C
C     PRINT THE RESULT OF CALCULATION
C
      WRITE (6,5) I
      IF(ANS(7)) 140,130,130
  130 SUMIP=ANS(4)-SUM
      IF(SUMIP) 140, 140, 150
  140 WRITE (6,13)
      GO TO 210
  150 WRITE (6,6) ANS(1)
      WRITE (6,7) (B(J),J=1,I)
      WRITE (6,8) I
      WRITE (6,9)
      SUM=ANS(4)
      WRITE (6,10) I,ANS(4),ANS(6),ANS(10),SUMIP
      NI=ANS(8)
      WRITE (6,11) NI,ANS(7),ANS(9)
      WRITE (6,12) NT,SUMSQ(MM)
C
C     SAVE COEFFICIENTS FOR CALCULATION OF Y ESTIMATES
C
```

```
      COE(1)=ANS(1)
      DO 160 J=1,I
  160 COE(J+1)=B(J)
      LA=I
  200 CONTINUE
C
C     TEST WHETHER PLOT IS DESIRED.
C
  210 IF(NPLOT) 100, 100, 220
C
C         CALCULATE ESTIMATES
C
  220 NP3=N+N
      DO 230 I=1,N
      NP3=NP3+1
      P(NP3)=COE(1)
      L=I
      DO 230 J=1,LA
      P(NP3)=P(NP3)+X(L)*COE(J+1)
  230 L=L+N
C
C         COPY OBSERVED DATA
C
      N2=N
      L=N*M
      DO 240 I=1,N
      P(I)=X(I)
      N2=N2+1
      L=L+1
  240 P(N2)=X(L)
C
C     PRINT TABLE OF RESIDUALS
C
      WRITE (6,3) PR,PR1
      WRITE (6,5) LA
      WRITE (6,14)
      NP2=N
      NP3=N+N
      DO 250 I=1,N
      NP2=NP2+1
      NP3=NP3+1
      RESID=P(NP2)-P(NP3)
  250 WRITE (6,15) I,P(I),P(NP2),P(NP3),RESID
C
      CALL PLOT (LA,P,N,3,0,1)
C
      GO TO 100
      END
C
C     ...............................................................
C
C        SUBROUTINE PLOT
C
C        PURPOSE
C           PLOT SEVERAL CROSS-VARIABLES VERSUS A BASE VARIABLE
C
C        USAGE
C           CALL PLOT (NO,A,N,M,NL,NS)
```

```
C
C        DESCRIPTION OF PARAMETERS
C           NO - CHART NUMBER (3 DIGITS MAXIMUM)
C           A  - MATRIX OF DATA TO BE PLOTTED. FIRST COLUMN REPRESENTS
C                BASE VARIABLE AND SUCCESSIVE COLUMNS ARE THE CROSS-
C                VARIABLES (MAXIMUM IS 9).
C           N  - NUMBER OF ROWS IN MATRIX A
C           M  - NUMBER OF COLUMNS IN MATRIX A (EQUAL TO THE TOTAL
C                NUMBER OF VARIABLES). MAXIMUM IS 10.
C           NL - NUMBER OF LINES IN THE PLOT. IF 0 IS SPECIFIED, 50
C                LINES ARE USED.
C           NS - CODE FOR SORTING THE BASE VARIABLE DATA IN ASCENDING
C                ORDER
C                  0  SORTING IS NOT NECESSARY (ALREADY IN ASCENDING
C                     ORDER).
C                  1  SORTING IS NECESSARY.
C
C        REMARKS
C           NONE
C
C        SUBROUTINES AND FUNCTION SUBPROGRAMS REQUIRED
C           NONE
C
C     ..................................................................
C
      SUBROUTINE PLOT(NO,A,N,M,NL,NS)
      DIMENSION OUT(101),YPR(11),ANG(9),A(1)
C
    1 FORMAT(1H1,60X,7H CHART ,I3,//)
    2 FORMAT(1H ,F11.4,5X,101A1)
    3 FORMAT(1H )
    4 FORMAT(10H 123456789)
    5 FORMAT(10A1)
    7 FORMAT(1H ,16X,101H.         .         .         .         .
     1    .         .         .         .         .         .)
    8 FORMAT(1H0,9X,11F10.4)
C
C     ..................................................................
C
      NLL=NL
C
      IF(NS) 16, 16, 10
C
C        SORT BASE VARIABLE DATA IN ASCENDING ORDER
C
   10 DO 15 I=1,N
      DO 14 J=I,N
      IF(A(I)-A(J)) 14, 14, 11
   11 L=I-N
      LL=J-N
      DO 12 K=1,M
      L=L+N
      LL=LL+N
      F=A(L)
      A(L)=A(LL)
   12 A(LL)=F
   14 CONTINUE
   15 CONTINUE
```

```
C
C        TEST NLL
C
   16 IF(NLL) 20, 18, 20
   18 NLL=50
C
C        PRINT TITLE
C
   20 WRITE(6,1)NO
C
C        DEVELOP BLANK AND DIGITS FOR PRINTING
C
      REWIND 13
      WRITE (13,4)
      REWIND 13
      READ (13,5) BLANK,(ANG(I),I=1,9)
      REWIND 13
C
C        FIND SCALE FOR BASE VARIABLE
C
      XSCAL=(A(N)-A(1))/(FLOAT(NLL-1))
C
C        FIND SCALE FOR CROSS-VARIABLES
C
      M1=N+1
      YMIN=A(M1)
      YMAX=YMIN
      M2=M*N
      DO 40 J=M1,M2
      IF(A(J)-YMIN) 28,26,26
   26 IF(A(J)-YMAX) 40,40,30
   28 YMIN=A(J)
      GO TO 40
   30 YMAX=A(J)
   40 CONTINUE
      YSCAL=(YMAX-YMIN)/100.0
C
C        FIND BASE VARIABLE PRINT POSITION
C
      XB=A(1)
      L=1
      MY=M-1
      I=1
   45 F=I-1
      XPR=XB+F*XSCAL
      IF(A(L)-XPR) 50,50,70
C
C        FIND CROSS-VARIABLES
C
   50 DO 55 IX=1,101
   55 OUT(IX)=BLANK
      DO 60 J=1,MY
      LL=L+J*N
      JP=((A(LL)-YMIN)/YSCAL)+1.0
      OUT(JP)=ANG(J)
   60 CONTINUE
C
C        PRINT LINE AND CLEAR, OR SKIP
```

```
C                                                                       PLOT1270
      WRITE(6,2)XPR,(OUT(IZ),IZ=1,101)                                  PLOT1280
      L=L+1                                                             PLOT1290
      GO TO 80                                                          PLOT1300
   70 WRITE(6,3)                                                        PLOT1310
   80 I=I+1                                                             PLOT1320
      IF(I-NLL) 45, 84, 86                                              PLOT1330
   84 XPR=A(N)                                                          PLOT1340
      GO TO 50                                                          PLOT1350
C                                                                       PLOT1360
C        PRINT CROSS-VARIABLES NUMBERS                                  PLOT1370
C                                                                       PLOT1380
   86 WRITE(6,7)                                                        PLOT1390
      YPR(1)=YMIN                                                       PLOT1400
      DO 90 KN=1,9                                                      PLOT1410
   90 YPR(KN+1)=YPR(KN)+YSCAL*10.0                                      PLOT1420
      YPR(11)=YMAX                                                      PLOT1430
      WRITE(6,8)(YPR(IP),IP=1,11)                                       PLOT1440
      RETURN                                                            PLOT1450
      END                                                               PLOT1460
```

```
C
C     ..................................................................
C
C        SUBROUTINE GDATA
C
C        PURPOSE
C           GENERATE INDEPENDENT VARIABLES UP TO THE M-TH POWER (THE
C           HIGHEST DEGREE POLYNOMIAL SPECIFIED) AND COMPUTE MEANS,
C           STANDARD DEVIATIONS, AND CORRELATION COEFFICIENTS.  THIS
C           SUBROUTINE IS NORMALLY CALLED BEFORE SUBROUTINES ORDER,
C           MINV AND MULTR IN THE PERFORMANCE OF A POLYNOMIAL
C           REGRESSION.
C
C        USAGE
C           CALL GDATA (N,M,X,XBAR,STD,D,SUMSQ)
C
C        DESCRIPTION OF PARAMETERS
C           N     - NUMBER OF OBSERVATIONS.
C           M     - THE HIGHEST DEGREE POLYNOMIAL TO BE FITTED.
C           X     - INPUT MATRIX (N BY M+1) .  WHEN THE SUBROUTINE IS
C                   CALLED, DATA FOR THE INDEPENDENT VARIABLE ARE
C                   STORED IN THE FIRST COLUMN OF MATRIX X, AND DATA FOR
C                   THE DEPENDENT VARIABLE ARE STORED IN THE LAST
C                   COLUMN OF THE MATRIX.  UPON RETURNING TO THE
C                   CALLING ROUTINE, GENERATED POWERS OF THE INDEPENDENT
C                   VARIABLE ARE STORED IN COLUMNS 2 THROUGH M.
C           XBAR  - OUTPUT VECTOR OF LENGTH M+1 CONTAINING MEANS OF
C                   INDEPENDENT AND DEPENDENT VARIABLES.
C           STD   - OUTPUT VECTOR OF LENGTH M+1 CONTAINING STANDARD
C                   DEVIATIONS OF INDEPENDENT AND DEPENDENT VARIABLES.
C           D     - OUTPUT MATRIX (ONLY UPPER TRIANGULAR PORTION OF THE
C                   SYMMETRIC MATRIX OF M+1 BY M+1) CONTAINING CORRELA-
C                   TION COEFFICIENTS.  (STORAGE MODE OF 1)
C           SUMSQ - OUTPUT VECTOR OF LENGTH M+1 CONTAINING SUMS OF
C                   PRODUCTS OF DEVIATIONS FROM MEANS  OF INDEPENDENT
C                   AND DEPENDENT VARIABLES.
C
C        REMARKS
C           N MUST BE GREATER THAN M+1.
C           IF M IS EQUAL TO 5 OR GREATER, SINGLE PRECISION MAY NOT BE
C           SUFFICIENT TO GIVE SATISFACTORY COMPUTATIONAL RESULTS.
C
C        SUBROUTINES AND FUNCTION SUBPROGRAMS REQUIRED
C           NONE
C
C        METHOD
C           REFER TO B. OSTLE, 'STATISTICS IN RESEARCH', THE IOWA STATE
C           COLLEGE PRESS, 1954, CHAPTER 6.
C
C     ..................................................................
C
      SUBROUTINE GDATA (N,M,X,XBAR,STD,D,SUMSQ)
      DIMENSION X(1),XBAR(1),STD(1),D(1),SUMSQ(1)
C
C        ...............................................................
C
C        IF A DOUBLE PRECISION VERSION OF THIS ROUTINE IS DESIRED, THE
```

```
C        C IN COLUMN 1 SHOULD BE REMOVED FROM THE DOUBLE PRECISION
C        STATEMENT WHICH FOLLOWS.
C
C     DOUBLE PRECISION X,XBAR,STD,D,SUMSQ,T1,T2
C
C        THE C MUST ALSO BE REMOVED FROM DOUBLE PRECISION STATEMENTS
C        APPEARING IN OTHER ROUTINES USED IN CONJUNCTION WITH THIS
C        ROUTINE.
C
C        THE DOUBLE PRECISION VERSION OF THIS SUBROUTINE MUST ALSO
C        CONTAIN DOUBLE PRECISION FORTRAN FUNCTIONS.  SQRT AND ABS IN
C        STATEMENT 180 MUST BE CHANGED TO DSQRT AND DABS.
C
C        ...........................................................
C
C     GENERATE INDEPENDENT VARIABLES
C
      IF(M-1) 105, 105, 90
   90 L1=0
      DO 100 I=2,M
      L1=L1+N
      DO 100 J=1,N
      L=L1+J
      K=L-N
  100 X(L)=X(K)*X(J)
C
C     CALCULATE MEANS
C
  105 MM=M+1
      DF=N
      L=0
      DO 115 I=1,MM
      XBAR(I)=0.0
      DO 110 J=1,N
      L=L+1
  110 XBAR(I)=XBAR(I)+X(L)
  115 XBAR(I)=XBAR(I)/DF
C
      DO 130 I=1,MM
  130 STD(I)=0.0
C
C     CALCULATE SUMS OF CROSS-PRODUCTS OF DEVIATIONS
C
      L=((MM+1)*MM)/2
      DO 150 I=1,L
  150 D(I)=0.0
      DO 170 K=1,N
      L=0
      DO 170 J=1,MM
      L2=N*(J-1)+K
      T2=X(L2)-XBAR(J)
      STD(J)=STD(J)+T2
      DO 170 I=1,J
      L1=N*(I-1)+K
      T1=X(L1)-XBAR(I)
      L=L+1
  170 D(L)=D(L)+T1*T2
      L=0
```

```fortran
      DO 175 J=1,MM                                                     GDAT1160
      DO 175 I=1,J                                                      GDAT1170
      L=L+1                                                             GDAT1180
  175 D(L)=D(L)-STD(I)*STD(J)/DF                                        GDAT1190
      L=0                                                               GDAT1200
      DO 180 I=1,MM                                                     GDAT1210
      L=L+I                                                             GDAT1220
      SUMSQ(I)=D(L)                                                     GDAT1230
  180 STD(I)= SQRT( ABS(D(L)))                                          GDAT1240
C                                                                       GDAT1250
C     CALCULATE CORRELATION COEFFICIENTS                                GDAT1260
C                                                                       GDAT1270
      L=0                                                               GDAT1280
      DO 190 J=1,MM                                                     GDAT1290
      DO 190 I=1,J                                                      GDAT1300
      L=L+1                                                             GDAT1310
  190 D(L)=D(L)/(STD(I)*STD(J))                                         GDAT1320
C                                                                       GDAT1330
C     CALCULATE STANDARD DEVIATIONS                                     GDAT1340
C                                                                       GDAT1350
      DF=SQRT(DF-1.0)                                                   GDAT1360
      DO 200 I=1,MM                                                     GDAT1370
  200 STD(I)=STD(I)/DF                                                  GDAT1380
      RETURN                                                            GDAT1390
      END                                                               GDAT1400
```

```
C
C     ..................................................................
C
C        SUBROUTINE ORDER
C
C        PURPOSE
C           CONSTRUCT FROM A LARGER MATRIX OF CORRELATION COEFFICIENTS
C           A SUBSET MATRIX OF INTERCORRELATIONS AMONG INDEPENDENT
C           VARIABLES AND A VECTOR OF INTERCORRELATIONS OF INDEPENDENT
C           VARIABLES WITH DEPENDENT VARIABLE.  THIS SUBROUTINE IS
C           NORMALLY USED IN THE PERFORMANCE OF MULTIPLE AND POLYNOMIAL
C           REGRESSION ANALYSES.
C
C        USAGE
C           CALL ORDER (M,R,NDEP,K,ISAVE,RX,RY)
C
C        DESCRIPTION OF PARAMETERS
C           M     - NUMBER OF VARIABLES AND ORDER OF MATRIX R.
C           R     - INPUT MATRIX CONTAINING CORRELATION COEFFICIENTS.
C                   THIS SUBROUTINE EXPECTS ONLY UPPER TRIANGULAR
C                   PORTION OF THE SYMMETRIC MATRIX TO BE STORED (BY
C                   COLUMN) IN R.  (STORAGE MODE OF 1)
C           NDEP  - THE SUBSCRIPT NUMBER OF THE DEPENDENT VARIABLE.
C           K     - NUMBER OF INDEPENDENT VARIABLES TO BE INCLUDED
C                   IN THE FORTHCOMING REGRESSION. K MUST BE GREATER
C                   THAN OR EQUAL TO 1.
C           ISAVE - INPUT VECTOR OF LENGTH K+1 CONTAINING, IN ASCENDING
C                   ORDER, THE SUBSCRIPT NUMBERS OF K INDEPENDENT
C                   VARIABLES TO BE INCLUDED IN THE FORTHCOMING REGRES-
C                   SION.
C                   UPON RETURNING TO THE CALLING ROUTINE, THIS VECTOR
C                   CONTAINS, IN ADDITION, THE SUBSCRIPT NUMBER OF
C                   THE DEPENDENT VARIABLE IN K+1 POSITION.
C           RX    - OUTPUT MATRIX (K X K) CONTAINING INTERCORRELATIONS
C                   AMONG INDEPENDENT VARIABLES TO BE USED IN FORTH-
C                   COMING REGRESSION.
C           RY    - OUTPUT VECTOR OF LENGTH K CONTAINING INTERCORRELA-
C                   TIONS OF INDEPENDENT VARIABLES WITH DEPENDENT
C                   VARIABLES.
C
C        REMARKS
C           NONE
C
C        SUBROUTINES AND FUNCTION SUBPROGRAMS REQUIRED
C           NONE
C
C        METHOD
C           FROM THE SUBSCRIPT NUMBERS OF THE VARIABLES TO BE INCLUDED
C           IN THE FORTHCOMING REGRESSION, THE SUBROUTINE CONSTRUCTS THE
C           MATRIX RX AND THE VECTOR RY.
C
C     ..................................................................
C
      SUBROUTINE ORDER (M,R,NDEP,K,ISAVE,RX,RY)
      DIMENSION R(1),ISAVE(1),RX(1),RY(1)
C
C        ...............................................................
```

```
C
C        IF A DOUBLE PRECISION VERSION OF THIS ROUTINE IS DESIRED, THE
C        C IN COLUMN 1 SHOULD BE REMOVED FROM THE DOUBLE PRECISION
C        STATEMENT WHICH FOLLOWS.
C
C     DOUBLE PRECISION R,RX,RY
C
C        THE C MUST ALSO BE REMOVED FROM DOUBLE PRECISION STATEMENTS
C        APPEARING IN OTHER ROUTINES USED IN CONJUNCTION WITH THIS
C        ROUTINE.
C
C        ..............................................................
C
C     COPY INTERCORRELATIONS OF INDEPENDENT VARIABLES
C     WITH DEPENDENT VARIABLE
C
      MM=0
      DO 130 J=1,K
      L2=ISAVE(J)
      IF(NDEP-L2) 122, 123, 123
  122 L=NDEP+(L2*L2-L2)/2
      GO TO 125
  123 L=L2+(NDEP*NDEP-NDEP)/2
  125 RY(J)=R(L)
C
C     COPY A SUBSET MATRIX OF INTERCORRELATIONS AMONG
C     INDEPENDENT VARIABLES
C
      DO 130 I=1,K
      L1=ISAVE(I)
      IF(L1-L2) 127, 128, 128
  127 L=L1+(L2*L2-L2)/2
      GO TO 129
  128 L=L2+(L1*L1-L1)/2
  129 MM=MM+1
  130 RX(MM)=R(L)
C
C     PLACE THE SUBSCRIPT NUMBER OF THE DEPENDENT
C     VARIABLE IN ISAVE(K+1)
C
      ISAVE(K+1)=NDEP
      RETURN
      END
```

```
C
C     ..............................................................
C
C        SUBROUTINE MINV
C
C        PURPOSE
C           INVERT A MATRIX
C
C        USAGE
C           CALL MINV(A,N,D,L,M)
C
C        DESCRIPTION OF PARAMETERS
C           A - INPUT MATRIX, DESTROYED IN COMPUTATION AND REPLACED BY
C               RESULTANT INVERSE.
C           N - ORDER OF MATRIX A
C           D - RESULTANT DETERMINANT
C           L - WORK VECTOR OF LENGTH N
C           M - WORK VECTOR OF LENGTH N
C
C        REMARKS
C           MATRIX A MUST BE A GENERAL MATRIX
C
C        SUBROUTINES AND FUNCTION SUBPROGRAMS REQUIRED
C           NONE
C
C        METHOD
C           THE STANDARD GAUSS-JORDAN METHOD IS USED. THE DETERMINANT
C           IS ALSO CALCULATED. A DETERMINANT OF ZERO INDICATES THAT
C           THE MATRIX IS SINGULAR.
C
C     ..............................................................
C
      SUBROUTINE MINV(A,N,D,L,M)
      DIMENSION A(1),L(1),M(1)
C
C        ...........................................................
C
C        IF A DOUBLE PRECISION VERSION OF THIS ROUTINE IS DESIRED, THE
C        C IN COLUMN 1 SHOULD BE REMOVED FROM THE DOUBLE PRECISION
C        STATEMENT WHICH FOLLOWS.
C
C     DOUBLE PRECISION A,D,BIGA,HOLD
C
C        THE C MUST ALSO BE REMOVED FROM DOUBLE PRECISION STATEMENTS
C        APPEARING IN OTHER ROUTINES USED IN CONJUNCTION WITH THIS
C        ROUTINE.
C
C        THE DOUBLE PRECISION VERSION OF THIS SUBROUTINE MUST ALSO
C        CONTAIN DOUBLE PRECISION FORTRAN FUNCTIONS.  ABS IN STATEMENT
C        10 MUST BE CHANGED TO DABS.
C
C        ...........................................................
C
C        SEARCH FOR LARGEST ELEMENT
C
      D=1.0
      NK=-N
```

```
      DO 80 K=1,N
      NK=NK+N
      L(K)=K
      M(K)=K
      KK=NK+K
      BIGA=A(KK)
      DO 20 J=K,N
      IZ=N*(J-1)
      DO 20 I=K,N
      IJ=IZ+I
   10 IF( ABS(BIGA)- ABS(A(IJ))) 15,20,20
   15 BIGA=A(IJ)
      L(K)=I
      M(K)=J
   20 CONTINUE
C
C        INTERCHANGE ROWS
C
      J=L(K)
      IF(J-K) 35,35,25
   25 KI=K-N
      DO 30 I=1,N
      KI=KI+N
      HOLD=-A(KI)
      JI=KI-K+J
      A(KI)=A(JI)
   30 A(JI) =HOLD
C
C        INTERCHANGE COLUMNS
C
   35 I=M(K)
      IF(I-K) 45,45,38
   38 JP=N*(I-1)
      DO 40 J=1,N
      JK=NK+J
      JI=JP+J
      HOLD=-A(JK)
      A(JK)=A(JI)
   40 A(JI) =HOLD
C
C        DIVIDE COLUMN BY MINUS PIVOT (VALUE OF PIVOT ELEMENT IS
C        CONTAINED IN BIGA)
C
   45 IF(BIGA) 48,46,48
   46 D=0.0
      RETURN
   48 DO 55 I=1,N
      IF(I-K) 50,55,50
   50 IK=NK+I
      A(IK)=A(IK)/(-BIGA)
   55 CONTINUE
C
C        REDUCE MATRIX
C
      DO 65 I=1,N
      IK=NK+I
      HOLD=A(IK)
      IJ=I-N
```

```
      DO 65 J=1,N                                                       MINV1160
      IJ=IJ+N                                                           MINV1170
      IF(I-K) 60,65,60                                                  MINV1180
   60 IF(J-K) 62,65,62                                                  MINV1190
   62 KJ=IJ-I+K                                                         MINV1200
      A(IJ)=HOLD*A(KJ)+A(IJ)                                            MINV1210
   65 CONTINUE                                                          MINV1220
C                                                                       MINV1230
C        DIVIDE ROW BY PIVOT                                            MINV1240
C                                                                       MINV1250
      KJ=K-N                                                            MINV1260
      DO 75 J=1,N                                                       MINV1270
      KJ=KJ+N                                                           MINV1280
      IF(J-K) 70,75,70                                                  MINV1290
   70 A(KJ)=A(KJ)/BIGA                                                  MINV1300
   75 CONTINUE                                                          MINV1310
C                                                                       MINV1320
C        PRODUCT OF PIVOTS                                              MINV1330
C                                                                       MINV1340
      D=D*BIGA                                                          MINV1350
C                                                                       MINV1360
C        REPLACE PIVOT BY RECIPROCAL                                    MINV1370
C                                                                       MINV1380
      A(KK)=1.0/BIGA                                                    MINV1390
   80 CONTINUE                                                          MINV1400
C                                                                       MINV1410
C        FINAL ROW AND COLUMN INTERCHANGE                               MINV1420
C                                                                       MINV1430
      K=N                                                               MINV1440
  100 K=(K-1)                                                           MINV1450
      IF(K) 150,150,105                                                 MINV1460
  105 I=L(K)                                                            MINV1470
      IF(I-K) 120,120,108                                               MINV1480
  108 JQ=N*(K-1)                                                        MINV1490
      JR=N*(I-1)                                                        MINV1500
      DO 110 J=1,N                                                      MINV1510
      JK=JQ+J                                                           MINV1520
      HOLD=A(JK)                                                        MINV1530
      JI=JR+J                                                           MINV1540
      A(JK)=-A(JI)                                                      MINV1550
  110 A(JI) =HOLD                                                       MINV1560
  120 J=M(K)                                                            MINV1570
      IF(J-K) 100,100,125                                               MINV1580
  125 KI=K-N                                                            MINV1590
      DO 130 I=1,N                                                      MINV1600
      KI=KI+N                                                           MINV1610
      HOLD=A(KI)                                                        MINV1620
      JI=KI-K+J                                                         MINV1630
      A(KI)=-A(JI)                                                      MINV1640
  130 A(JI) =HOLD                                                       MINV1650
      GO TO 100                                                         MINV1660
  150 RETURN                                                            MINV1670
      END                                                               MINV1680
```

```
C
C     ..................................................................
C
C        SUBROUTINE MULTR
C
C        PURPOSE
C           PERFORM A MULTIPLE LINEAR REGRESSION ANALYSIS FOR A
C           DEPENDENT VARIABLE AND A SET OF INDEPENDENT VARIABLES.  THIS
C           SUBROUTINE IS NORMALLY USED IN THE PERFORMANCE OF MULTIPLE
C           AND POLYNOMIAL REGRESSION ANALYSES.
C
C        USAGE
C           CALL MULTR (N,K,XBAR,STD,D,RX,RY,ISAVE,B,SB,T,ANS)
C
C        DESCRIPTION OF PARAMETERS
C           N     - NUMBER OF OBSERVATIONS.
C           K     - NUMBER OF INDEPENDENT VARIABLES IN THIS REGRESSION.
C           XBAR  - INPUT VECTOR OF LENGTH M CONTAINING MEANS OF ALL
C                   VARIABLES. M IS NUMBER OF VARIABLES IN OBSERVATIONS.
C           STD   - INPUT VECTOR OF LENGTH M CONTAINING STANDARD DEVI-
C                   ATIONS OF ALL VARIABLES.
C           D     - INPUT VECTOR OF LENGTH M CONTAINING THE DIAGONAL OF
C                   THE MATRIX OF SUMS OF CROSS-PRODUCTS OF DEVIATIONS
C                   FROM MEANS FOR ALL VARIABLES.
C           RX    - INPUT MATRIX (K X K) CONTAINING THE INVERSE OF
C                   INTERCORRELATIONS AMONG INDEPENDENT VARIABLES.
C           RY    - INPUT VECTOR OF LENGTH K CONTAINING INTERCORRELA-
C                   TIONS OF INDEPENDENT VARIABLES WITH DEPENDENT
C                   VARIABLE.
C           ISAVE - INPUT VECTOR OF LENGTH K+1 CONTAINING SUBSCRIPTS OF
C                   INDEPENDENT VARIABLES IN ASCENDING ORDER.  THE
C                   SUBSCRIPT OF THE DEPENDENT VARIABLE IS STORED IN
C                   THE LAST, K+1, POSITION.
C           B     - OUTPUT VECTOR OF LENGTH K CONTAINING REGRESSION
C                   COEFFICIENTS.
C           SB    - OUTPUT VECTOR OF LENGTH K CONTAINING STANDARD
C                   DEVIATIONS OF REGRESSION COEFFICIENTS.
C           T     - OUTPUT VECTOR OF LENGTH K CONTAINING T-VALUES.
C           ANS   - OUTPUT VECTOR OF LENGTH 10 CONTAINING THE FOLLOWING
C                   INFORMATION..
C                   ANS(1)  INTERCEPT
C                   ANS(2)  MULTIPLE CORRELATION COEFFICIENT
C                   ANS(3)  STANDARD ERROR OF ESTIMATE
C                   ANS(4)  SUM OF SQUARES ATTRIBUTABLE TO REGRES-
C                           SION (SSAR)
C                   ANS(5)  DEGREES OF FREEDOM ASSOCIATED WITH SSAR
C                   ANS(6)  MEAN SQUARE OF SSAR
C                   ANS(7)  SUM OF SQUARES OF DEVIATIONS FROM REGRES-
C                           SION (SSDR)
C                   ANS(8)  DEGREES OF FREEDOM ASSOCIATED WITH SSDR
C                   ANS(9)  MEAN SQUARE OF SSDR
C                   ANS(10) F-VALUE
C
C        REMARKS
C           N MUST BE GREATER THAN K+1.
C
C        SUBROUTINES AND FUNCTION SUBPROGRAMS REQUIRED
```

```
C           NONE
C
C        METHOD
C           THE GAUSS-JORDAN METHOD IS USED IN THE SOLUTION OF THE
C           NORMAL EQUATIONS.  REFER TO W. W. COOLEY AND P. R. LOHNES,
C           'MULTIVARIATE PROCEDURES FOR THE BEHAVIORAL SCIENCES',
C           JOHN WILEY AND SONS, 1962, CHAPTER 3, AND B. OSTLE,
C           'STATISTICS IN RESEARCH', THE IOWA STATE COLLEGE PRESS,
C           1954, CHAPTER 8.
C
C     ..................................................................
C
      SUBROUTINE MULTR (N,K,XBAR,STD,D,RX,RY,ISAVE,B,SB,T,ANS)
      DIMENSION XBAR(1),STD(1),D(1),RX(1),RY(1),ISAVE(1),B(1),SB(1),
     1          T(1),ANS(1)
C
C        ...............................................................
C
C        IF A DOUBLE PRECISION VERSION OF THIS ROUTINE IS DESIRED, THE
C        C IN COLUMN 1 SHOULD BE REMOVED FROM THE DOUBLE PRECISION
C        STATEMENT WHICH FOLLOWS.
C
C     DOUBLE PRECISION XBAR,STD,D,RX,RY,B,SB,T,ANS,RM,BO,SSAR,SSDR,SY,
C    1                 FN,FK,SSARM,SSDRM,F
C
C        THE C MUST ALSO BE REMOVED FROM DOUBLE PRECISION STATEMENTS
C        APPEARING IN OTHER ROUTINES USED IN CONJUNCTION WITH THIS
C        ROUTINE.
C
C        THE DOUBLE PRECISION VERSION OF THIS SUBROUTINE MUST ALSO
C        CONTAIN DOUBLE PRECISION FORTRAN FUNCTIONS.  SQRT AND ABS IN
C        STATEMENTS 122, 125, AND 135 MUST BE CHANGED TO DSQRT AND DABS.
C
C        ...............................................................
C
      MM=K+1
C
C           BETA WEIGHTS
C
      DO 100 J=1,K
  100 B(J)=0.0
      DO 110 J=1,K
      L1=K*(J-1)
      DO 110 I=1,K
      L=L1+I
  110 B(J)=B(J)+RY(I)*RX(L)
      RM=0.0
      BO=0.0
      L1=ISAVE(MM)
C
C           COEFFICIENT OF DETERMINATION
C
      DO 120 I=1,K
      RM=RM+B(I)*RY(I)
C
C           REGRESSION COEFFICIENTS
C
      L=ISAVE(I)
```

```
      B(I)=B(I)*(STD(L1)/STD(L))
C
C        INTERCEPT
C
  120 BO=BO+B(I)*XBAR(L)
      BO=XBAR(L1)-BO
C
C        SUM OF SQUARES ATTRIBUTABLE TO REGRESSION
C
      SSAR=RM*D(L1)
C
C        MULTIPLE CORRELATION COEFFICIENT
C
  122 RM= SQRT( ABS(RM))
C
C        SUM OF SQUARES OF DEVIATIONS FROM REGRESSION
C
      SSDR=D(L1)-SSAR
C
C        VARIANCE OF ESTIMATE
C
      FN=N-K-1
      SY=SSDR/FN
C
C        STANDARD DEVIATIONS OF REGRESSION COEFFICIENTS
C
      DO 130 J=1,K
      L1=K*(J-1)+J
      L=ISAVE(J)
  125 SB(J)= SQRT( ABS((RX(L1)/D(L))*SY))
C
C        COMPUTED T-VALUES
C
  130 T(J)=B(J)/SB(J)
C
C        STANDARD ERROR OF ESTIMATE
C
  135 SY= SQRT( ABS(SY))
C
C        F VALUE
C
      FK=K
      SSARM=SSAR/FK
      SSDRM=SSDR/FN
      F=SSARM/SSDRM
C
      ANS(1)=BO
      ANS(2)=RM
      ANS(3)=SY
      ANS(4)=SSAR
      ANS(5)=FK
      ANS(6)=SSARM
      ANS(7)=SSDR
      ANS(8)=FN
      ANS(9)=SSDRM
      ANS(10)=F
      RETURN
      END
```

```
C
C     ...............................................................
C
C        SAMPLE MAIN PROGRAM FOR ANALYSIS OF VARIANCE - ANOVA
C
C        PURPOSE
C           (1) READ THE PROBLEM PARAMETER CARD FOR ANALYSIS OF VARI-
C           ANCE, (2) CALL THE SUBROUTINES FOR THE CALCULATION OF SUMS
C           OF SQUARES, DEGREES OF FREEDOM AND MEAN SQUARE, AND
C           (3) PRINT FACTOR LEVELS, GRAND MEAN AND ANALYSIS OF VARI-
C           ANCE TABLE.
C
C        REMARKS
C           THE PROGRAM HANDLES ONLY COMPLETE FACTORIAL DESIGNS.  THERE-
C           FORE, OTHER EXPERIMENTAL DESIGN MUST BE REDUCED TO THIS FORM
C           PRIOR TO THE USE OF THE PROGRAM.
C
C        SUBROUTINES AND FUNCTION SUBPROGRAMS REQUIRED
C           AVDAT
C           AVCAL
C           MEANQ
C
C        METHOD
C           THE METHOD IS BASED ON THE TECHNIQUE DISCUSSED BY H. O.
C           HARTLEY IN 'MATHEMATICAL METHODS FOR DIGITAL COMPUTERS',
C           EDITED BY A. RALSTON AND H. WILF, JOHN WILEY AND SONS,
C           1962, CHAPTER 20.
C
C     ...............................................................
C
C     THE FOLLOWING DIMENSION MUST BE GREATER THAN OR EQUAL TO THE
C     CUMULATIVE PRODUCT OF EACH FACTOR LEVEL PLUS ONE (LEVEL(I)+1)
C     FOR I=1 TO K, WHERE K IS THE NUMBER OF FACTORS..
C
      DIMENSION X(3000)
C
C     THE FOLLOWING DIMENSIONS MUST BE GREATER THAN OR EQUAL TO THE
C     NUMBER OF FACTORS..
C
      DIMENSION HEAD(6),LEVEL(6),ISTEP(6),KOUNT(6),LASTS(6)
C
C     THE FOLLOWING DIMENSIONS MUST BE GREATER THAN OR EQUAL TO 2 TO
C     THE K-TH POWER MINUS 1, ((2**K)-1)..
C
      DIMENSION SUMSQ(63),NDF(63),SMEAN(63)
C
C     THE FOLLOWING DIMENSION IS USED TO PRINT FACTOR LABELS IN ANALYSIS
C     OF VARIANCE TABLE AND IS FIXED..
C
      DIMENSION FMT(15)
C     ...............................................................
C
C        IF A DOUBLE PRECISION VERSION OF THIS ROUTINE IS DESIRED, THE
C        C IN COLUMN 1 SHOULD BE REMOVED FROM THE DOUBLE PRECISION
C        STATEMENT WHICH FOLLOWS.
C
C     DOUBLE PRECISION X,GMEAN,SUMSQ,SMEAN,SUM
```

```
C
C       THE C MUST ALSO BE REMOVED FROM DOUBLE PRECISION STATEMENTS
C       APPEARING IN OTHER ROUTINES USED IN CONJUNCTION WITH THIS
C       ROUTINE.
C
C       ..........................................................
C
    1 FORMAT(A4,A2,I2,A4,3X,11(A1,I4)/(A1,I4,A1,I4,A1,I4,A1,I4,A1,I4))
    2 FORMAT(26H1ANALYSIS OF VARIANCE.....A4,A2//)
    3 FORMAT(18H0LEVELS OF FACTORS/(3X,A1,7X,I4))
    4 FORMAT(1H0//11H GRAND MEANF20.5////)
    5 FORMAT(10H0SOURCE OF18X,7HSUMS OF10X,10HDEGREES OF9X,4HMEAN/10H VA
     1RIATION18X,7HSQUARES11X,7HFREEDOM10X,7HSQUARES/)
    6 FORMAT(1H 15A1,F20.5,10X,I6,F20.5)
    7 FORMAT(6H TOTAL10X,F20.5,10X,I6)
    8 FORMAT(12F6.0)
C
C     ............................................................
C
C     READ PROBLEM PARAMETER CARD
C
  100 READ (5,1) PR,PR1,K,BLANK,(HEAD(I),LEVEL(I),I=1,K)
C        PR.....PROBLEM NUMBER (MAY BE ALPHAMERIC)
C        PR1....PROBLEM NUMBER (CONTINUED)
C        K......NUMBER OF FACTORS
C        BLANK..BLANK FIELD
C        HEAD...FACTOR LABELS
C        LEVEL..LEVELS OF FACTORS
C
C     PRINT PROBLEM NUMBER AND LEVELS OF FACTORS
C
      WRITE (6,2) PR,PR1
      WRITE (6,3) (HEAD(I),LEVEL(I),I=1,K)
C
C     CALCULATE TOTAL NUMBER OF DATA
C
      N=LEVEL(1)
      DO 102 I=2,K
  102 N=N*LEVEL(I)
C
C     READ ALL INPUT DATA
C
      READ (5,8) (X(I),I=1,N)
C
      CALL AVDAT (K,LEVEL,N,X,L,ISTEP,KOUNT)
      CALL AVCAL (K,LEVEL,X,L,ISTEP,LASTS)
      CALL MEANQ (K,LEVEL,X,GMEAN,SUMSQ,NDF,SMEAN,ISTEP,KOUNT,LASTS)
C
C     PRINT GRAND MEAN
C
      WRITE (6,4) GMEAN
C
C     PRINT ANALYSIS OF VARIANCE TABLE
C
      WRITE (6,5)
      LL=(2**K)-1
      ISTEP(1)=1
      DO 105 I=2,K
```

```
105 ISTEP(I)=0
    DO 110 I=1,15
110 FMT(I)=BLANK
    NN=0
    SUM=0.0
120 NN=NN+1
    L=0
    DO 140 I=1,K
    FMT(I)=BLANK
    IF(ISTEP(I)) 130, 140, 130
130 L=L+1
    FMT(L)=HEAD(I)
140 CONTINUE
    WRITE (6,6) (FMT(I),I=1,15),SUMSQ(NN),NDF(NN),SMEAN(NN)
    SUM=SUM+SUMSQ(NN)
    IF(NN-LL) 145, 170, 170
145 DO 160 I=1,K
    IF(ISTEP(I)) 147, 150, 147
147 ISTEP(I)=0
    GO TO 160
150 ISTEP(I)=1
    GO TO 120
160 CONTINUE
170 N=N-1
    WRITE (6,7) SUM,N
    GO TO 100
    END
```

```
C
C     ..................................................................
C
C        SUBROUTINE AVDAT
C
C        PURPOSE
C           PLACE DATA FOR ANALYSIS OF VARIANCE IN PROPERLY DISTRIBUTED
C           POSITIONS OF STORAGE.  THIS SUBROUTINE IS NORMALLY FOLLOWED
C           BY CALLS TO AVCAL AND MEANQ SUBROUTINES IN THE PERFORMANCE
C           OF ANALYSIS OF VARIANCE FOR A COMPLETE FACTORIAL DESIGN.
C
C        USAGE
C           CALL AVDAT (K,LEVEL,N,X,L,ISTEP,KOUNT)
C
C        DESCRIPTION OF PARAMETERS
C           K     - NUMBER OF VARIABLES (FACTORS). K MUST BE .GT. ONE.
C           LEVEL - INPUT VECTOR OF LENGTH K CONTAINING LEVELS (CATE-
C                   GORIES) WITHIN EACH VARIABLE.
C           N     - TOTAL NUMBER OF DATA POINTS READ IN.
C           X     - WHEN THE SUBROUTINE IS CALLED, THIS VECTOR CONTAINS
C                   DATA IN LOCATIONS X(1) THROUGH X(N).  UPON RETURNING
C                   TO THE CALLING ROUTINE, THE VECTOR CONTAINS THE DATA
C                   IN PROPERLY REDISTRIBUTED LOCATIONS OF VECTOR X.
C                   THE LENGTH OF VECTOR X IS CALCULATED BY (1) ADDING
C                   ONE TO EACH LEVEL OF VARIABLE AND (2) OBTAINING THE
C                   CUMULATIVE PRODUCT OF ALL LEVELS.  (THE LENGTH OF
C                   X = (LEVEL(1)+1)*(LEVEL(2)+1)*...*(LEVEL(K)+1).)
C           L     - OUTPUT VARIABLE CONTAINING THE POSITION IN VECTOR X
C                   WHERE THE LAST INPUT DATA IS STORED.
C           ISTEP - OUTPUT VECTOR OF LENGTH K CONTAINING CONTROL STEPS
C                   WHICH ARE USED TO LOCATE DATA IN PROPER POSITIONS
C                   OF VECTOR X.
C           KOUNT - WORKING VECTOR OF LENGTH K.
C
C        REMARKS
C           INPUT DATA MUST BE ARRANGED IN THE FOLLOWING MANNER.
C           CONSIDER THE 3-VARIABLE ANALYSIS OF VARIANCE DESIGN, WHERE
C           ONE VARIABLE HAS 3 LEVELS AND THE OTHER TWO VARIABLES HAVE
C           2 LEVELS.  THE DATA MAY BE REPRESENTED IN THE FORM X(I,J,K),
C           I=1,2,3  J=1,2  K=1,2.  IN ARRANGING DATA, THE INNER
C           SUBSCRIPT, NAMELY I, CHANGES FIRST.  WHEN I=3, THE NEXT
C           INNER SUBSCRIPT, J, CHANGES AND SO ON UNTIL I=3, J=2, AND
C           K=2.
C
C        SUBROUTINES AND FUNCTION SUBPROGRAMS REQUIRED
C           NONE
C
C        METHOD
C           THE METHOD IS BASED ON THE TECHNIQUE DISCUSSED BY H. O.
C           HARTLEY IN 'MATHEMATICAL METHODS FOR DIGITAL COMPUTERS',
C           EDITED BY A. RALSTON AND H. WILF, JOHN WILEY AND SONS,
C           1962, CHAPTER 20.
C
C     ..................................................................
C
      SUBROUTINE AVDAT (K,LEVEL,N,X,L,ISTEP,KOUNT)
      DIMENSION LEVEL(1),X(1),ISTEP(1),KOUNT(1)
```

```
C
C        ..........................................................
C
C        IF A DOUBLE PRECISION VERSION OF THIS ROUTINE IS DESIRED, THE
C        C IN COLUMN 1 SHOULD BE REMOVED FROM THE DOUBLE PRECISION
C        STATEMENT WHICH FOLLOWS.
C
C     DOUBLE PRECISION X
C
C        THE C MUST ALSO BE REMOVED FROM DOUBLE PRECISION STATEMENTS
C        APPEARING IN OTHER ROUTINES USED IN CONJUNCTION WITH THIS
C        ROUTINE.
C
C        ..........................................................
C
C     CALCULATE TOTAL DATA AREA REQUIRED
C
      M=LEVEL(1)+1
      DO 105 I=2,K
  105 M=M*(LEVEL(I)+1)
C
C     MOVE DATA TO THE UPPER PART OF THE ARRAY X
C     FOR THE PURPOSE OF REARRANGEMENT
C
      N1=M+1
      N2=N+1
      DO 107 I=1,N
      N1=N1-1
      N2=N2-1
  107 X(N1)=X(N2)
C
C     CALCULATE MULTIPLIERS TO BE USED IN FINDING STORAGE LOCATIONS FOR
C     INPUT DATA
C
      ISTEP(1)=1
      DO 110 I=2,K
  110 ISTEP(I)=ISTEP(I-1)*(LEVEL(I-1)+1)
      DO 115 I=1,K
  115 KOUNT(I)=1
C
C     PLACE DATA IN PROPER LOCATIONS
C
      N1=N1-1
      DO 135 I=1,N
      L=KOUNT(1)
      DO 120 J=2,K
  120 L=L+ISTEP(J)*(KOUNT(J)-1)
      N1=N1+1
      X(L)=X(N1)
      DO 130 J=1,K
      IF(KOUNT(J)-LEVEL(J)) 124, 125, 124
  124 KOUNT(J)=KOUNT(J)+1
      GO TO 135
  125 KOUNT(J)=1
  130 CONTINUE
  135 CONTINUE
      RETURN
      END
```

```
C
C     ..................................................................
C
C        SUBROUTINE AVCAL
C
C        PURPOSE
C           PERFORM THE CALCULUS OF A FACTORIAL EXPERIMENT USING
C           OPERATOR SIGMA AND OPERATOR DELTA.  THIS SUBROUTINE IS
C           PRECEDED BY SUBROUTINE ADVAT AND FOLLOWED BY SUBROUTINE
C           MEANQ IN THE PERFORMANCE OF ANALYSIS OF VARIANCE FOR A
C           COMPLETE FACTORIAL DESIGN.
C
C        USAGE
C           CALL AVCAL (K,LEVEL,X,L,ISTEP,LASTS)
C
C        DESCRIPTION OF PARAMETERS
C           K     - NUMBER OF VARIABLES (FACTORS). K MUST BE .GT. ONE.
C           LEVEL - INPUT VECTOR OF LENGTH K CONTAINING LEVELS (CATE-
C                   GORIES) WITHIN EACH VARIABLE.
C           X     - INPUT VECTOR CONTAINING DATA.  DATA HAVE BEEN PLACED
C                   IN VECTOR X BY SUBROUTINE AVDAT.  THE LENGTH OF X
C                   IS (LEVEL(1)+1)*(LEVEL(2)+1)*...*(LEVEL(K)+1).
C           L     - THE POSITION IN VECTOR X WHERE THE LAST INPUT DATA
C                   IS LOCATED.  L HAS BEEN CALCULATED BY SUBROUTINE
C                   AVDAT.
C           ISTEP - INPUT VECTOR OF LENGTH K CONTAINING STORAGE CONTROL
C                   STEPS WHICH HAVE BEEN CALCULATED BY SUBROUTINE
C                   AVDAT.
C           LASTS - WORKING VECTOR OF LENGTH K.
C
C        REMARKS
C           THIS SUBROUTINE MUST FOLLOW SUBROUTINE AVDAT.
C
C        SUBROUTINES AND FUNCTION SUBPROGRAMS REQUIRED
C           NONE
C
C        METHOD
C           THE METHOD IS BASED ON THE TECHNIQUE DISCUSSED BY H. O.
C           HARTLEY IN 'MATHEMATICAL METHODS FOR DIGITAL COMPUTERS',
C           EDITED BY A. RALSTON AND H. WILF, JOHN WILEY AND SONS,
C           1962, CHAPTER 20.
C
C     ..................................................................
C
      SUBROUTINE AVCAL (K,LEVEL,X,L,ISTEP,LASTS)
      DIMENSION LEVEL(1),X(1),ISTEP(1),LASTS(1)
C
C        ...............................................................
C
C        IF A DOUBLE PRECISION VERSION OF THIS ROUTINE IS DESIRED, THE
C        C IN COLUMN 1 SHOULD BE REMOVED FROM THE DOUBLE PRECISION
C        STATEMENT WHICH FOLLOWS.
C
C     DOUBLE PRECISION X,SUM
C
C        THE C MUST ALSO BE REMOVED FROM DOUBLE PRECISION STATEMENTS
C        APPEARING IN OTHER ROUTINES USED IN CONJUNCTION WITH THIS
```

```
C        ROUTINE.
C
C        ..............................................................
C
C     CALCULATE THE LAST DATA POSITION OF EACH FACTOR
C
      LASTS(1)=L+1
      DO 145 I=2,K
  145 LASTS(I)=LASTS(I-1)+ISTEP(I)
C
C     PERFORM CALCULUS OF OPERATION
C
  150 DO 175 I=1,K
      L=1
      LL=1
      SUM=0.0
      NN=LEVEL(I)
      FN=NN
      INCRE=ISTEP(I)
      LAST=LASTS(I)
C
C     SIGMA OPERATION
C
  155 DO 160 J=1,NN
      SUM=SUM+X(L)
  160 L=L+INCRE
      X(L)=SUM
C
C     DELTA OPERATION
C
      DO 165 J=1,NN
      X(LL)=FN*X(LL)-SUM
  165 LL=LL+INCRE
      SUM=0.0
      IF(L-LAST) 167, 175, 175
  167 IF(L-LAST+INCRE) 168, 168, 170
  168 L=L+INCRE
      LL=LL+INCRE
      GO TO 155
  170 L=L+INCRE+1-LAST
      LL=LL+INCRE+1-LAST
      GO TO 155
  175 CONTINUE
      RETURN
      END
```

```
C
C     ..................................................................
C
C        SUBROUTINE MEANQ
C
C        PURPOSE
C           COMPUTE SUM OF SQUARES, DEGREES OF FREEDOM, AND MEAN SQUARE
C           USING THE MEAN SQUARE OPERATOR.  THIS SUBROUTINE NORMALLY
C           FOLLOWS CALLS TO AVDAT AND AVCAL SUBROUTINES IN THE PER-
C           FORMANCE OF ANALYSIS OF VARIANCE FOR A COMPLETE FACTORIAL
C           DESIGN.
C
C        USAGE
C           CALL MEANQ (K,LEVEL,X,GMEAN,SUMSQ,NDF,SMEAN,MSTEP,KOUNT,
C                       LASTS)
C
C        DESCRIPTION OF PARAMETERS
C           K     - NUMBER OF VARIABLES (FACTORS). K MUST BE .GT. ONE.
C           LEVEL - INPUT VECTOR OF LENGTH K CONTAINING LEVELS (CATE-
C                   GORIES) WITHIN EACH VARIABLE.
C           X     - INPUT VECTOR CONTAINING THE RESULT OF THE SIGMA AND
C                   DELTA OPERATORS. THE LENGTH OF X IS
C                   (LEVEL(1)+1)*(LEVEL(2)+1)*...*(LEVEL(K)+1).
C           GMEAN - OUTPUT VARIABLE CONTAINING GRAND MEAN.
C           SUMSQ - OUTPUT VECTOR CONTAINING SUMS OF SQUARES.  THE
C                   LENGTH OF SUMSQ IS 2 TO THE K-TH POWER MINUS ONE,
C                   (2**K)-1.
C           NDF   - OUTPUT VECTOR CONTAINING DEGREES OF FREEDOM.  THE
C                   LENGTH OF NDF IS 2 TO THE K-TH POWER MINUS ONE,
C                   (2**K)-1.
C           SMEAN - OUTPUT VECTOR CONTAINING MEAN SQUARES.  THE
C                   LENGTH OF SMEAN IS 2 TO THE K-TH POWER MINUS ONE,
C                   (2**K)-1.
C           MSTEP - WORKING VECTOR OF LENGTH K.
C           KOUNT - WORKING VECTOR OF LENGTH K.
C           LASTS - WORKING VECTOR OF LENGTH K.
C
C        REMARKS
C           THIS SUBROUTINE MUST FOLLOW SUBROUTINE AVCAL
C
C        SUBROUTINES AND FUNCTION SUBPROGRAMS REQUIRED
C           NONE
C
C        METHOD
C           THE METHOD IS BASED ON THE TECHNIQUE DISCUSSED BY H. O.
C           HARTLEY IN 'MATHEMATICAL METHODS FOR DIGITAL COMPUTERS',
C           EDITED BY A. RALSTON AND H. WILF, JOHN WILEY AND SONS,
C           1962, CHAPTER 20.
C
C     ..................................................................
C
      SUBROUTINE MEANQ (K,LEVEL,X,GMEAN,SUMSQ,NDF,SMEAN,MSTEP,KOUNT,
     1                  LASTS)
      DIMENSION LEVEL(1),X(1),SUMSQ(1),NDF(1),SMEAN(1),MSTEP(1),
     1          KOUNT(1),LASTS(1)
C
C        ...............................................................
```

```
C
C        IF A DOUBLE PRECISION VERSION OF THIS ROUTINE IS DESIRED, THE
C        C IN COLUMN 1 SHOULD BE REMOVED FROM THE DOUBLE PRECISION
C        STATEMENT WHICH FOLLOWS.
C
C     DOUBLE PRECISION X,GMEAN,SUMSQ,SMEAN,FN1
C
C        THE C MUST ALSO BE REMOVED FROM DOUBLE PRECISION STATEMENTS
C        APPEARING IN OTHER ROUTINES USED IN CONJUNCTION WITH THIS
C        ROUTINE.
C
C        ...........................................................
C
C     CALCULATE TOTAL NUMBER OF DATA
C
      N=LEVEL(1)
      DO 150 I=2,K
  150 N=N*LEVEL(I)
C
C     SET UP CONTROL FOR MEAN SQUARE OPERATOR
C
      LASTS(1)=LEVEL(1)
      DO 178 I=2,K
  178 LASTS(I)=LEVEL(I)+1
      NN=1
C
C     CLEAR THE AREA TO STORE SUMS OF SQUARES
C
      LL=(2**K)-1
      MSTEP(1)=1
      DO 180 I=2,K
  180 MSTEP(I)=MSTEP(I-1)*2
      DO 185 I=1,LL
  185 SUMSQ(I)=0.0
C
C     PERFORM MEAN SQUARE OPERATOR
C
      DO 190 I=1,K
  190 KOUNT(I)=0
  200 L=0
      DO 260 I=1,K
      IF(KOUNT(I)-LASTS(I)) 210, 250, 210
  210 IF(L) 220, 220, 240
  220 KOUNT(I)=KOUNT(I)+1
      IF(KOUNT(I)-LEVEL(I)) 230, 230, 250
  230 L=L+MSTEP(I)
      GO TO 260
  240 IF(KOUNT(I)-LEVEL(I)) 230, 260, 230
  250 KOUNT(I)=0
  260 CONTINUE
      IF(L) 285, 285, 270
  270 SUMSQ(L)=SUMSQ(L)+X(NN)*X(NN)
      NN=NN+1
      GO TO 200
C
C     CALCULATE THE GRAND MEAN
C
  285 FN=N
```

```
      GMEAN=X(NN)/FN
C
C     CALCULATE FIRST DIVISOR REQUIRED TO FORM SUM OF SQUARES AND SECOND
C     DIVISOR, WHICH IS EQUAL TO DEGREES OF FREEDOM, REQUIRED TO FORM
C     MEAN SQUARES
C
      DO 310 I=2,K
  310 MSTEP(I)=0
      NN=0
      MSTEP(1)=1
  320 ND1=1
      ND2=1
      DO 340 I=1,K
      IF(MSTEP(I)) 330, 340, 330
  330 ND1=ND1*LEVEL(I)
      ND2=ND2*(LEVEL(I)-1)
  340 CONTINUE
      FN1=N*ND1
      FN2=ND2
      NN=NN+1
      SUMSQ(NN)=SUMSQ(NN)/FN1
      NDF(NN)=ND2
      SMEAN(NN)=SUMSQ(NN)/FN2
      IF(NN-LL) 345, 370, 370
  345 DO 360 I=1,K
      IF(MSTEP(I)) 347, 350, 347
  347 MSTEP(I)=0
      GO TO 360
  350 MSTEP(I)=1
      GO TO 320
  360 CONTINUE
  370 RETURN
      END
```